FINITE ELEMENT ANALYSIS FOR STEADY STATE NATURAL CONVECTION IN AN OPEN SQUARE CAVITY HAVING PARTIALLY HEATED CIRCULAR CYLINDER

BY

MOHAMMED NASIR UDDIN
Student No. 100709010P
Registration No. 100709010, Session: October-2007

MASTER OF PHILOSOPHY
IN
MATHEMATICS

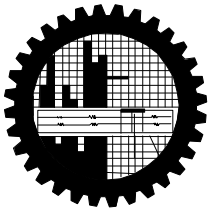

DEPARTMENT OF MATHEMATICS
BANGLADESH UNIVERSITY OF ENGINEERING AND TECHNOLOGY
DHAKA-1000
January-2011

The thesis titled

FINITE ELEMENT ANALYSIS FOR STEADY STATE NATURAL CONVECTION IN AN OPEN SQUARE CAVITY HAVING PARTIALLY HEATED CIRCULAR CYLINDER

Submitted by

MOHAMMED NASIR UDDIN
Student No. 100709010P, Registration No. 100709010, Session: October-2007, a part time student of M. Phil. (Mathematics) has been accepted as satisfactory in partial fulfillment for the degree of
Master of Philosophy in Mathematics
On 22, January- 2011

Board of Examiners

1. _____
   Dr. Md. Abdul Alim — Chairman (Supervisor)
   Associate Professor
   Department of Mathematics
   BUET, Dhaka-1000

2. _____
   Dr. Md. Abdul Hakim Khan — Member (Ex-Officio)
   Professor and Head
   Department of Mathematics
   BUET, Dhaka-1000

3. _____
   Dr. Md. Mustafa Kamal Chowdhury — Member
   Professor
   Department of Mathematics,
   BUET, Dhaka-1000

4. _____
   Md. Obayedullah — Member
   Associate Professor
   Department of Mathematics,
   BUET, Dhaka-1000

5. _____
   Dr. Amal Krishna Halder — Member (External)
   Professor
   Department of Mathematics,
   Dhaka University, Dhaka-1000

Author's Declaration

I am hereby declaring that the work in this dissertation was carried out in accordance with the regulations of Bangladesh University of Engineering and Technology (BUET), Dhaka, Bangladesh. The work is also original except where indicated by and attached with special reference in the context and no part of it has been submitted for any attempt to get other degrees or diplomas.

All views expressed in the dissertation are those of the author and in no way or by no means represent those of Bangladesh University of Engineering and Technology, Dhaka. This dissertation has not been submitted to any other University for examination either in home or abroad.

(MOHAMMED NASIR UDDIN)

Date: 22, January, 2011

Permit of Research

This is to endorse that the work presented in this thesis is carried out by the author under the supervision of Dr. Md. Abdul Alim, Associate Professor, Department of Mathematics, Bangladesh University of Engineering & Technology [BUET], Dhaka.

---------- ----------

Dr. Md. Abdul Alim **Md. Nasir Uddin**

Dedicated to my Parents

Acknowledgements

With great pleasure the author takes this opportunity to place on record her deepest respect and sincerest gratitude to Dr. Md. Abdul Alim, Associate Professor, Department of Mathematics, Bangladesh University of Engineering and Technology, Dhaka for his expert guidance and valuable suggestions through out this work. It would not have been possible to carry out this study successfully without the continuous inspiration and encouragement from supervisor.

I am also deeply indebted to Prof. Dr. Md Abdul Hakim Khan, Head of the Department of Mathematics, Prof. Dr. Md. Mustafa Kamal Chowdhury, and Prof. Dr. Md. Abdul Maleque, Department of Mathematics, BUET for their wise and liberal co-operation in providing me all necessary help from the department during my course of M.Phil. Degree.

I would also like to extend my thanks to Prof. Dr. Md. Monirul Alam Sarker and all other teachers and concerned of this department for their thoroughly help and co-operation.

Finally I express my devoted affection to my wife Mrs. Tahmina Haque and all my family members and relatives specially my parents for creating a delightful atmosphere as well as excusing me from family duties in order to complete the courses, research studies and final production of the thesis work.

Abstract

Natural convection in open cavities has received considerable attention because of its importance in several thermal engineering problems, for example, in the design of electronic devices, solar thermal receivers, uncovered flat plate solar collectors having rows of vertical strips geothermal reservoirs etc. In this thesis under the title "Finite Element Analysis for Steady State Natural Convection in a Square Open Cavity Having Partially Heated Circular Cylinder" two problems have been studied. The study as well depending on various kinds of cylinder and boundary conditions are abstracted below.

Firstly, Numerical analysis of two-dimensional laminar steady-state natural convection in a tilted square open cavity with a partially heated circular cylinder has been investigated. A partially heated circular cylinder is placed at the center of the cavity and the opposite wall to the aperture is placed at iso-flux heat source. The other two remaining walls were kept cooled with Temperature T_c (Top wall) and heated with temperature T_h (bottom wall). The fluid is concerned with Prandtl numbers 0.72, 1.0 and 7.0. The properties of the fluid were assumed to be constant. The physical problems are represented mathematically by different sets of governing equations along with the corresponding boundary conditions. The non-dimensional governing equations are discretized by using Galerkin weighted residual method of finite element formulation. The obtained results are presented in terms of streamlines and isotherms, heat transfer characteristics Nusselt numbers for Grashof numbers from 10^3 to 10^6 and for inclination angles of the cavity from 0^o to 45^o. The obtained results are also presented with the variation of different diameter ratios of the cylinder. The results show that the Nusselt numbers increase with the increase of Grashof numbers. Also the average Nusselt number changes substantially with the inclination angle of the cavity while better thermal performance is also sensitive to the boundary condition of the heated wall. The computational results also indicate that the average Nusselt number at the hot wall of the cavity is depending on the dimensionless parameters.

Finally, Numerical analysis of two-dimensional laminar steady-state natural convection in a tilted square open cavity with a partially heated square cylinder has been investigated. A partially heated square cylinder is placed at the center of the cavity and remains all of properties unchanged. The obtained results are presented in terms of streamlines and isotherms, heat transfer characteristics Nusselt numbers for Grashof

numbers from 10^3 to 10^6 and cavity angle ranges of 0º to 45º. The obtained results are also presented with the variation of different aspect ratios of the square cylinder. The results show that the Nusselt numbers increase with the increase of Grashof numbers. Also the average Nusselt number changes substantially with the inclination angle of the cavity while better thermal performance is also sensitive to the boundary condition of the heated wall. The computational results also indicate that the average Nusselt number at the hot wall of the cavity depends on the dimensionless parameters.

Contents

Nomenclature

g	gravitational acceleration (ms^{-2})
Gr	Grashof number
k	thermal conductivity of the fluid ($Wm^{-1}K^{-1}$)
L	height and width of the enclosure (m)
D	Diameter of the cylinder
Nu	Nusselt number
p	pressure (Nm^{-2})
P	non-dimensional pressure
Pr	Prandtl number, υ/α
q	heat flux (Wm^{-2})
dr	Diameter ratio
T	temperature (K)
u, v	velocity components (ms^{-1})
U, V	non-dimensional velocity components
x, y	Cartesian coordinates (m)
X, Y	non-dimensional Cartesian coordinates

Greek symbols

α	thermal diffusivity, (m^2s^{-1})
β	thermal expansion coefficient (K^{-1})
ρ	density of the fluid (kgm^{-3})
υ	kinematic viscosity of the fluid (m^2s^{-1})
θ	non-dimensional temperature
Φ	inclination angle of the cavity

List of Tables

List of Figures

CHAPTER 1

Introduction and Historical Review

1.1 Introduction

Heat transfer is that science which seeks to predict the energy transfer which may take place between material bodies as a result of a temperature difference. Thermodynamics teaches that this energy transfer is defined as heat. The science of heat transfer seeks not merely to explain how heat energy may be transferred, but also to predict the rate at which the exchange will take place under certain specified conditions.

The phenomenon of heat transfer was known to human being even in the primitive age when they used to use solar energy as a source of heat. Heat transfer in its initial stage was conceived with the invention of fire in the early age of human civilization. Since then its knowledge and use has been progressively increasing each day as it is directly related to the growth of human civilization. With the invention of steam engine by James watt in 1765 A. D., the phenomenon of heat transfer got its first industrial recognition and after that its use extended to a great extent and spread out in different spheres of engineering fields. In the past three decades, digital computers, numerical techniques and development of numerical models of heat transfer have made it possible to calculate heat transfer of considerable complexity and thereby create a new approach to the design of heat transfer equipment.

The study of temperature and heat transfer is of great importance to the engineers because of its almost universal occurrence in many branches of science and engineering. Although heat transfer analysis is most important for the proper sizing of fuel elements in the nuclear reactors cores to prevent burnout, the performance of aircraft also depends upon the case with which the structure and engines can be cooled. The design of chemical plants is usually done on the basis of heat transfer analysis and the analogous mass transfer processes. The transfer and conversion of energy from one form to another is the basis to all heat transfer process and hence, they are governed by the first as well as the second law of thermodynamics. Heat transfer is commonly associated with fluid dynamics. The knowledge of temperature distribution is essential in heat transfer studies because of the fact that the heat flow takes place only wherever there is a temperature gradient in a system. The heat flux which is defined as the amount of heat transfer per

unit area in per unit time can be calculated from the physical laws relating to the temperature gradient and the heat flux.

Natural convection in open cavities has received considerable attention because of its importance in several thermal engineering problems, for example, in the design of electronic devices, solar thermal receivers, uncovered flat plate solar collectors having rows of vertical strips, geothermal reservoirs, etc. During the past two decades, several experiments and numerical calculations have been presented for describing the phenomenon of natural convection in open cavities. Those studies have been focused to study the effect on flow and heat transfer for different Rayleigh numbers, aspect ratios, and tilt angles.

Natural convection in an air filled, differentially heated, inclined square cavity with a diathermal partition placed at the middle of its cold wall was numerically studied for Rayleigh numbers 10^3 to 10^5. It was observed that due to suppression of convection, heat transfer reductions up to 47 percent in comparison to the cavity without partition by Frederick [11]. Laminar natural convection and conduction in enclosures with multiple vertical partitions were studied theoretically by Kangni et al. [18]. The study covered Rayleigh number Ra in the range 10^3–10^7, Pr = 0.72 (air) aspect ratio 5–20, cavity width 0.1–0.9 and partition thickness 0.01–0.1. They found that the heat transfer decreases with increasing partition number at high Rayleigh number for all conductivity ratios Kr and heat transfer decreases with increasing partition thickness C at all Ra except in the conduction regime where the effect is negligibly small. The offender partitions are less effective in decreasing the heat transfer. Nusselt number is also a decreasing function in the aspect ratio. Tasnim and Collins [34] determined the effect of a horizontal baffle placed on hot (left) wall of a differentially heated square cavity. It has been found that adding baffle on the hot wall can increase the rate of heat transfer by as much as 31.46 percent compared with a wall without baffle for Ra = 10^4. When Ra = 10^5 the increase in heat transfer is 15.3 percent for the same baffle length and the increases in heat transfer is 19.73 percent, when the longest baffle is attached at the middle of the cavity. Bilgen and Oztop [2] studied numerically the steady-state heat transfer by natural convection in partially open inclined square cavities.

1.2 Historical Review

Natural convection in fluid-filled rectangular enclosures has received considerable attention over the past several years due to the wide variety of applications that involve

natural convection processes. These applications span such diverse fields as solar energy collection, nuclear reactor operation and safety, the energy efficient design of building, room, and machinery, waste disposal, and fire prevention and safety. The oscillation-induced heat transport has been studied by a number of researchers due to its many industrial applications, such as bioengineering, chemical engineering, and so forth. Kuhn and Oosthuizen [19] numerically studied unsteady natural convection in a partially heated rectangular cavity. They concluded that as the heated location moves from the top to the bottom, the Nusselt number increases up to a maximum and then decreases. Lakhal et al. [21] studied the transient natural convection in a square cavity partially heated from side. In the first, the temperature is varied sinusoidal with time while in the second; it varies with a pulsating manner. The results showed that the mean values of heat transfer and flow intensity are considerably different with those obtained in stationary regime. Le Quere et al [22] investigated the effect on the flow field and heat transfer of the Grashof number as it was varied from 10^4 to $3x10^7$; the temperature difference between the cavity walls and ambient changed from 50 to 500 K, the aspect ratio varied between 0.5 and 2, and the inclination angle of the cavity was modified from 0 to 45^o (for 0^o the wall opposite the aperture was vertical and the angles were taken clockwise). The results of the paper showed that the Nusselt number diminished with the increase in the inclination angle, and that the unsteadiness in the flow takes place for values of the Grashof number greater than 10^6 and inclination angles of 0^o. Showole and Tarasuk [32] investigated, experimentally and numerically, the natural steady state convection in a two dimensional isothermal open cavity. They obtained experimental results for air, varying the Rayleigh number from 10^4 to $5.5\ x10^5$, cavity aspect ratios of 0.25, 0.5 and 1.0, and inclination angles of 0, 30^o, 45^o and 60^o (for 0^o, the wall opposite the aperture was horizontal and the angles were taken clockwise). The numerical results were calculated for Rayleigh numbers between 10^4 and $5.5x10^5$, inclination angles of 0 and 45^o, and an aspect ratio equal to one. The results showed that, for all Rayleigh numbers, the first inclination of the cavity caused a significant increase in the average heat transfer rate, but a further increase in the inclination angle caused very little increase in the heat transfer rate. Another result observed was that, for 0^o, two symmetric counter rotating eddies were formed, while at inclination angles greater than 0^o, the symmetric flow and temperature patterns disappear.

Mohamad [25] studied numerically the natural convection in an inclined two-dimensional open cavity with one heated wall opposite the aperture and two adiabatic walls. The author analyzed the influence on fluid flow and heat transfer, with the inclination angle in the range 10^o-90^o (for 90^o the wall opposite the aperture was vertical and the angles were taken clockwise), the Rayleigh number from 10^3 to 10^7, and the aspect ratio between 0.5 and 2. The study concludes that the inclination angle did not have a significant effect on the average Nusselt number from the isothermal wall, but a substantial one on the local Nusselt number. Polat and Bilgen [31] made a numerical study of the conjugate heat transfer by conduction and natural convection in an inclined, open shallow cavity with a uniform heat flux in the wall opposite to the aperture. The parameters studied were: the Rayleigh number from 10^6 to 10^{12}, the conductivity ratio from 1 to 60, the cavity aspect ratio from 1 to 0.125, the dimensionless wall thickness from 0.05 to 0.20, and the inclination angle from 0 to 45^o from the horizontal (for 0^o, the wall opposite the aperture was vertical and the angles were taken counterclockwise).

Le Quere et al [22] investigated thermally driven laminar natural convection in enclosures with isothermal sides, one of which facing the opening. They used primitive variables and finite difference expressions suitable for treating problems with large temperature and density variations. The computational domain was an enlarged domain comprising a square open cavity and a far field surrounding it. Penot [29] studied a similar problem using stream function-vorticity formulation. He also used an enlarged computational domain similar to that of Le Quere et al [22] with approximate boundary conditions. Chan and Tien [4] studied numerically a square open cavity, which had an isothermal vertical heated side facing the opening and two adjoining adiabatic horizontal sides. The boundary conditions at far field were approximated to obtain satisfactory solutions in the open cavity. Chan and Tien [3] studied numerically shallow open cavities and also made a comparison study using a square cavity in an enlarged computational domain. They found that for a square open cavity having an isothermal vertical side facing the opening and two adjoining adiabatic horizontal sides, satisfactory heat transfer results could be obtained, especially at high Rayleigh numbers. In a similar way, Mohamad [25] studied inclined open square cavities, by considering a restricted computational domain. Different from those by Chan and Tien [4], gradients of both velocity components were set to zero at the opening plane. It was found that heat transfer was not sensitive to inclination angle and the flow was unstable at high Rayleigh

numbers and small inclinations angles. Polat and Bilgen [31] studied numerically inclined open shallow cavities in which the side facing the opening was heated by constant heat flux, two adjoining walls were insulated and the opening was in contact with a reservoir at constant temperature and pressure. The computational domain was restricted to the cavity.

The finite element method is one of the numerical methods that have received popularity due to its capability for solving complex structural problems (Cook, [6], Zienkiewicz,[37]. The method has been extended to solve problems in several fields such as in the field of heat transfer (Lewis et al., [23], Dechaumphai, [8]), electromagnetics (Jini, [17]), biomechanics (Gallagher et al., [13]), etc. In spite of the great success of the method in these fields, its application to fluid mechanics is still under intensive research. This is due to the fact that the governing differential equations for general flow problems consist of several coupled equations which are inherently nonlinear. Accurate numerical solutions thus require a vast amount of computer time and data storage. One-way to minimize the amount of computer time and data storage used is to employ an adaptive meshing technique (Dechaumphai, [8], Peraire et al., [30]). The technique places small elements in the regions of large change in the solution gradients to increase solution accuracy, and at the same time, uses large elements in the other regions to reduce the computational time and computer memory.

Goutam Saha et al [14] studied a numerical simulation of two-dimensional laminar steady-state natural convection in a square tilt open cavity. The opposite wall to the aperture was kept at either constant surface temperature or constant heat flux, while the surrounding fluid interacting with the aperture was maintained at an ambient temperature. The two remaining walls were assumed to be adiabatic. The fluid concerned is air with Prandtl number fixed at 0.71. The governing mass, momentum and energy equations are expressed in a normalized primitive variables formulation. A finite element method for steady-state incompressible natural convection flows has been developed. The streamlines and isotherms are produced, heat transfer characteristics is obtained for Rayleigh numbers from 10^3 to 10^6 and an inclination angles of the cavity ranges from 0º to 60º.

In experimental studies of Ozoe et al. [26], Arnold et al. [1], Linthorst et al. [24] and Hamady et al. (1989) found as the tilt angle changes from 0° to 90°, the heat transfer decreases until a minimum point was reached, and then gradually increases again and the

minimum point occurs at the angle where flow changes its mode from the three-dimensional roll pattern caused by the thermal instability to the two-dimensional circulation caused by the hydrodynamic effect. Most of these experimental researches only studied cavities with small to medium aspect ratios, with the maximum aspect ratio 15.5. In the study of Elsherbiny et al. [10], six aspect ratios between 5 and 110 were examined experimentally to find the influence of the tilt angle and the aspect ratio on the heat transfer rate. A correlation for tilt angle 60° was developed, and a suggestion of a straight-line interpolation between 60° and 90° was proposed. A lot of numerical studies were also performed. Most of them are two dimensional and only studied flow in an inclined square cavity, such as Ozoe et al. [27], Chen et al. [5], Kuyper et al. [20] and Zhong et al.[26]. However, these two-dimensional numerical studies could not work well at small tilt angles close to horizontal position. In the recent paper of Soong et al. [33], the same model of square cavity from Ozoe et al. [27] was studied with the imperfect constant wall temperature boundary conditions, and the results showed good agreement with the experimental curve even at small tilt angles.

In the present thesis a numerical analysis of two-dimensional laminar steady-state natural convection in a square open cavity have numerically been studied. A partially heated circular cylinder and square cylinder are placed at the center of the cavity and the opposite wall to the aperture is heated by a constant heat flux. The top and bottom walls have kept at the cooled with temperature and heated with temperature. The fluid is concerned with Prandtl number at 0.72, 1.0 and 7.0. The governing mass, momentum and energy equations are expressed in a normalized primitive variables formulation. In this thesis, a finite element method for steady-state incompressible natural convection flows has been developed. The streamlines and isotherms are produced; heat transfer characteristics are obtained for Grashof numbers from 10^3 to 10^6 and inclination angles of the cavity from 0º to 45º. The results show that the Nusselt number increases with the Grashof numbers. Also the Nusselt number has changed substantially with the inclination angle of the cavity while better thermal performance is also sensitive to the boundary condition of the heated wall.

1.3 Heat Transfer Mechanism

Heat is the form of energy that can be transferred from one system to another as a result of temperature difference. A thermodynamic analysis is concerned with the amount of heat transfer as a system undergoes a process from one equilibrium state to another. The

science that deals with the determination of the rates of such energy transfers is the heat transfer. The transfer of energy as heat is always from the higher temperature medium to the lower temperature one, and heat transfer stops when the two mediums reach the same temperature.

Heat can be transferred in three different mechanisms or modes: conduction, convection and radiation. All modes of heat transfer require the existence of a temperature difference, and all modes are from the high temperature medium to a lower temperature one. In reality, the combined effect of these three modes of heat transfer control temperature distribution in a medium. A brief description of convection mode is given below.

1.3.1 Convection

Convective heat transfer is the heat transfer mechanism affected by the flow of fluids. The amount of energy and matter are conveyed by the fluid can be predicted through the convective heat transfer. The convective heat transfer bifurcates into two branches; the natural convection and the forced convection. Forced convection regards the heat transport by induced fluid motion that is forced to happen. This induced flow needs consistent mechanical power. But natural convection differs from the forced convection through the fluid flow driving force that happens naturally. The flows are driven by the buoyancy effect due to the presence of density gradient and gravitational field. The density difference gives rise to buoyancy effects due to which the flow is generated. Buoyancy is due to the combined presence of the fluid density gradient and the body force. As the temperature distribution in the natural convection depends on the intensity of the fluid currents that is dependent on the temperature potential itself, the qualitative and quantitative analysis of natural convection heat transfer is very difficult. Numerical investigation instead of theoretical analysis is more needed in this field. Two types of natural convection heat transfer phenomena can be observed in the nature. One is that external free convection that is caused by the heat transfer interaction between a single wall and a very large fluid reservoir adjacent to the wall. Another is that internal free convection which befalls within an enclosure. The thermo-fluid fields developed inside the cavity depend on the orientation and geometry of the cavity. Reviewing the nature and the practical applications, the enclosure phenomena can be organized into two classes. One of these is enclosure heated from the side which is found in solar collectors, double wall insulations, laptop cooling system and air circulation inside the room and

another one is enclosure heated from below which happens in geophysical system like natural circulation in the atmosphere, the hydrosphere and the molten core of the earth.

Convective heat transfer or, simply, convection is the study of heat transport processes affected by the flow of fluids. Convective heat transfer, clearly, is a field at the interface between two older fields-heat transfer and fluid mechanics. Before reviewing the foundations of convective heat transfer methodology, it is worth reexamining the historic relationship between fluid mechanics and heat transfer at the interface. Especially during the past 100 years, heat transfer and fluid mechanics have enjoyed a symbiotic relationship in their parallel development. Convection is that mode of heat transfer where energy exchange occurs between the particles by convection current. It may be explained as; when fluid flows over a solid body or inside a channel while temperatures of the fluid and the solid surface are different, heat transfer between the fluid and the solid surface takes place as a consequences of the motion of the fluid relative to the surfaces; the mechanism of heat transfer called convection. In the diversity of the studies related to heat transfer, considerable effort has been directed at the convective mode, in which the relative motion of the fluid provides an additional mechanism for the transfer of heat and materials. Convection is inevitably coupled with the conductive mechanism, since though the fluid motion modifies the transport process, the eventual transfer of heat from one fluid element to another in its neighborhood is through conduction.

The convection mode of heat transfer is further divided into two basic processes. If the motion of the fluid arises due to an external agent, such as the externally imposed flow of fluid stream over a heated object, the process is termed as forced convection. The fluid flow may be the results of, for instance, a fan, a blower, the wind or the motion of the heated object itself. Such problems are very frequently encountered in technology where heat transfer to, or from, a body is often due to an imposed flow of a fluid at a temperature different from that of the body. It has wide applications in compact heat exchanger, central air conditioning system, cooling tower, gas turbine blade, internal cooling passage, chemical engineering process industries, nuclear reactors and many other cases. If, on the other hand, no such externally induced flow is provided and the flow arises “naturally” simply due to the effect of a density difference, resulting from a temperature difference, in a body force field, such as gravitational field, the process is termed as natural or free convection. The density deference gives rise to buoyancy effects due to which the flow is generated. A heated body cooling in ambient air

generates such a flow in the region surrounding it. Similarly, the buoyant flow arising from heat rejection to the atmosphere and to other ambient media, Heat transfer by free convection occurs in many engineering applications, such as heat transfer from hot radiators, refrigerator coils, transmission lines, electric transformers, electric heating elements and electronic equipment etc.

The convection heat transfer that is neither dominated by pure forced nor pure free convection, but is rather a combination of the two is referred as combined or mixed convection. The buoyancy forces that arise as the results of the temperature differences and which cause the fluid flow in free convection also exist when there is a forced flow. The effects of these buoyancy forces are however; usually negligible when there is a forced flow. In some cases, however, these buoyancy forces do have a significant influence on the flow and consequently on the heat transfer rate. In such cases, the flow about the body is a combination of forced and free convection; such flows are referred to as mixed convection. For example, heat transfer from one fluid to another fluid through the walls of pipe occurs in many practical devices. In this case, heat is transferred by convection from the hotter fluid to the one surface of the pipe. Heat is then transferred by conduction through the walls of the pipe. Finally, heat is transferred by convection from the other surface to the colder fluid.

1.3.2 Conduction

Conduction is the mode of heat transfer in which energy exchange takes place from the region of high temperature to that of law temperature by the kinetic motion or direct impact of molecules, as in the case of fluid at rest, and by the drift of electrons, as in the case of metals. In a solid which is a good electric conductor, a large number of free electrons move about in the lattice, hence materials that are good electric conductors are generally good heat conductors (i.e. copper, silver.etc).

1.3.3 Thermal Conductivity

Thermal conductivity of a material can be defined as the rate of heat transfer through a unit thickness of the material per unit area per unit temperature difference. Therefore the thermal conductivity of a material is a measure of the ability of the material to conduct heat. A high value for thermal conductivity indicates that the material is a good heat conductor, and a low value for thermal conductivity indicates that the material is a poor heat conductor or insulator. For example the materials such as copper and silver that are good electric conductors are also good heat conductors, and have high values of thermal

conductivity. Materials such as rubber, wood are poor conductors of heat and have low conductivity values. The rate of heat conduction through a medium depends on the geometry of the medium, its thickness, and the material of the medium, as well as the temperature difference across the medium. The proportionality constant k is called thermal conductivity of the material.

1.3.4 Thermal Diffusivity

The time dependent heat conduction equation for constant k contains a quantity α, called the thermal diffusivity. Thermal diffusivity represents how fast heat diffuses through a material and is defined as

$$\alpha = \frac{\kappa}{\rho C_p}$$

Here the thermal conductivity κ represents how well a material conducts heat, and the heat capacity ρCp represents how much energy a material stores per unit volume. Therefore, the thermal diffusivity of a material can be viewed as the ratio of the heat conducted through the material to the heat stored per unit volume. A material that has a high thermal conductivity or a low heat capacity will obviously have a large thermal diffusivity. The larger thermal diffusivity means that the propagation of heat into the medium is faster. A small value of thermal diffusivity means the material mostly absorbs the heat and a small amount of heat is conducted further.

1.3.5 Internal and External Flows

A fluid flow is classified as being internal or external, depending on whether the fluid is forced to flow in a confined channel or over a surface. An internal flow is bounded on all sides by solid surfaces except, possibly, for an inlet and exit. Flows through a pipe or in an air-conditioning duct are the examples of internal flow. Internal flows are dominated by the influence of viscosity throughout the flow field. The internal flow configuration represents a convenient geometry for the heating and cooling of fluids used in the chemical processing, environmental control, and energy conversion areas. The flow of an unbounded fluid over a surface is external flow. The flows over curved surfaces such as sphere, cylinder, airfoil, or turbine blade are the example of external flow. In external flows the viscous effects are limited to boundary layers near solid surfaces.

1.3.6 Boundary Layer

Since fluid motion is the distinguishing feature of heat convection, it is necessary to understand some of the principles of fluid dynamics in order to describe adequately the processes of convection. When a fluid flows over a body, the velocity and temperature distribution at the immediate vicinity of the surface strongly influence by the convective heat transfer. In order to simplify the analysis of convective heat transfer the boundary layer concept frequently is introduced to model the velocity and temperature fields near the solid surface in order to simplify the analysis of convective heat transfer. So we are concerned with two different kinds of boundary layers, the velocity boundary layer and the thermal boundary layer.

The velocity boundary layer is defined as the narrow region, near the solid surface, over which velocity gradients and shear stresses are large, but in the region outside the boundary layer, called the potential-flow region, the velocity gradients and shear stresses are negligible. The exact limit of the boundary layer cannot be precisely defined because of the asymptotic nature of the velocity variation. The limit of the boundary layer is usually taken to be at the distance from the surface, at which the fluid velocity is equal to a predetermined percentage of the free stream value, U_∞. This percentage depends on the accuracy desired, 99 or 95% being customary. Although, outside the boundary layer region the flow is assumed to be inviscid, but inside the boundary layer the viscous flow may be either laminar or turbulent. In the case of laminar boundary layer, fluid motion is highly ordered and it is possible to identify streamlines along which particles move. Fluid motion along a streamline is characterized by velocity components in both the x and y directions. Since the velocity component v is in the direction normal to the surface, it can contribute significantly to the transfer of momentum, energy or species through the boundary layer. Fluid motion normal to the surface is necessitated by boundary layer growth in the x direction. In contrast, fluid motion in the turbulent boundary layer is highly irregular and is characterized by velocity fluctuations. These fluctuations enhance the transfer of momentum, energy and species and hence increase surface friction, as well as convection transfer rates. Due to fluid mixing resulting from the fluctuations, turbulent boundary layer thicknesses are larger and boundary layer profiles are flatter than in laminar flow. The thermal boundary layer may be defined (in the same sense that the velocity boundary layer was defined above) as the narrow region between the surface and the point at which the fluid temperature has reached a certain percentage of ambient

temperature T_∞. Outside the thermal boundary layer the fluid is assumed to be a heat sink at a uniform temperature of T_∞. The thermal boundary layer is generally not coincident with the velocity boundary layer, although it is certainly dependent on it. If the fluid has high thermal conductivity, it will be thicker than the velocity boundary layer, and if conductivity is low, it will be thinner than the velocity boundary layer.

1.3.7 Flow within an Enclosure

The flow within an enclosure consisting of two horizontal walls, at different temperatures, is an important circumstance encountered quite frequently in practice. In all the applications having this kind of situation, heat transfer occurs due to the temperature difference across the fluid layer, one horizontal solid surface being at a temperature higher than the other. If the upper plate is the hot surface, then the lower surface has heavier fluid and by virtue of buoyancy the fluid would not come to the lower plate. Because in this case the heat transfer mode is restricted to only conduction. But if the fluid is enclosed between two horizontal surfaces of which the upper surface is at lower temperature, there will be the existence of cellular natural convective currents which are called as Benard cells. For fluids whose density decreases with increasing temperature, this leads to an unstable situation.

1.3.8 Slanted Enclosure

The tilted enclosure geometry has received considerable attention in the heat transfer literature because of mostly growing interest of solar collector technology. The angle of tilt has a dramatic impact on the flow housed by the enclosure. Consider an enclosure heated from below is rotated about a reference axis. When the tilted angle becomes 90º, the flow and thermal fields inside the enclosure experience the heating from side condition. Thereby convective currents may pronounce over the diffusive currents. When the enclosure rotates to 180º, the heat transfer mechanism switches to the diffusion because the top wall is heated.

1.3.9 Boussinesq Approximation

The governing equations for convection flow are coupled elliptic partial differential equations and are, therefore, of considerable complexity. The major problems in obtaining a solution to these equations lie in the inevitable variation of density with temperature, or concentration, and in their partial, elliptic nature. Several approximations are generally made to considerably simplify these equations. Among them Boussinesq

approximation attributed to Boussinesq (1903) is considered here. In flows accompanied by heat transfer, the fluid properties are normally functions of temperature. The variations may be small and yet be the cause of the fluid motion. If the density variation is not large, one may treat the density as constant in the unsteady and convection terms, and treat it as variable only in the gravitational term. This is called the Boussinesq approximation.

1.4 Dimensionless Parameters

The dimensionless parameters can be thought of as measures of the relative importance of certain aspects of the flow. Some dimensionless parameters related to our study are discussed below:

Grashof number *Gr*

The flow regime in free convection is governed by the dimensionless Grashof number, which represent the ratio of the buoyancy force to the viscous forces acting on the fluid, and is defined as

$$Gr = \frac{g\beta L^3 \left(T_w - T_\infty\right)}{\nu^2}$$

where g is the acceleration due to gravity, β is the volumetric thermal expansion coefficient, T_w is the wall temperature, T_∞ is the ambient temperature, L is the characteristic length and ν is the kinematics viscosity. The Grashof number Gr plays same role in free convection as the Reynolds number Re plays in forced convection. As such, the Grashof number provides the main criterion in determining whether the fluid flow is laminar or turbulent in free convection. For vertical plates, the critical value of the Grashof number is observed to be about 10^9. Therefore, the flow regime on a vertical plate becomes turbulent at Grashof numbers greater than10^9.

Prandtl Number *Pr*

The relative thickness of the velocity and the thermal boundary layers is best described by the dimensionless parameter Prandtl number, defined as

Pr = Molecular diffusivity of momentum / Molecular diffusivity of heat = $\boldsymbol{\upsilon / \alpha}$

It is named after Ludwig Prandtl, who introduced the concept of boundary layer in 1904 and made significant contributions to boundary layer theory. The Prandtl numbers of

fluids range from less than 0.01 for liquid metals to more than 100,000 for heavy oils. Note that the Prandtl number is in the order of 7 for water. The Prandtl numbers of gases are about 1, which indicates that both momentum and heat dissipate through the fluid at about the same rate. Consequently the thermal boundary layer is much thicker for liquid metals and much thinner for oils relative to the velocity boundary layer.

Nusselt Number *Nu*

The Nusselt number represents the enhancement of heat transfer through a fluid layer as a result of convection relative to conduction across the same fluid layer, and is defined as

$$Nu = hL / k$$

where k is the thermal conductivity of the fluid, h is the heat transfer coefficient and L is the characteristics length. The Nusselt number is named after Wilhelm Nusselt, who made significant contributions to convective heat transfer in the first half of the twentieth century, and it is viewed as the dimensionless convection heat transfer coefficient. The larger Nusselt number indicates a large temperature gradient at the surface and hence, high heat transfer by convection. A Nusselt number of $Nu = 1$, for a fluid layer represents heat transfer across the layer by pure conduction. To understand the physical significance of the Nusselt number, consider the following daily life problems. We remedy to forced convection whenever we want to increase the rate of heat transfer from a hot object. In free convection flow velocities are produced by the buoyancy forces hence there are no externally induced flow velocities.

1.5 Enthusiasm Behind The Selection of Current Work

From the historical review it is clear that during the past two decades, several experiments and numerical calculations have been presented for describing the phenomenon of natural convection in open cavities. Those studies have been focused to study the effect on flow and heat transfer for different Rayleigh numbers, aspect ratios, and tilt angles. Natural convection in open cavities has received considerable attention because of its importance in several thermal engineering problems, for example, in the design of electronic devices, solar thermal receivers, uncovered flat plate solar collectors having rows of vertical strips, geothermal reservoirs, etc. In the present thesis a numerical analysis of two-dimensional laminar steady-state natural convection in a square open cavity has numerically studied. A partially heated circular cylinder is placed at the center of the cavity and the opposite wall to the aperture by a constant iso-flux heat

source. The top and bottom walls have kept at the cooled with temperature and heated with temperature. In this thesis, a finite element method for steady-state incompressible natural convection flows has been developed. Numerical studies are therefore essential to observe the variation in fluid flow and heat transfer due to the above physical changes with boundary conditions, which forms the basis of the motivation behind the present study.

1.6 Main Objectives of The Present Study

The present study has focused on the development of a mathematical model and numerical techniques regarding the effects of natural convection flow around a partially heated circular cylinder placed in a square open cavity.

The specific objectives of the present research work are as follows:

- A mathematical model regarding the effect of natural convection flow around a partially heated circular cylinder placed in a square open cavity have been developed.
- To visualize the fluid flow and temperature distribution inside the enclosure in terms of streamline and isotherm plots.
- The analytical model has numerically solved using finite element method.
- To investigate the effects of Grashof number and Prandtl number on the heat transfer characteristics (Nusselt number).
- To investigate the effects of diameter ratio of a partially heated cylinder on natural convection placed inside an open cavity.
- To carry out the validation of the present finite element model by investigating the effect of natural convection heat transfer in a square open cavity.
- To examine the effects of inclination angles of the enclosure on the heat transfer characteristics.

1.7 Outline of The Thesis

This dissertation contains five chapters. In this chapter a brief introduction is presented with aim and objective. This chapter also consists of a literature review of the past studies on fluid flow and heat transfer in cavities or channels. The different aspects of the previous studies have been mentioned categorically. This is followed by the post-mortem of a recent historical event for the illustration of fluid flow and heat transfer effects in cavities or channels.

CHAPTER 1

Chapter 2, the computational technique of the problem have discussed for viscous incompressible flow.

In Chapter 3, a detailed parametric study on Numerical simulation of two-dimensional laminar steady-state natural convection in a tilted square open cavity with a partially heated circular cylinder is placed at the center. Effects of the major parameters such as Grashof number and Prandtl number, and of different angles of the cavity and different diameter ratio of the cylinder have been presented for a better understanding of the heat transfer mechanisms in square open cavity. The results of isotherms and streamlines for Grashof number, Prandtl number, different angle of the cavity and different diameter ratio of the cylinder with natural convection have been studied.

In Chapter 4, I have discussed a same type of problem using a partially heated square cylinder instead of a partially heated circular cylinder in an open square cavity. I have also discussed the result of isotherms and streamlines of different parameters (Grashof number Gr and Prandtl number Pr) and different angles of cavity and different aspect ratio of the partially heated square cylinder.

Finally, in Chapter 5 the study is rounded of with the conclusions, comparison of both cylinders and recommendations for further study of the present problem are outlined.

CHAPTER 2
COMPUTATIONAL TECHNIQUE

Computational Technique

Computational fluid dynamics (CFD) has been rapidly gaining popularity over the past several years for technological as well as scientific interests. For many problems of industrial interest, experimental techniques are extremely expensive or even impossible due to the complex nature of the flow configuration. Analytical methods are often useful in studying the basic physics involved in a certain flow problem, however, in many interesting problems; these methods have limited direct applicability. The dramatic increase in computational power over the past several years has led to a heightened interest in numerical simulations as a cost effective method of providing additional flow information, not readily available from experiments, for industrial applications, as well as a complementary tool in the investigation of the fundamental physics of turbulent flows, where analytical solutions have so far been unattainable. It is not expected (or advocated), however, that numerical simulations replace theory or experiment, but that they be used in conjunction with these other methods to provide a more complete understanding of the physical problem at hand.

Mathematical model of physical phenomena may be ordinary or partial differential equations, which have been the subject of analytical and numerical investigations. The partial differential equations of fluid mechanics and heat transfer are solvable for only a limited number of flows. To obtain an approximate solution numerically, we have to use a discretization method, which approximated the differential equations by a system of algebraic equations, which can then be solved on a computer. The approximations are applied to small domains in space and / or time so the numerical solution provides results at discrete locations in space and time. Much as the accuracy of experimental data depends on the quality of the tools used, the accuracy of numerical solutions depend on the quality of discretizations used.Computational fluid dynamics (CFD) computation involves the formation of a set numbers that constitutes a practical approximation of a real life system. The outcome of computation process improves the understanding of the performance of a system. Thereby, engineers need CFD codes that can make physically realistic results with good quality accuracy in simulations with finite grids. Contained within the broad field of computational fluid dynamics are activities that cover the range from the automation of well established engineering design methods to the use of

detailed solutions of the Navier-Stokes equations as substitutes for experimental research into the nature of complex flows. CFD have been used for solving wide range of fluid dynamics problem. It is more frequently used in fields of engineering where the geometry is complicated or some important feature that cannot be dealt with standard methods. More details are available in Ferziger & Perić [12] and Patankar [28].

2.1 Elements of Numerical Solution Methods

Several components of numerical solution methods are available in Ferziger and Perić [12], here only the main steps will be demonstrate in the following.

2.1.1 Mathematical Model

The starting point of any numerical method is the mathematical model, i.e. the set of partial differential equations and boundary conditions. A solution method is usually designed for a particular set of equations. Trying to produce a general-purpose solution method, i.e. one which is applicable to all flows, is impractical, is not impossible and as with most general purpose tools, they are usually not optimum for any one application.

2.1.2 Discretization Process

After selecting the mathematical model, one has to choose a suitable discretization method, i.e. a method of approximating the differential equations by a system of algebraic equations for the variable at some set of discrete locations in space and time.

2.1.3 Numerical Grid

The numerical grid defines the discrete locations, at which the variables are to be calculated, which is essentially a discrete representation of the geometric domain on which the problem is to be solved. It divided the solution domain into a finite number of sub-domains (elements, control volumes etc). Some of the options available are structural (regular) grid, block structured grid, unstructured grids etc.

2.1.4 Finite Approximations

Following the choice of grid type, one has to select the approximations to be used in the discretization process. In a finite difference method, approximations for the derivatives at the grid points have to be selected. In a finite volume method, one has to select the methods of approximating surface and volume integrals. In a finite element method, one has to choose the functions and weighting functions.

2.1.5 Solution Technique

Discretization yields a large system of non-linear algebraic equations. The method of solution depends on the problem. For unsteady flows, methods based on those used for initial value problems for ordinary differential equation (marching in time) is used. At each time step an elliptic problem has to be solved. Pseudo-time marching or an equivalent iteration scheme usually solves steady flow problems. Since the equations are non-linear, an iteration scheme is used to solve them. These methods use successive linearization of the equations and the resulting linear systems are almost always solved by iterative techniques. The choice of solver depends on the grid type and the number of nodes involved in each algebraic equation.

2.2 Discretization Approaches

The first step to numerically solve a mathematical model of physical phenomena is its numerical discretization. This means that each component of the differential equations is transformed into a “numerical analogue” which can be represented in the computer and then processed by a computer program, built on some algorithm. There are many different methodologies were devised for this purpose in the past and the development still continues. In order to short them, we can at first divide the spatial discretisation schemes into the following three main categories: finite difference (FD), finite volume (FV) finite element (FE) methods, Boundary element (BE) method and Boundary volume (BV) method.

In the present numerical computation, Galerkin finite element method (FEM) is used. Detailed discussion of this method is available in Chung [7] and Dechaumphai [9].

Finite Element Analysis

The finite element method (FEM) is a powerful computational method for solving problems, which are described by partial differential equations. The fundamental idea of the finite element method is to outlook a given domain as an assemblage of simple geometric shapes, called finite elements, for which it is possible to systematically generate the approximation functions needed in the solution of partial differential equations by the weighted residual method. The computational domains with irregular geometries by a collection of finite elements makes the method a valuable practical tool for the solution of boundary value problems arising in various fields of engineering. The approximation functions, which satisfy the governing equations and boundary

conditions, are often constructed using ideas from interpolation theory. Approximating functions in finite elements are determined in terms of nodal values of a physical field, which is required. A continuous physical problem is transformed into a discretized finite element problem with unknown nodal values. For a linear problem, a system of linear algebraic equations should be solved. Values inside finite elements can be recovered using nodal values.

The finite element method is one of the numerical methods that have received popularity due to its capability for solving complex structural problems. The method has been extended to solve problems in several other fields such as in the field of heat transfer, computational fluid dynamics, electromagnetic, biomechanics etc. In spite of the great success of the method in these fields, its application to fluid mechanics, particularly to convective viscous flows, is still under intensive research.

The major steps involved in finite element analysis of a typical problem are:

1. Discretization of the domain into a set of finite elements (mesh generation).
2. Weighted-integral or weak formulation of the differential equation to be analyzed.
3. Development of the finite element model of the problem using its weighted-integral or weak form.
4. Assembly of finite elements to obtain the global system of algebraic equations.
5. Imposition of boundary conditions.
6. Solution of equations.
7. Post-computation of solution and quantities of interest.

2.2.1 Mesh Generation

The area of numerical grid generation is relatively young in practice, although its roots in mathematics are old. The arrangement of discrete points throughout the flow field is simply called a grid. The determination of a proper grid for the flow through a given geometric shape is important. The way that such a grid is determined is called grid generation. The grid generation is a significant consideration in CFD. Finite element method can be applied to unstructured grids. This is because the governing equations in this method are written in integral form and numerical integration can be carried out directly on the unstructured grid domain in which no coordinate transformation is required. A two-dimensional domain may be triangulated as shown in Figure 2.1. In

finite element method, the mesh generation is the technique to subdivide a domain into a set of sub-domains, called finite elements. Figure 2.1 shows a domain, Λ is subdivided into a set of sub-domains, Λ^e with boundary Γ^e. Detailed discussion of this issue is available in Anderson and Chung [7].

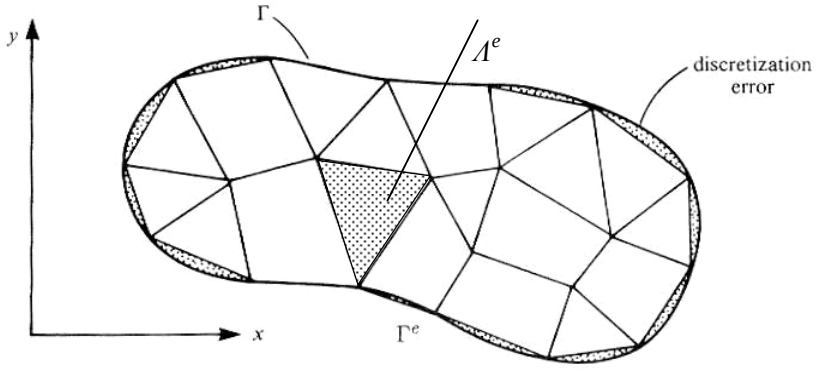

Figure 2.1: A typical FE discretization of a domain, Reddy & Gartling [32].

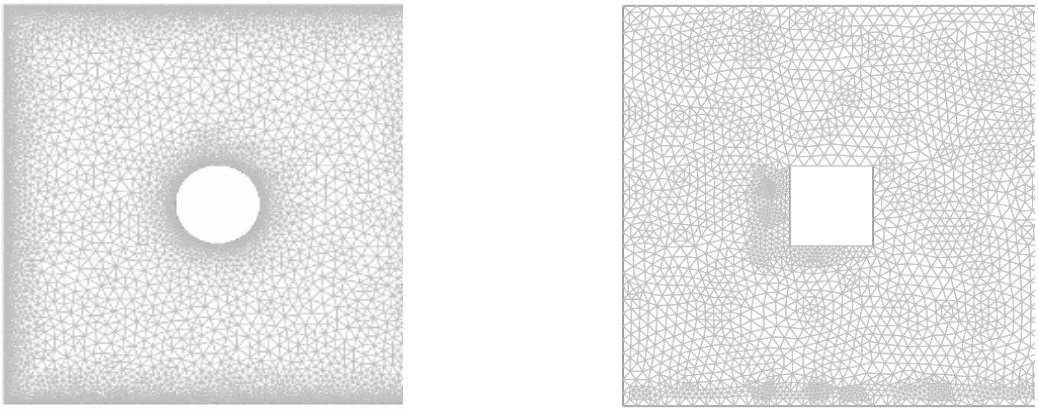

Figure 2.2: Current mesh structure of elements for square open cavity.

2.2.2 Finite Element Formulation and Computational Technique

Viscous incompressible thermal flows have been the subject of our investigation. The problem is relatively complex due to the coupling between the energy equation and the Navier-Stokes equations, which govern the fluid motion. These equations comprise a set of coupled nonlinear partial differential equations, which is difficult to solve especially with complicated geometries and boundary conditions. The finite element formulation and computational procedure for Navier-Stokes equations along with energy equations will be discuss in the chapter 3.

2.2.3 Algorithm

The algorithm was originally put forward by the iterative Newton-Raphson algorithm; the discrete forms of the continuity, momentum and energy equations are solved to find out the value of the velocity and the temperature. It is essential to guess the initial values of the variables. Then the numerical solutions of the variables are obtained while the convergent criterion is fulfilled. The simple algorithm is shown by the flow chart below.

CHAPTER 2

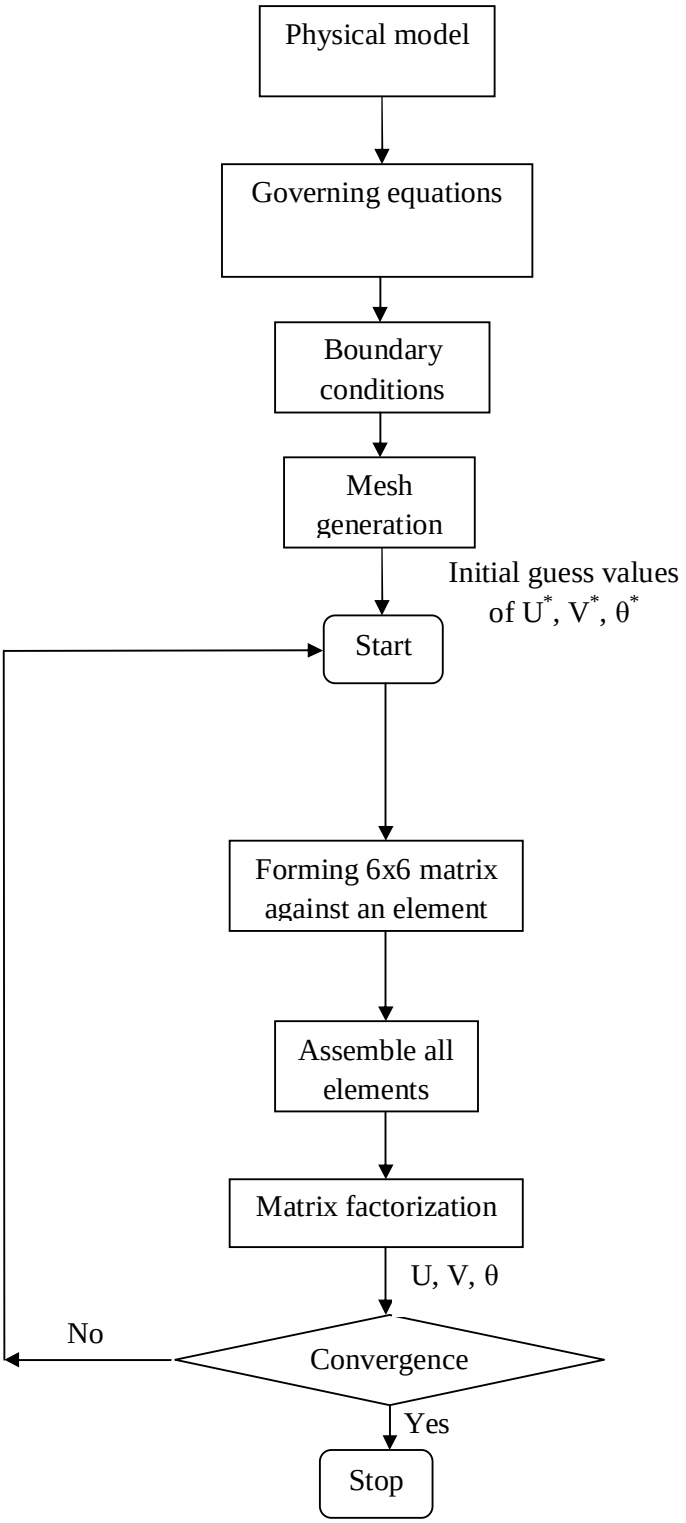

Figure 2.3: Flow chart of the computational procedure

2.2.4 Solution of System of Equations

A system of linear algebraic equations has been solved by the UMFPACK with COMSOL MULTIPHYSICS package interface. UMFPACK is a set of routines for solving asymmetric sparse linear systems Ax = b, using the Asymmetric MultiFrontal method and direct sparse LU factorization. Five primary UMFPACK routines are required to factorize A or Ax = b:

1. Pre-orders the columns of A to reduce fill-in and performs a symbolic analysis.
2. Numerically scales and then factorizes a sparse matrix.
3. Solves a sparse linear system using the numeric factorization.
4. Frees the Symbolic object.
5. Frees the Numeric object.

Additional routines are:

1. Passing a different column ordering
2. Changing default parameters
3. Manipulating sparse matrices
4. Getting LU factors
5. Solving the LU factors
6. Computing determinant

UMFPACK factorizes PAQ, PRAQ, or $PR^{-1}AQ$ into the product LU, where L and U are lower and upper triangular, respectively, P and Q are permutation matrices, and R is a diagonal matrix of row scaling factors (or R = I if row-scaling is not used). Both P and Q are chosen to reduce fill-in (new nonzeros in L and U that are not present in A). The permutation P has the dual role of reducing fill-in and maintaining numerical accuracy (via relaxed partial pivoting and row interchanges). The sparse matrix A can be square or rectangular, singular or non-singular, and real or complex (or any combination). Only square matrices A can be used to solve Ax = b or related systems. Rectangular matrices can only be factorized. UMFPACK first finds a column pre-ordering that reduces fill-in, without regard to numerical values. It scales and analyzes the matrix, and then automatically selects one of three strategies for pre-ordering the rows and columns: asymmetric, 2-by-2 and symmetric. These strategies are described below.

One notable attribute of the UMFPACK is that whenever a matrix is factored, the factorization is stored as a part of the original matrix so that further operations on the

matrix can reuse this factorization. Whenever a factorization or decomposition is calculated, it is preserved as a list (element) in the factor slot of the original object. In this way a sequence of operations, such as determining the condition number of a matrix and then solving a linear system based on the matrix, do not require multiple factorizations of the intermediate results.

Conceptually, the simplest representation of a sparse matrix is as a triplet of an integer vector **i** giving the row numbers, an integer vector **j** giving the column numbers, and a numeric vector **x** giving the non-zero values in the matrix. The triplet representation is row-oriented if elements in the same row were adjacent and column-oriented if elements in the same column were adjacent. The compressed sparse row (csr) or compressed sparse column (csc) representation is similar to row-oriented triplet or column-oriented triplet respectively. These compressed representations remove the redundant row or column in indices and provide faster access to a given location in the matrix.

2.3 Chapter Summary

This chapter has presented an introduction to computational method with advantages of numerical investigation. Because numerical method has played a central role in this thesis. Various components of numerical method have been also explained. Finally, the major steps involved in finite element analysis of a typical problem have been discussed.

CHAPTER 3

Numerical Analysis of Two Dimentional Laminar Steady-State Natural Convection Flow in a Tilted Open Square Cavity Having Partially Heated Circular Cylinder

3.1 Problem Definition

The heat transfer and the fluid flow in a two-dimensional open square cavity of length L was considered, as shown in the schematic diagram of figure3.1. The opposite wall to the aperture was first kept to constant heat flux q, while the surrounding fluid interacting with the aperture was maintained to an ambient temperature T_∞. The other two remaining walls were kept cooled with temperature T_c (Top wall) and heated with temperature T_h (bottom wall). The remaining circular cylinder was assumed to be partially heated. The fluid was assumed with Prandtl number (*Pr* = 0.72, 1.0, 7.0) and Newtonian, and the fluid flow is considered to be laminar. The properties of the fluid were assumed to be constant.

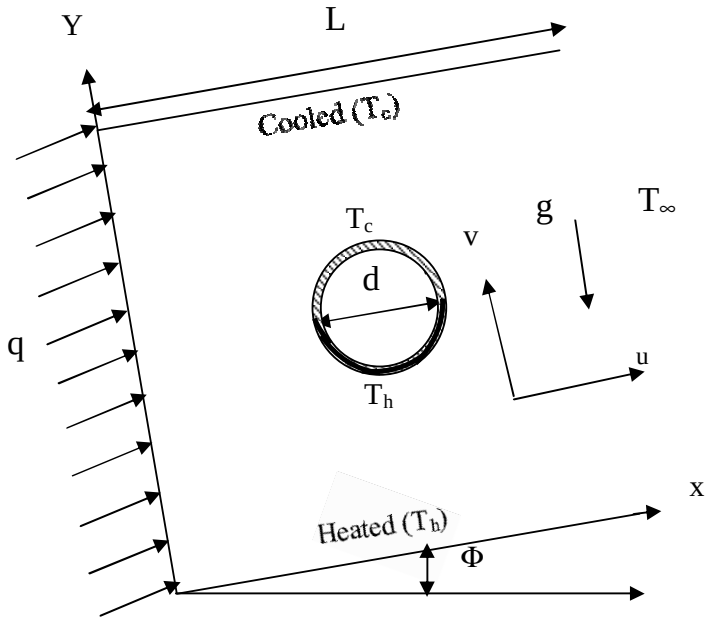

Figure-3.1. Schematic diagram of the physical system

3.2 Mathematical Modeling

The several steps of the mathematical formulation for the above physical configurations are shown as follows

CHAPTER 3

3.2.1 Governing Equations

Natural convection is governed by the differential equations expressing conservation of mass, momentum and energy. The present flow is considered steady, laminar, incompressible and two-dimensional. The viscous dissipation term in the energy equation is neglected. The Boussinesq approximation is invoking for the fluid properties to relate density changes to temperature changes, and to couple in this way the temperature field to the flow field. The governing equations for steady natural convection flow can be written as:

Continuity Equation

$$\frac{\partial \mathrm{u}}{\partial \mathrm{x}} + \frac{\partial \mathrm{u}}{\partial \mathrm{y}} = 0 \tag{1}$$

Momentum Equations

$$u\frac{\partial u}{\partial x} + v\frac{\partial u}{\partial y} = -\frac{1}{\rho}\frac{\partial p}{\partial x} + \gamma \left(\frac{\partial^2 u}{\partial x^2} + \frac{\partial^2 u}{\partial y^2}\right) + g \quad \beta \quad \left(T - T_\infty\right) \quad \sin\Phi \tag{2}$$

$$u\frac{\partial v}{\partial x} + v\frac{\partial v}{\partial y} = -\frac{1}{\rho}\frac{\partial p}{\partial y} + \gamma \left(\frac{\partial^2 v}{\partial x^2} + \frac{\partial^2 v}{\partial y^2}\right) + g \quad \beta \quad \left(T - T_\infty\right) \quad \cos\Phi \tag{3}$$

Energy Equation

$$u\frac{\partial T}{\partial x} + v\frac{\partial T}{\partial y} = \alpha \left(\frac{\partial^2 T}{\partial x^2} + \frac{\partial^2 T}{\partial y^2}\right) \tag{4}$$

3.2.2 Boundary Conditions

The boundary conditions for the present problem are specified as follows:

On the left wall (x = 0): u = v= 0 , $\frac{\partial T(0, y)}{\partial x} = -\frac{q}{k}$

On the right wall (x = 1): u = v = 0, $T_{in} = T_\infty$, $\frac{\partial T}{\partial x}(L, y) = 0$

On the bottom wall (y = 0): u = v = 0, $T = T_h$

On the Upper wall (y = 1): u = v = 0, T = T_c

On the cylinder,

At the bottom side: u = v = 0, $T = T_h$

At the upper side: u = v = 0, T = T_c

where x and y are the distances measured along the horizontal and vertical directions, respectively; u and v are the velocity components in the x- and y-direction, respectively; T denotes the temperature; γ and α are the kinematics viscosity and the thermal diffusivity, respectively; p is the pressure and ρ is the density; T_h ,T_c and T_∞ are heated, cooled and ambient temperatures respectively.

3.2.3 Dimensional Analysis

The governing equations in non-dimensional form are written as follows:

Continuity Equation

$$\frac{\partial \mathrm{U}}{\partial \mathrm{X}} + \frac{\partial \mathrm{V}}{\partial \mathrm{Y}} = 0 \tag{5}$$

Momentum Equations

$$U\frac{\partial U}{\partial X} + V\frac{\partial U}{\partial Y} = -\frac{\partial P}{\partial X} + \frac{1}{\sqrt{Gr}}\left(\frac{\partial^2 U}{\partial X^2} + \frac{\partial^2 U}{\partial Y^2}\right) + \theta \sin\Phi \tag{6}$$

$$U\frac{\partial V}{\partial X} + V\frac{\partial V}{\partial Y} = -\frac{\partial P}{\partial Y} + \frac{1}{\sqrt{Gr}}\left(\frac{\partial^2 V}{\partial X^2} + \frac{\partial^2 V}{\partial Y^2}\right) + \theta \cos\Phi \tag{7}$$

Energy Equation

$$U\frac{\partial \theta}{\partial X} + V\frac{\partial \theta}{\partial Y} = \frac{1}{\mathrm{Pr}\sqrt{Gr}}\left(\frac{\partial^2 \theta}{\partial X^2} + \frac{\partial^2 \theta}{\partial Y^2}\right) \tag{8}$$

Equations (5)-(8) were non-dimensional using the following dimensionless scales:

CHAPTER 3

$$X = \frac{x}{L},\ Y = \frac{y}{L},\ U = \frac{u}{U_o},\ V = \frac{v}{U_o},\ P = \frac{p - p_\infty}{\rho U_o^2},\ \theta = \frac{T - T_c}{\Delta t}$$

$$= \frac{\nu}{\alpha},\ Gr = \frac{g\,\beta\,\Delta t\,L^3}{\nu^2},\ dr = \frac{D}{L},\ \Delta t = (T_h - T_c),\ \Delta t = \frac{q\,L}{k}$$

Here Gr and Pr are Grashof and Prandtl numbers, respectively. The Grashof number represents the ratio of the buoyancy force to the viscous force acting on the fluid. The reference velocity U_o is related to the buoyancy force term and is defined as

$$U_o = \sqrt{g\,\beta\,L\,(T_h - T_c)}.$$

The Nusselt number (Nu) is one of the important dimensionless parameters to be computed for heat transfer analysis in natural convection flow. Also the Nusselt number for free convection is a function of the Grashof number only. The local Nusselt number can be obtained from the temperature field by applying

$$Nu = \frac{1}{\theta(x,0)}dx$$

and the average or overall Nusselt number was calculated by integrating the temperature gradient over the heated wall as

$$Nu_{av} = \int_0^1 \frac{1}{\theta(x,0)}dx$$

with the boundary conditions

On the left wall (X = 0): U = V= 0 , $\frac{\partial\theta(0,Y)}{\partial X} = -1$

On the right wall (X = 1): U = V = 0, θ(1,Y) = 0 if U < 0 and $\frac{\partial\theta}{\partial X}(1,Y) = 0$ if U > 0

On the bottom wall (Y = 0): U = V = 0, θ = 1

On the Upper wall (Y = 1): U = V = 0, θ = 0

On the cylinder,

At the bottom side: U = V = 0, $\theta = 1$

At the upper side: U = V = 0, $\theta = 0$

3.3 Numerical Analysis

The governing equations along with the boundary conditions are solved numerically, employing Galerkin weighted residual finite element techniques discussed below.

3.3.1 Finite Element Formulation and Computational Technique

The numerical procedure used to solve the governing equations for the present work is based on the Galerkin weighted residual method of finite-element formulation. The non-linear parametric solution method is chosen to solve the governing equations. This approach will result in substantially fast convergence assurance. A non-uniform triangular mesh arrangement is implemented in the present investigation especially near the walls to capture the rapid changes in the dependent variables.

The velocity and thermal energy equations (5)-(8) result in a set of non-linear coupled equations for which an iterative scheme is adopted. To ensure convergence of the numerical algorithm the following criteria is applied to all dependent variables over the solution domain

$$\sum \left| \psi_{ij}^{n} - \psi_{ij}^{n-1} \right| \leq 10^{-5}$$

where Ψ represents a dependent variable U, V, P, and T; the indexes i, j indicate a grid point; and the index n is the current iteration at the grid level. The six node triangular element is used in this work for the development of the finite element equations. All six nodes are associated with velocities as well as temperature; only the corner nodes are associated with pressure. This means that a lower order polynomial is chosen for pressure and which is satisfied through continuity equation. The velocity component and the temperature distributions and linear interpolation for the pressure distribution according to their highest derivative orders in the differential Eqs (5)-(8) as

$$U(X,Y) = N_\alpha U_\alpha \tag{9}$$

$$V(X,Y) = N_\alpha V_\alpha \tag{10}$$

CHAPTER 3

$$\theta(X,\ Y) = N_\alpha \quad \theta_\alpha \tag{11}$$

$$\mathrm{P}(\mathrm{X},\mathrm{Y}) = \mathrm{H}_\lambda\, \mathrm{P}_\lambda \tag{12}$$

where α = 1, 2, … …, 6; λ= 1, 2, 3; N_α are the element interpolation functions for the velocity components and the temperature, and H_λ are the element interpolation functions for the pressure.

To derive the finite element equations, the method of weighted residuals (Zienkiewicz, [37]) is applied to the continuity Eq. (5), the momentum Eqs (6)-(7), and the energy Eq. (8), we get

$$\int_{\mathrm{A}} \mathrm{N}\alpha\left(\frac{\partial \mathrm{U}}{\partial \mathrm{X}} + \frac{\partial \mathrm{V}}{\partial \mathrm{Y}}\right)\mathrm{dA} = 0 \tag{13}$$

$$\begin{aligned}\int_A N_\alpha\left(U\frac{\partial U}{\partial X} + V\frac{\partial U}{\partial Y}\right)\ dA &= -\int_A H_\lambda\left(\frac{\partial P}{\partial X}\right)\ dA \\ &+ \frac{1}{\sqrt{Gr}}\ \int_A N_\alpha\left(\frac{\partial^2 U}{\partial X^2} + \frac{\partial^2 U}{\partial Y^2}\right)\ dA + \int_A N_\alpha(\sin\Phi)\theta dA\end{aligned} \tag{14}$$

$$\begin{aligned}\int_A N_\alpha\left(U\frac{\partial V}{\partial X} + V\frac{\partial V}{\partial Y}\right)\ dA &= -\int_A H_\lambda\left(\frac{\partial P}{\partial Y}\right)\ dA \\ &+ \frac{1}{\sqrt{Gr}}\int_A N_\alpha\left(\frac{\partial^2 V}{\partial X^2} + \frac{\partial^2 V}{\partial Y^2}\right)dA + \int_A N_\alpha(\cos\Phi)\theta dA\end{aligned} \tag{15}$$

$$\int_A N_\alpha\ \left(U\frac{\partial \theta}{\partial X} + V\frac{\partial \theta}{\partial Y}\right)\ dA = \frac{1}{\mathrm{Pr}\sqrt{Gr}}\ \int_A N_\alpha\ \left(\frac{\partial^2 \theta}{\partial X^2} + \frac{\partial^2 \theta}{\partial Y^2}\right)\ dA \tag{16}$$

where A is the element area. Gauss's theorem is then applied to Eqs (14)-(16) to generate the boundary integral terms associated with the surface tractions and heat flux. Then Eqs (14)-(16) become,

$$\begin{aligned}&\int_A N_\alpha\left(U\frac{\partial U}{\partial X} + V\frac{\partial U}{\partial Y}\right)\ dA + \int_A H_\lambda\left(\frac{\partial P}{\partial X}\right)\ dA + \\ &\frac{1}{\sqrt{Gr}}\int_A\left(\frac{\partial N_\alpha}{\partial X}\frac{\partial U}{\partial X} + \frac{\partial N_\alpha}{\partial Y}\frac{\partial U}{\partial Y}\right)dA - \int_A \sin\Phi N_\alpha\theta dA = \int_{S_0} N_\alpha S_x dS_0\end{aligned} \tag{17}$$

CHAPTER 3

$$\int_A N_\alpha \left(U\frac{\partial V}{\partial X} + V\frac{\partial V}{\partial Y} \right) dA + \int_A H_\lambda \left(\frac{\partial P}{\partial Y} \right) dA + \frac{1}{\sqrt{Gr}} \int_A \left(\frac{\partial N_\alpha}{\partial X}\frac{\partial V}{\partial X} + \frac{\partial N_\alpha}{\partial Y}\frac{\partial V}{\partial Y} \right) dA - \int_A \cos\Phi N_\alpha \theta dA = \int_{S_0} N_\alpha S_y dS_0 \tag{18}$$

$$\int_A N_\alpha \left(U\frac{\partial \theta}{\partial X} + V\frac{\partial \theta}{\partial Y} \right) dA + \frac{1}{\Pr\sqrt{Gr}} \int_A \left(\frac{\partial N_\alpha}{\partial X}\frac{\partial \theta}{\partial X} + \frac{\partial N_\alpha}{\partial Y}\frac{\partial \theta}{\partial Y} \right) dA = \int_{S_w} N_\alpha \; q_w \; dS_w \tag{19}$$

Here (14)-(15) specifying surface tractions (S_x, S_y) along outflow boundary S_0 and (16) specifying velocity components and fluid temperature or heat flux that flows into or out from domain along wall boundary S_w. Substituting the element velocity component distributions, the temperature distribution, and the pressure distribution from Eqs (9)-(12), the finite element equations can be written in the form,

$$K_{\alpha\beta}^{x} U_\beta + K_{\alpha\beta}^{y} V_\beta = 0 \tag{20}$$

$$K_{\alpha\beta\gamma}^{x} U_\beta U_\gamma + K_{\alpha\beta\gamma}^{y} V_\gamma U_\gamma + M_{\alpha\mu}^{x} P_\mu + \frac{1}{\sqrt{Gr}} \left(S_{\alpha\beta}^{xx} + S_{\alpha\beta}^{yy} \right) U_\beta - \sin\Phi \; K_{\alpha\beta}\theta_\beta = Q_{\alpha^u} \tag{21}$$

$$K_{\alpha\beta\gamma}^{x} U_\beta V_\gamma + K_{\alpha\beta\gamma}^{y} V_\gamma V_\gamma + M_{\alpha\mu}^{y} P_\mu + \frac{1}{\sqrt{Gr}} \left(S_{\alpha\beta}^{xx} + S_{\alpha\beta}^{yy} \right) V_\beta - \cos\Phi \; K_{\alpha\beta}\theta_\beta = Q_{\alpha^v} \tag{22}$$

$$K_{\alpha\beta\gamma}^{x} U_\beta \theta_\gamma + K_{\alpha\beta\gamma}^{y} V_\beta \theta_\gamma + \frac{1}{\Pr\sqrt{Gr}} \left(S_{\alpha\beta}^{xx} + S_{\alpha\beta}^{yy} \right) \theta_\beta = Q_{\alpha^T} \tag{23}$$

where the coefficients in element matrices are in the form of the integrals over the element area and along the element edges S_0 and S_w as,

$$K_{\alpha\beta}^{x} = \int_A N_\alpha N_{\beta,x} dA, \tag{24a}$$

$$K_{\alpha\beta}^{y} = \int_A N_\alpha N_{\beta,y} dA, \tag{24b}$$

$$K_{\alpha\beta\gamma}^{x} = \int_A N_\alpha N_\beta N_{\gamma,x} dA, \tag{24c}$$

$$K_{\alpha\beta\gamma}{}^{y} = \int_A N\alpha N\beta N\gamma, y dA , \tag{24d}$$

$$K\alpha\beta = \int_A N\alpha N\beta dA , \tag{24e}$$

$$S_{\alpha\beta}{}^{xx} = \int_A N\alpha, x N\beta, x dA , \tag{24f}$$

$$S_{\alpha\beta}{}^{yy} = \int_A N\alpha, y N\beta, y dA , \tag{24g}$$

$$M_{\alpha\mu}{}^{x} = \int_A H\alpha H\mu, x dA , \tag{24h}$$

$$M_{\alpha\mu}{}^{y} = \int_A H\alpha H\mu, y dA , \tag{24i}$$

$$Q_{\alpha}{}^{u} = \int_{S_0} N\alpha S_x dS_0 , \tag{24j}$$

$$Q_{\alpha}{}^{v} = \int_{S_0} N\alpha S_y dS_0 , \tag{24k}$$

$$Q_\alpha \theta = \int_{S_w} N_\alpha \quad q_w dS_w . \tag{24*l*}$$

These element matrices are evaluated in closed-form ready for numerical analysis. Details of the derivation for these element matrices are omitted herein for brevity.

The derived finite element equations, Eqs (20)-(23), are nonlinear. These nonlinear algebraic equations are solved by applying the Newton-Raphson iteration technique (Dechaumphai, [9]) by first writing the unbalanced values from the set of the finite element Eqs (20)-(23) as,

$$F_{\alpha}{}^{p} = K_{\alpha\beta}{}^{x} U\beta + K_{\alpha\beta}{}^{y} V\beta \tag{25a}$$

$$F_{\alpha^\mu} = K_{\alpha\beta\gamma^x} U_\beta U_\gamma + K_{\alpha\beta\gamma^y} V_\gamma U_\gamma + M_{\alpha\mu^x} P_\mu + \frac{1}{\sqrt{Gr}} \quad (S_{\alpha\beta^{xx}} + S_{\alpha\beta^{yy}}) \quad U_\beta - \quad \sin\Phi \quad K_{\alpha\beta}\theta_\beta - Q_{\alpha^\mu} \tag{25b}$$

$$F_{\alpha^v} = K_{\alpha\beta\gamma^x} U_\beta V_\gamma + K_{\alpha\beta\gamma^y} V_\gamma V_\gamma + M_{\alpha\mu^y} P_\mu + \frac{1}{\sqrt{Gr}} (S_{\alpha\beta^{xx}} + S_{\alpha\beta^{yy}}) V_\beta - \cos\Phi \quad K_{\alpha\beta}\theta_\beta - Q_{\alpha^v} \tag{25c}$$

$$F_{\alpha^T} = K_{\alpha\beta\gamma^x} U_\beta \theta_\gamma + K_{\alpha\beta\gamma^y} V_\beta \theta_\gamma + \frac{1}{\Pr\sqrt{Gr}} \left(S_{\alpha\beta^{xx}} + S_{\alpha\beta^{yy}} \right) \theta_\beta - Q_{\alpha^T} \quad (25d)$$

This leads to a set of algebraic equations with the incremental unknowns of the element nodal velocity components, temperatures, and pressures in the form,

$$\begin{bmatrix} K_{uu} & K_{uv} & K_{u\theta} & K_{up} \\ K_{vu} & K_{vv} & K_{v\theta} & K_{vp} \\ K_{Tu} & K_{\theta v} & K_{\theta\theta} & 0 \\ K_{pu} & K_{pv} & 0 & 0 \end{bmatrix} \begin{Bmatrix} \Delta u \\ \Delta v \\ \Delta\theta \\ \Delta p \end{Bmatrix} = - \begin{Bmatrix} F_{\alpha^\mu} \\ F_{\alpha^\nu} \\ F_{\alpha^\theta} \\ F_{\beta^p} \end{Bmatrix} \quad (26)$$

where

$$K_{uu} = K_{\alpha\beta\gamma^x} U_\gamma + K_{\alpha\gamma\beta^x} U_\gamma + K_{\alpha\beta\gamma^y} V_\beta + \frac{1}{\sqrt{Gr}} \left(S_{\alpha\beta^{xx}} + S_{\alpha\beta^{yy}} \right)$$

$$\mathrm{K_{uv}} = \mathrm{K_{\alpha\beta\gamma^y}\, U\gamma},$$

$$K_{u\theta} = -\sin\Phi \quad K_{\alpha\beta},$$

$$\mathrm{K_{up}} = \mathrm{M_{\alpha\mu^x}},$$

$$\mathrm{K_{vu}} = \mathrm{K_{\alpha\beta\gamma^x}\, V\gamma},$$

$$K_{vv} = K_{\alpha\beta\gamma^x} U_\beta + K_{\alpha\gamma\beta^y} V_\gamma + K_{\alpha\beta\gamma^y} V_\gamma + \frac{1}{\sqrt{Gr}} \left(S_{\alpha\beta^{xx}} + S_{\alpha\beta^{yy}} \right)$$

$$K_{v\theta} = -\cos\Phi \quad K_{\alpha\beta},$$

$$\mathrm{K_{vp}} = \mathrm{M_{\alpha\mu^y}},$$

$$K_{\theta u} = K_{\alpha\beta\gamma^x} \theta\gamma,$$

$$K_{\theta v} = K_{\alpha\beta\gamma^y} \theta\gamma$$

$$K_{\theta\theta} = K_{\alpha\beta\gamma^x} U_\beta + K_{\alpha\beta\gamma^y} V_\beta + \frac{1}{\Pr\sqrt{Gr}} \left(S_{\alpha\beta^{xx}} + S_{\alpha\beta^{yy}} \right)$$

$K_{\theta p} = 0$, $K_{pu} = K_{\alpha\beta^x}$, $K_{pv} = K_{\alpha\beta^y}$ and $K_{p\theta} = 0 = K_{pp}$.

The iteration process is terminated if the percentage of the overall change compared to the previous iteration is less than the specified value.

To solve the sets of the global nonlinear algebraic equations in the form of matrix, the Newton-Raphson iteration technique has been adapted through PDE solver with COMSOL MULTIPHYSIS interface.

3. 3.2 Grid Independence Test

Preliminary results are obtained to inspect the field variables grid independency solutions. Test for the accuracy of grid fineness has been carried out to find out the optimum grid number.

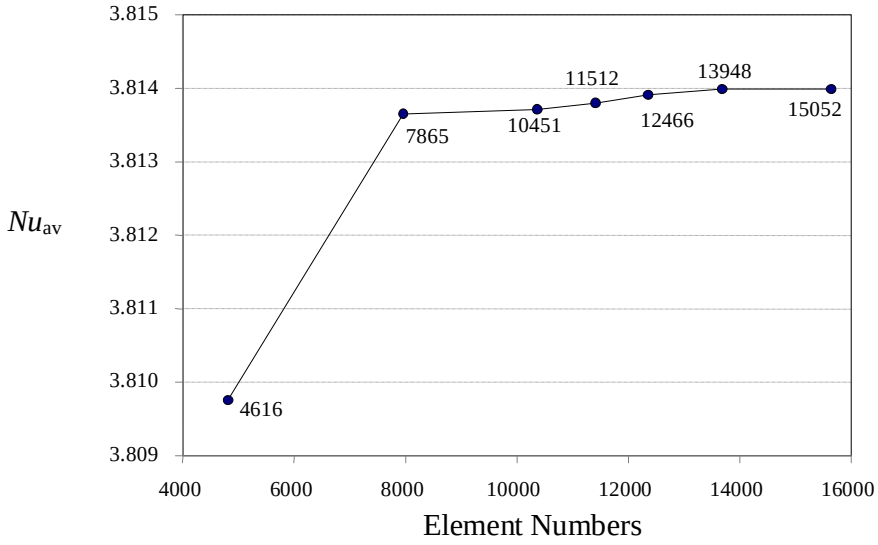

Figure 3.2 Convergence of average Nusselt number with grid refinement for *Gr* = 10^6 and *dr* = 0.2

In order to obtain grid independent solution, a grid refinement study is performed for a square open cavity with *Gr* = 10^6 and *dr* = 0.2. Figure 3.2 shows the convergence of the average Nusselt number, Nu_{av} at the heated surface with grid refinement. It is observed that grid independence is achieved with 13984 elements where there is insignificant change in Nu with further increase of mesh elements. Six different non-uniform grids with the following number of nodes and elements were considered for the grid refinement tests: 28442 nodes, 4616 elements; 50346 nodes, 7865 elements; 64240

nodes, 10451 elements; 69887 nodes, 11512 elements; 82584 nodes, 12466 elements; 92573 nodes, 13948 elements, 98388 nodes, 15052 elements. From these values, 92573 nodes, 13984 elements can be chosen throughout the simulation to optimize the relation between the accuracy required and the computing time.

Nodes (elements)	28442 (4616)	50346 (7865)	64240 (10451)	69887 (11512)	82584 (12466)	92573 (13948)	98388 (15052)
Nu	3.80956	3.81324	3.81344	3.81354	3.81366	3.81424	3.81426
Time (s)	283.610	300.43	337.51	444.21	455.56	551.61	1007.65

Table 3.1: Grid Sensitivity Check at $Pr = 0.72$, dr = 0.2 and $Gr = 10^6$.

3.4 Results and Discussion

Two-dimensional laminar steady state natural convection flow in a square open cavity with the left vertical wall at iso-heat flux has been studied numerically, as shown in Figure 3.1. A partially heated circular cylinder is placed at the center of the cavity and the opposite wall to the aperture is heated by iso-flux heat source. The other two remaining walls are kept cool with Temperature T_c (Top wall) and heated with temperature T_h (bottom wall). Two-dimensional forms of Navier-Stokes equations along with the energy equations are solved using Galerkin finite element method. Results are obtained for a range of Grashof number from 10^3 to 10^6 at Pr = 0.72, 1.00 and 7.00 with constant physical properties. The parametric studies for a wide range of governing parameters show consistent performance of the present numerical approach to obtain as stream functions and temperature profiles. The computational results indicate that the heat transfer coefficient is strongly affected by Grashof number. The use of Nusselt number and Grashof number develops an empirical correlation. Obviously for high values of Grashof number the errors encountered are appreciable and hence it is necessary to perform some grid size testing in order to establish a suitable grid size. Grid independent solution is ensured by comparing the results of different grid meshes for Gr = 10^6, which has been the highest Grashof number. The total domain is discretized into 13948 elements that results in 92573 nodes.

The effect of inclination angle is examined for Φ = 0º, 15º, 30º, 45º with aspect ratio A = 1. A comparison between the steady-state patterns of streamlines from Grashof numbers of 10^3 to 10^6 with different angles is presented in Figure 3.3 – 3.12. Also a comparison between the steady-state patterns of isotherms from Grashof numbers of 10^3 to 10^6 with different angles is presented in Figure 3.3 – 3.12. For the isotherm, the figures show that as the Grashof number and the inclination angle increase, the buoyancy force increases and the thermal boundary layers become thinner. We observe that the heat transfer in the cavity is qusi-conductive at Gr = 10^3 and becomes dominated by convective regime as Gr increases to 10^6 in fig: 3.3-3.19. As Gr is increased to 10^6, the isotherms show that the cold fluid penetrates right to the heated wall, where steep temperature gradients exit. At Gr = 10^5 and 10^6 from the figure, shows that heat transfer rate increases and flow is boundary layer type-specially left and cold wall. The cold fluid penetrates to the heated wall and the heated cylinder. Then the isotherms and streamlines become more packed to the cold wall. This suggests that the flow moves faster as natural convection is rigorous.

Flow of the hot fluid from the opening is choked, as a result of which the fluid velocity is increased and boundary layer becomes thinner. For the streamlines, the figures show that the fluid enters from the bottom of the aperture, circulates in a clockwise direction following the shape of the cavity, and leaves toward the upper part of the aperture. At Gr = 10^3 and 10^4 , the stream lines in the cavity show that for quasi-conductive regime entrance and exit sections of the fluid at the opening are unequal. The discharging fluid from the upper part of the cavity occupies smaller and smaller sections of the opening. The velocity of the air flow moving toward the aperture increases, and the area that is occupied by the leaving hot fluid decreases, compared with that of the entering fluid. Streamlines show that as the inclination angle of the heated wall increases, the velocity gradient increases at heated wall, and also the strength of the circulation increases. The results are presented in terms of streamlines and isotherm patterns. The variations of the average Nusselt number are also highlighted. The results in the steady state are obtained for a Grashof range from 10^3 to $10^6$and for a range of 0^o-45^o for the inclination angles of the cavity. The results show that for high Grashof numbers, the Nusselt number changes substantially with the inclination angle of the cavity. The numerical model predictes Nusselt number oscillations for low angles and high Grashof numbers.

In order to validate the numerical code, pure natural convection with *Pr* = 0.72 in a square open cavity was solved, and the results were compared with those reported by Hinojosa et al. [16], obtained with an extended computational domain. In Table 3.2, a comparison between the average Nusselt numbers are presented. The results from the present experiment are almost same as Hinojosa et al.

Table 3.2: Comparison of the results for the constant surface temperature with Pr = 0.71.

Gr	Nu_{av}	
	Present work	Hinojosa et al. (2005)
10^3	1.33	1.30
10^4	3.42	3.44
10^5	7.40	7.44
10^6	14.41	14.51

3.4.1 Effects of Inclination Angle

With the increase of the Grashof number, complex flow pattern characteristics were found for some inclination angles. To show this, the profiles of isotherm and streamline and inclination angles of 0^o, 15^o, 30^o and 45^o are presented in Fig. 3.3 to 3.8. For inclination angles of the cavity from 0^o to 45^o, the steady state become unstable; the pictorial diagram show that the fluid enters and leaves in a very asymmetrical way, indicating an unsteady convection. The cold fluid enters by the lower section of the aperture plane, without symmetry, and the hot fluid leaves by the upper section. The velocity magnitude of the leaving fluid is greater than the incoming fluid, and thus the thermal boundary layer at the top wall becomes much thinner. For the tilted angle of 45^o, the air flow entering and leaving the cavity decreases its velocity considerably.

In Table 3.3, average Nusselt number for different cavity angles and Grashof numbers, obtained with the present model for Pr = 0.72 and dr = 0.2 are presented. Table 3.3 presents the average Nusselt numbers for four Grashof numbers (10^3, 10^4, 10^5 and 10^6) for a range of 0^o - 45^o for the tilted angles of an open square cavity. For different angles and Gr numbers, mainly for lower angles and for higher Gr, the average Nusselt number increases. Therefore, in Table 3.3, the average Nusselt numbers are reported.

In Fig.3.13, we observe that the heat transfer rate Nu increases with the increase of inclination angles and Grashof number.

Table 3.3: Average Nusselt number Nu for different cavity's inclination angles Φ and Grasof numbers for Pr =0.72 and dr = 0.2.

Nu_{av}				
Φ	Gr=10^3	Gr=10^4	Gr=10^5	Gr=10^6
0^o	3.795779	4.608153	6.373589	9.947833
15^o	3.943523	4.528235	6.345305	10.062273
30^o	4.117558	4.020996	5.791963	9.583794
45^o	4.893168	4.48368	6.500447	11.429212

3.4.2 Effects of Prandtl Number

A study of Pr = 0.72, 1.00 and 7.00 has been done for investigating the effects of Prandtl number on the flow and heat transfer characteristics. The predicted isotherms and stream lines are shown in figure 3.9 and 3.10. It is seen that the fluid that moves clock wise around the cylinder creates vortices in the cavity.

In 3.4, average Nusselt numbers for different Prandlt numbers (Pr = 0.72, 1.00 and 7.00) and Grashof numbers, obtained with the present model for angle $\Phi = 0^o$ and diameter ratio dr = 0.2 are presented.

Figure 3.16 shows the average Nusselt number variation for different Prandtl numbers while Pr = 0.72, 1.00, 7.00. In Fig.3.16, we observe that average Nusselt number Nu increases with the increasing of Grashof number Gr and decreases with the increasing of Prandtl number Pr. The similar behavior is observed in Fig.3.17, 3.18 and 3.19. Heat transfer characteristics become low for higher Prandtl number Pr = 7 and high for lower Pr = 0.72. So the results show insignificant for different angles.

We observe that the flow patterns become more of a boundary layer type at the walls for Gr = 10^5 and 10^6 with the increase of prandtl number Pr. This implies that the flow becomes slower and velocity gradient decreases as natural conduction is intensified. It is also seen that the region between cylinder and cavity wall is dominated by a slow moving stratified cellular pattern.

The temperature is superior in the case of Pr = 7.0 than in the case of Pr = 0.72. This is because, the fluid with Pr = 7.0 has a lower thermal diffusivity than that of the fluid with Pr = 0.72. Hence, the fluid with Pr = 7.0 will tend to exchange less heat with surrounding fluid by diffusion.

Table 3.4: Average Nusselt numbers for different Prandtl number while Pr = 0.72, 1.00 and 7.00, angle $\Phi = 0^o$ and dr = 0.2.

	Nu_{av}			
Pr	Gr=10^3	Gr=10^4	Gr=10^5	Gr=10^6
0.72	3.795779	4.608153	6.373589	9.947833
1.0	3.615149	4.135585	5.788313	9.260708
7.0	3.274197	1.944154	3.326285	5.488287

3.4.3 Effects of Diameter Ratio

In Table 3.5, average Nusselt numbers for different diameter ratios (*dr* = 0. 2, 0.3 and 0.4) and Grashof numbers, obtained with the present model for angle $\Phi = 0^o$ and Prandlt number = 0.72 are presented. Figure 3.20 shows average Nusselt number decreases with increasing of diameter ratio of the cylinder for Gr = 10^3 to 10^5. Again average Nusselt number increases with the increasing of diameter ratio of the cylinder for Gr = 10^6.At Gr = 10^3 – 10^5, thermal boundary layer increases along with the increase of diameter ratio (dr) because of the restriction of heat flow from bottom to upper in the cavity. But at Gr = 10^6, the thermal boundary layer decreases with the increase of diameter ratio due to the increase of convective heat transfer. For stream line, velocity gradient decreases with diameter ratio at heated wall. Entering fluid flow patterns become flat and create more vortices with the increase of diameter ratio. At Gr = 10^4 , fluid flow more packed at diameter ratio dr = 0.4 than other diameter ratio dr and the flow type is boundary layer.

Table 3.5: Average Nusselt numbers for different diameter ratios while *dr* = 0. 2, 0.3 and 0.4, angle $\Phi = 0^o$ and *Pr* = 0.72.

Nu_{av}				
dr	Gr=10^3	Gr=10^4	Gr=10^5	Gr=10^6
0. 2	3.795779	4.608153	6.373589	9.947833
0.3	3.341359	4.392743	5.846771	9.963084
0.4	3.199761	5.51039	5.61039	10.244008

3.5 Chapter Summary

Two-dimensional laminar steady state natural convection flow in a square open cavity with the left vertical wall at iso-heat flux has been studied numerically. A finite element method for steady-state incompressible natural convection flow is presented. The finite element equations derived from the governing flow equations that consist of the conservation of mass, momentum, and energy equations. The derived finite element equations are nonlinear requiring an iterative technique solver. The Newton-Raphson iteration method has been applied to solve these nonlinear equations for solutions of the nodal velocity component, temperature, and pressure by considering Prandtl numbers of 0.72, 1.00 and 7.00 and Grashof numbers of 10^3 to 10^6. The results show the following aspects:

- Heat transfer depends on Prandtl number and heat transfer rate decreases for higher Prandtl number.
- Thermal boundary layer thickness is thinner due to the increasing of Grashof number.
- The heat transfer rate increases for Grashof number 10^3 to 10^6 gradually but different behavior is found for angle 30^0.
- The heat transfer rate Nu_{av} increases with the increase of inclination angles for Grashof number 10^3 and it varies for rest of Gr.
- The heat transfer rate Nu_{av} decreases with the increase of diameter ratio for $10^3 - 10^5$ and increase for Grashof number Gr^6.
- Various vortices entering the flow field and a secondary vortex at the center and bottom wall of the cavity are seen in the streamlines.

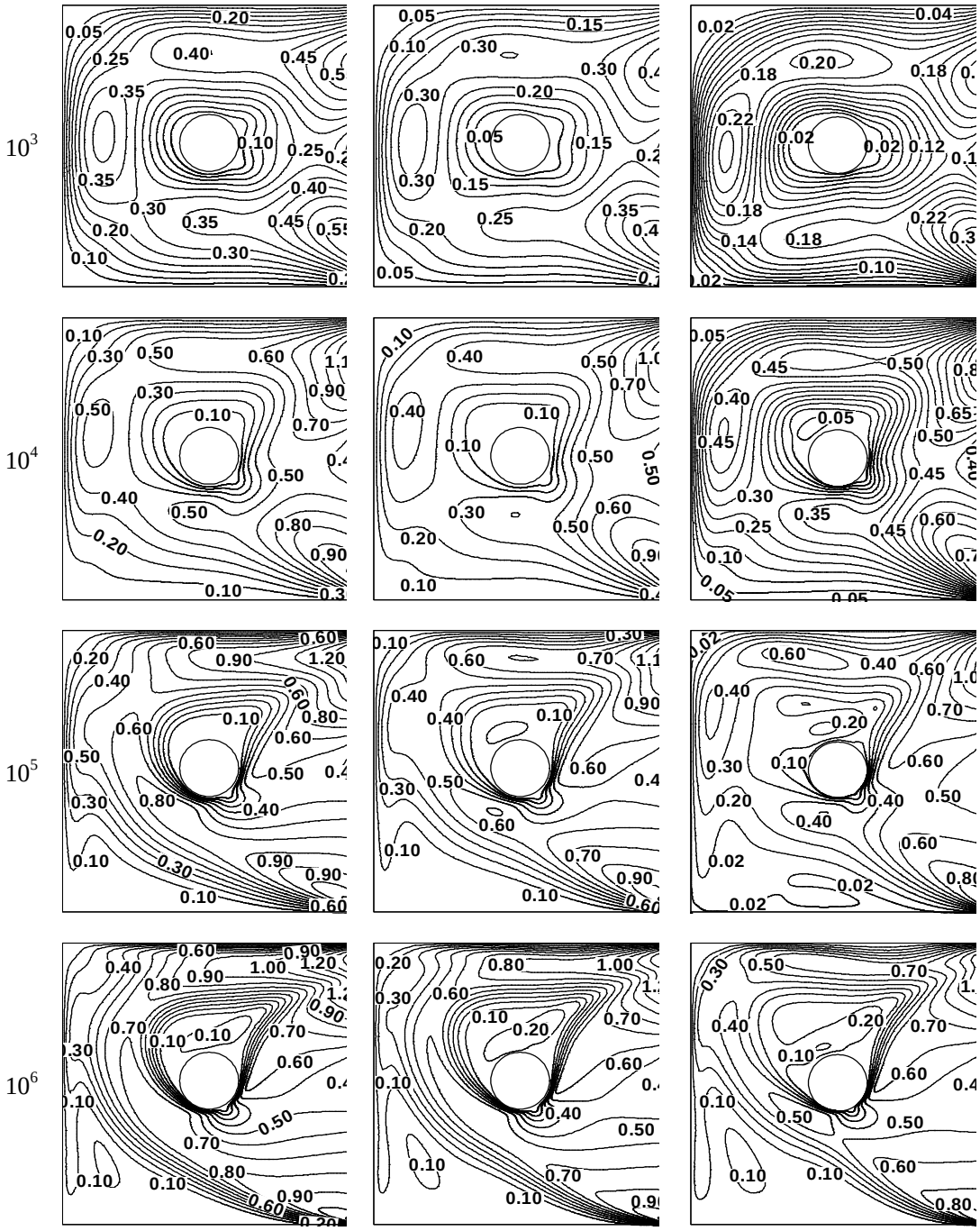

Fig 3.3: Streamline patterns for different angles with *dr* = 0.2 and *Pr* = 0.72

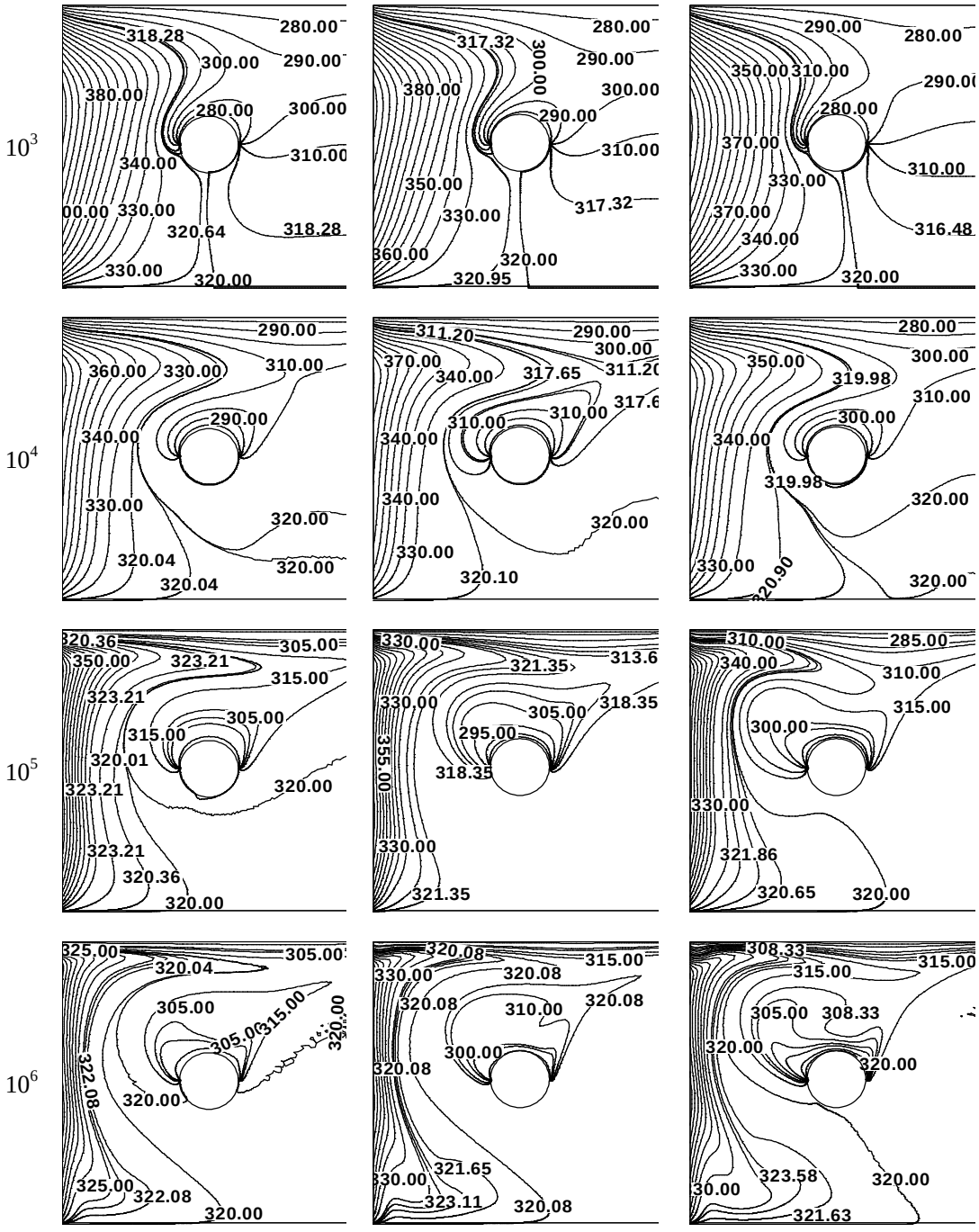

Fig 3.4: Isotherm patterns for different angles with *dr* = 0.2 and *Pr* = 0.72

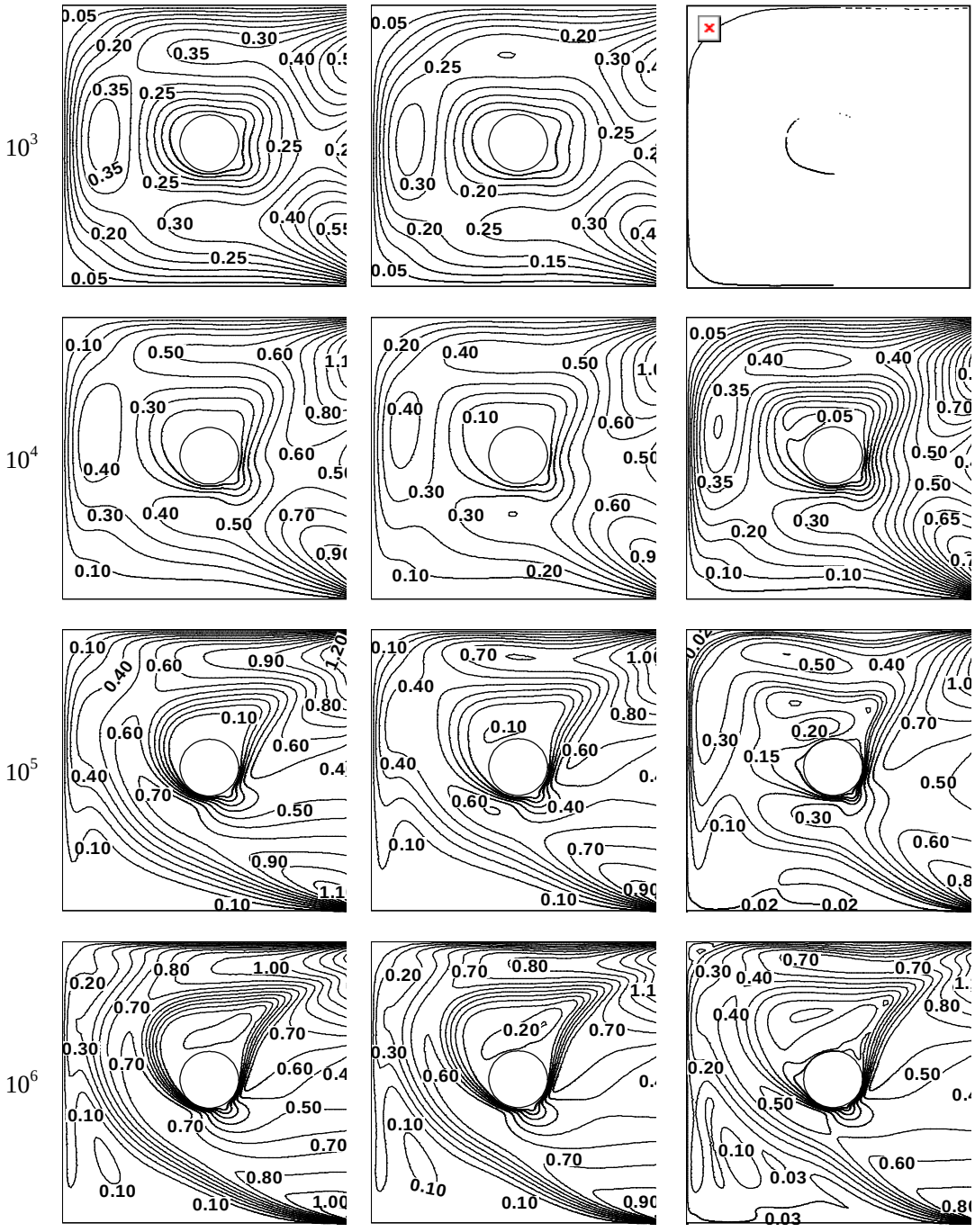

Fig 3.5: Streamline patterns for different angles with *dr* = 0.2 and *Pr* = 1.00

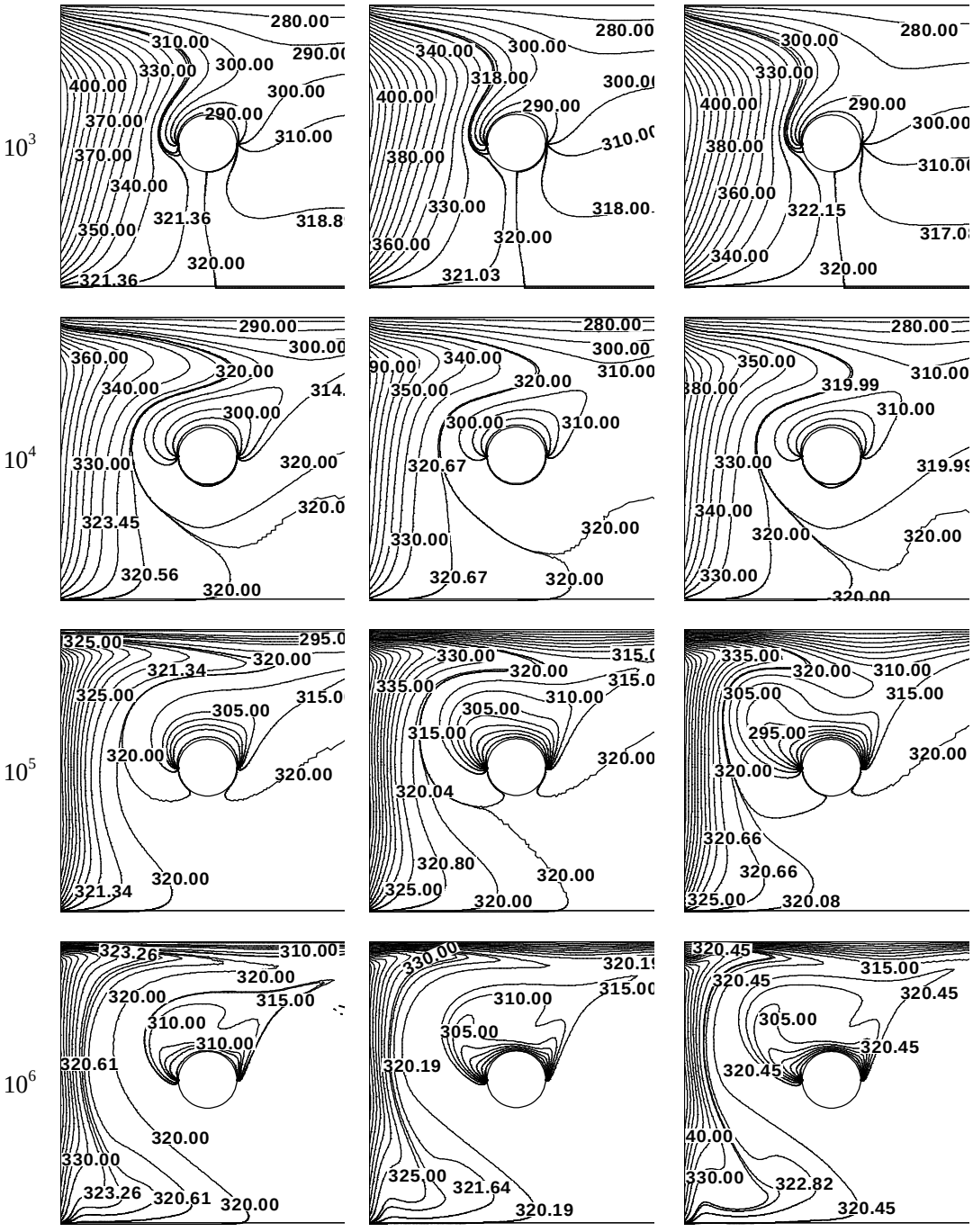

Fig 3.6: Isotherm patterns for different angles with *dr* = 0.2 and *Pr* = 1.00

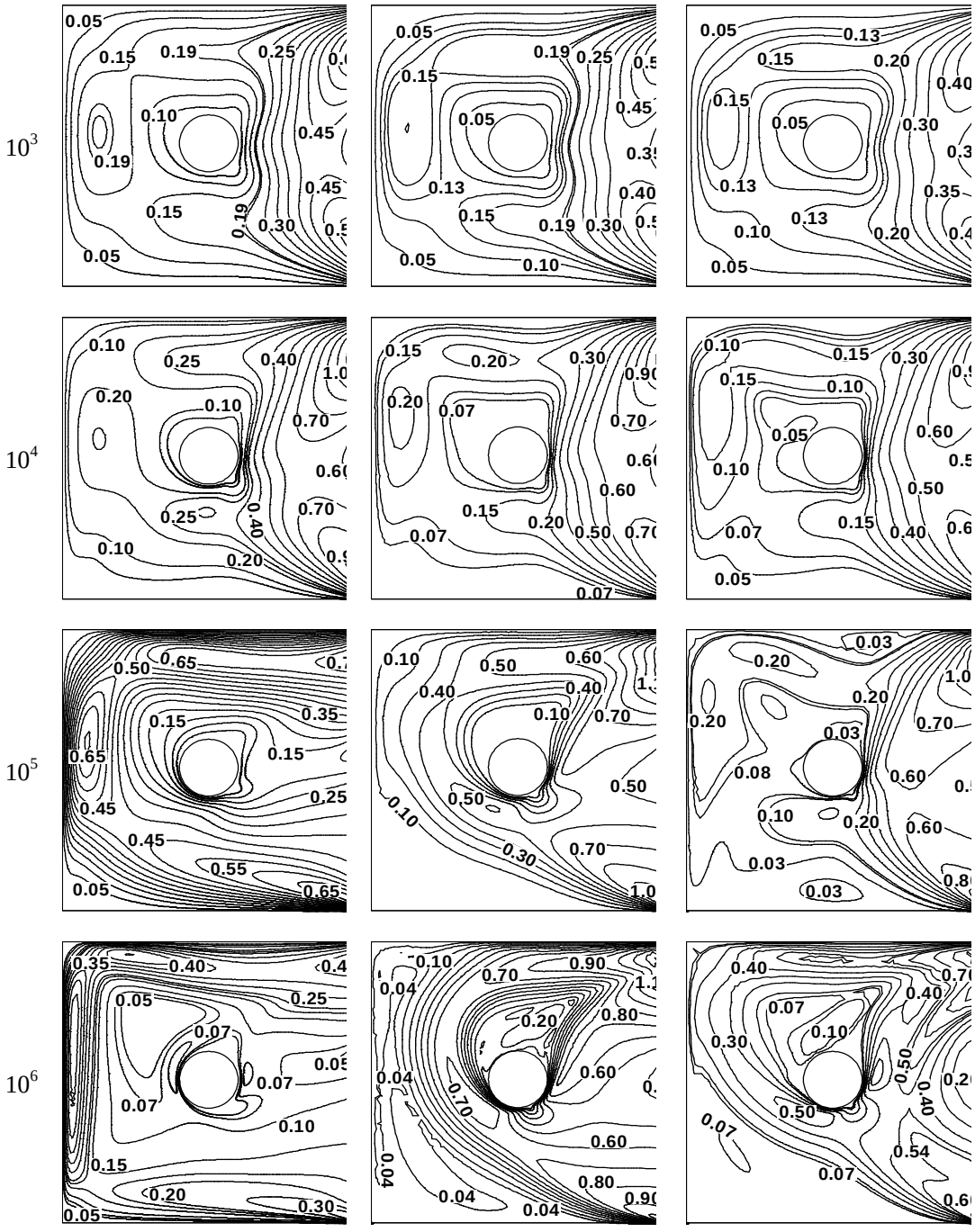

Fig 3.7: Streamline patterns for different angles with *dr* = 0.2 and *Pr* = 7.00

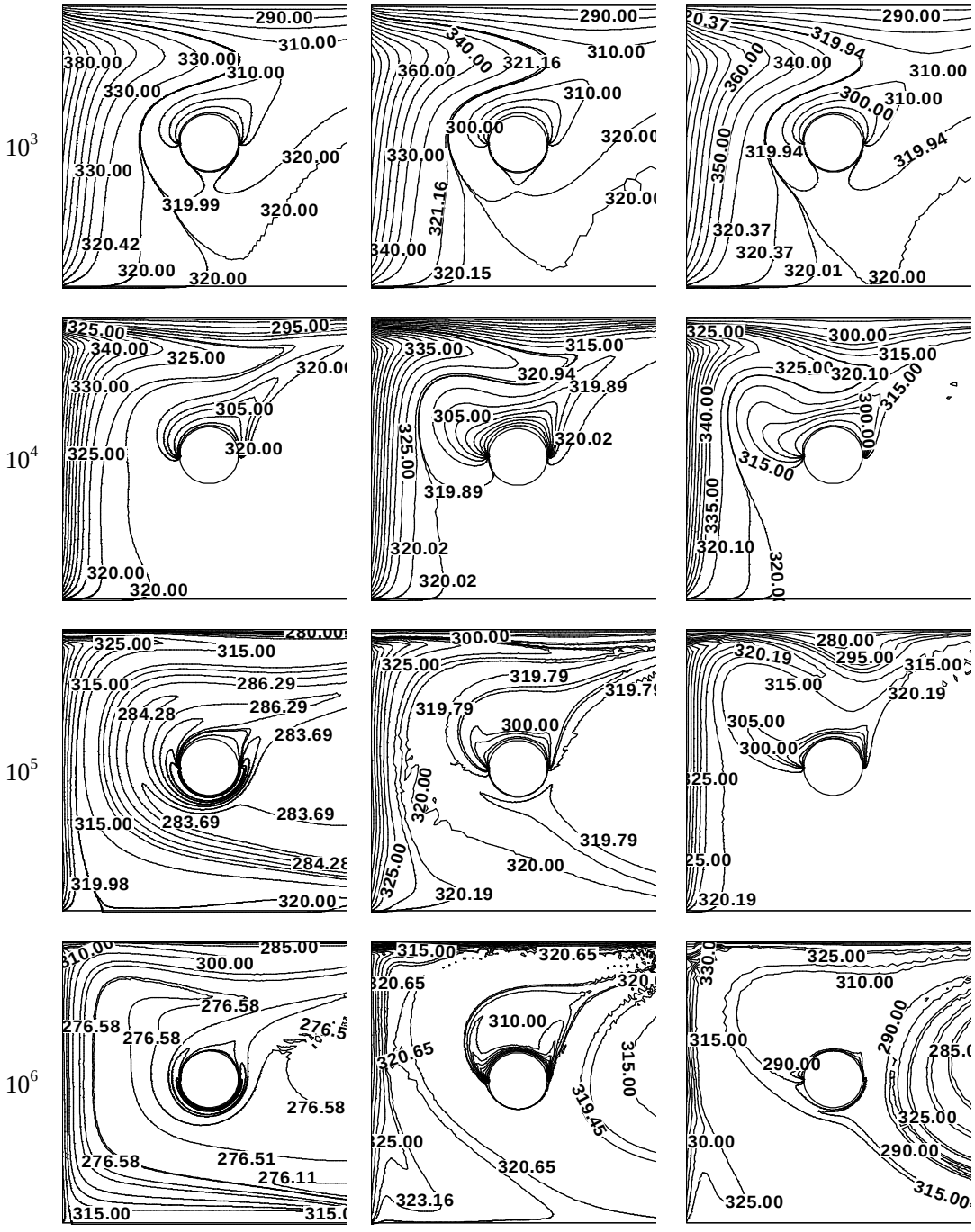

Fig 3.8: Isotherm patterns for different angles with *dr* = 0.2 and *Pr* = 7.00

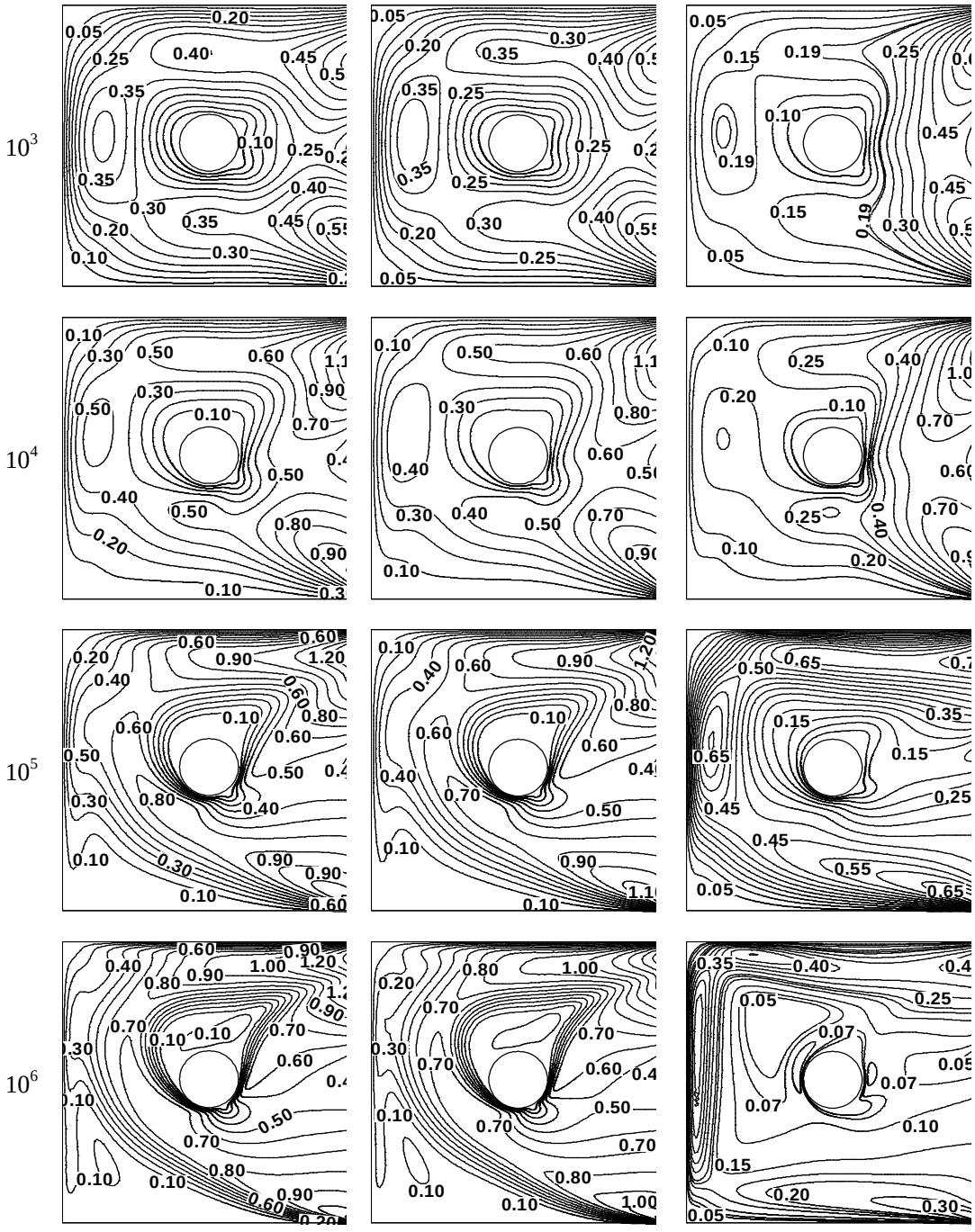

Fig 3.9: Streamline patterns for different angles with *dr* = 0.2 and *Pr* = 0.72

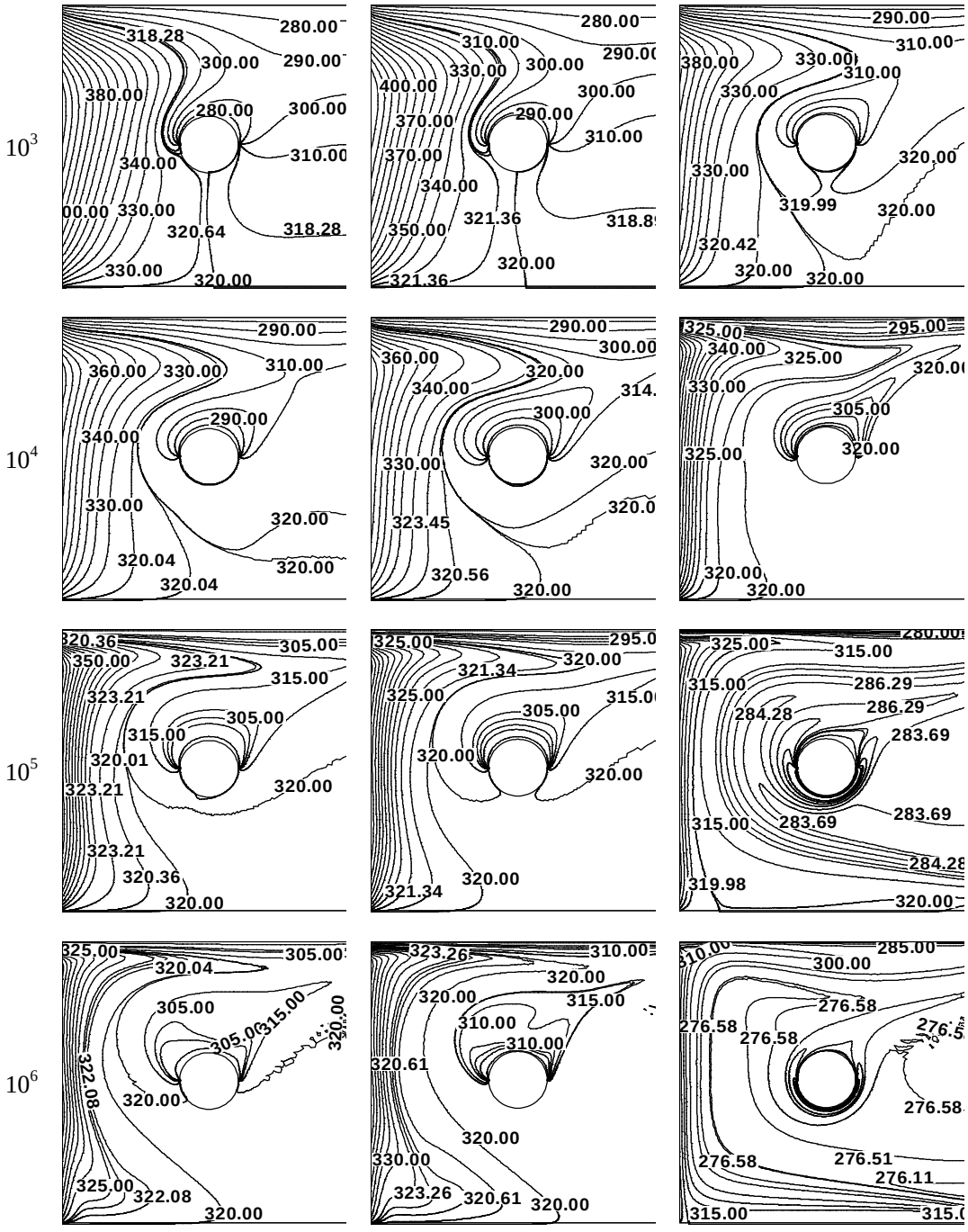

Fig 3.10: Isotherm patterns for different Pr with $dr = 0.2$ and $\Phi = 0^0$

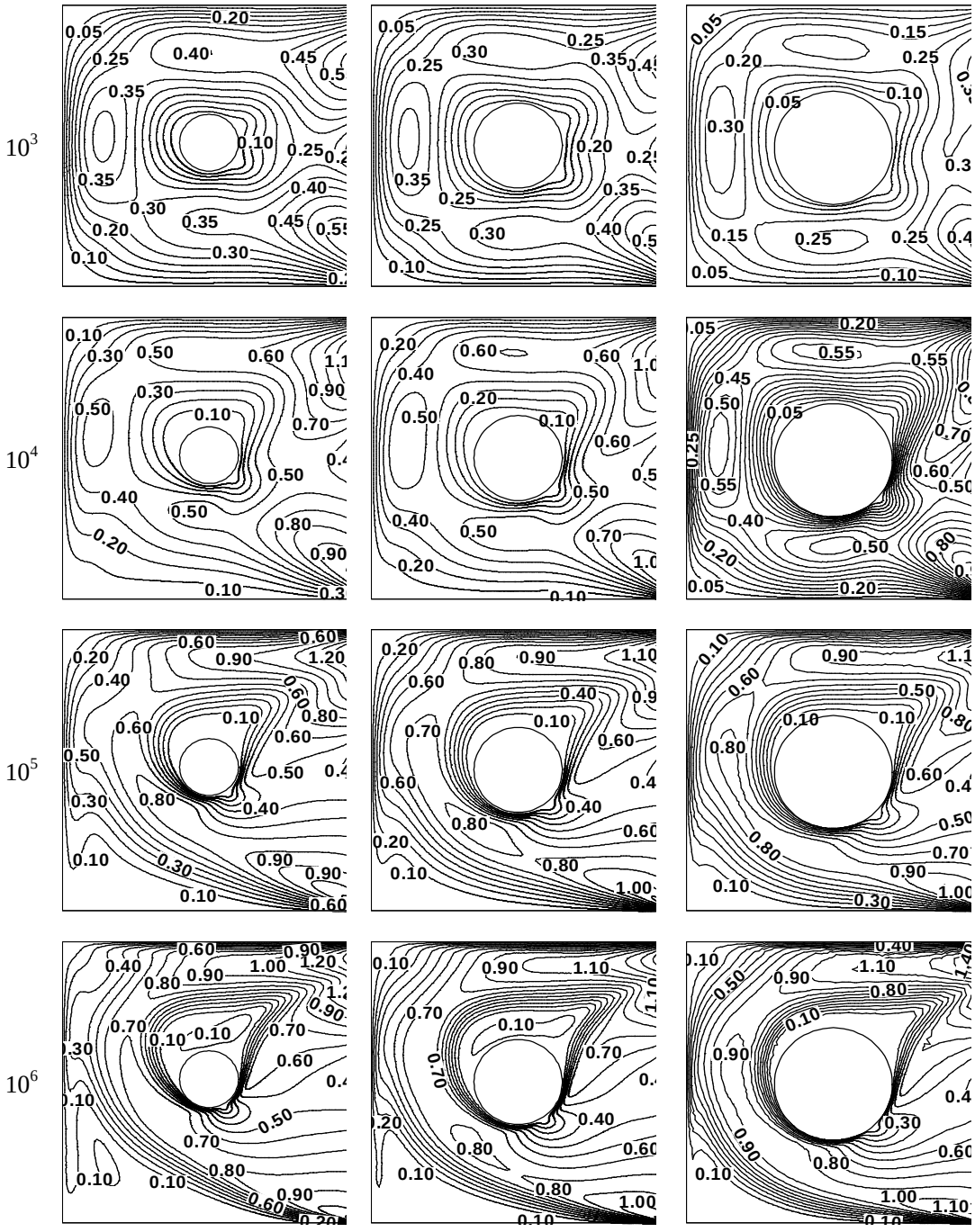

Fig 3.11: Streamline patterns for different dr with P*r* = 0.72 and $\Phi = 0^0$

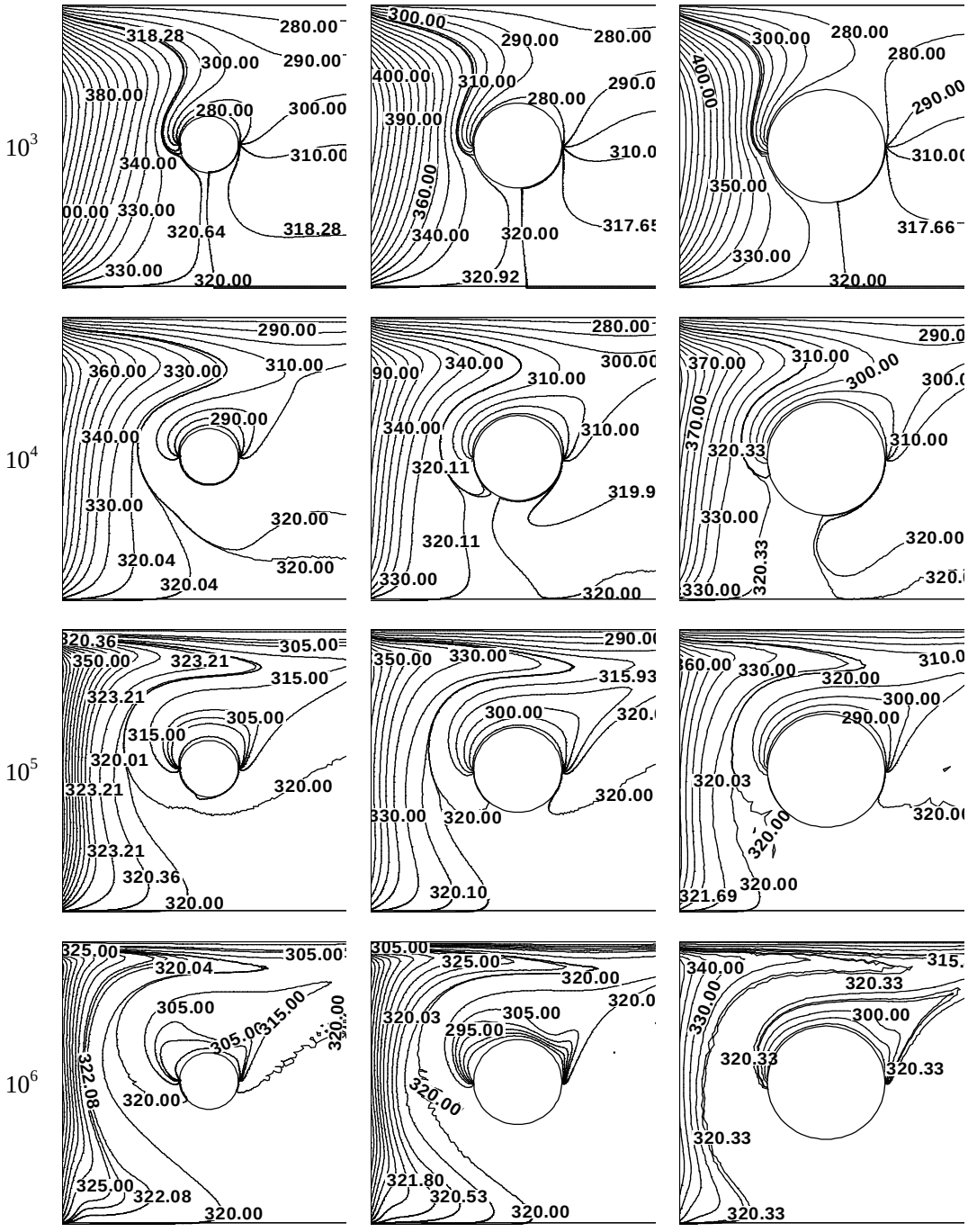

Fig 3.12: Isotherm patterns for different dr with pr = 0.72 and $\Phi = 0^0$

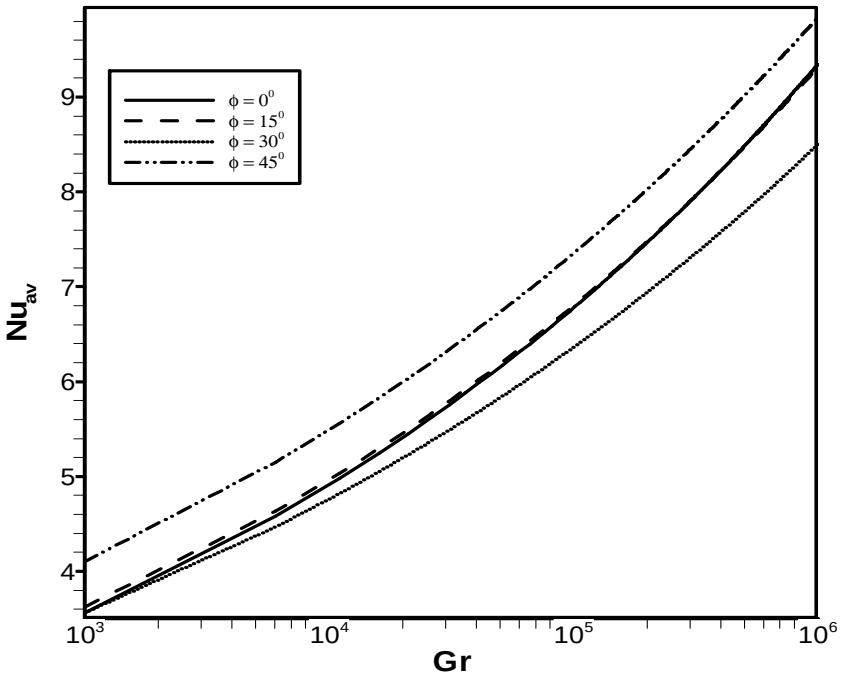

Fig.3.13: Effect of inclination angle on average Nusselt number and Grashof number while *Pr* = 0.72, *dr* = 0.2.

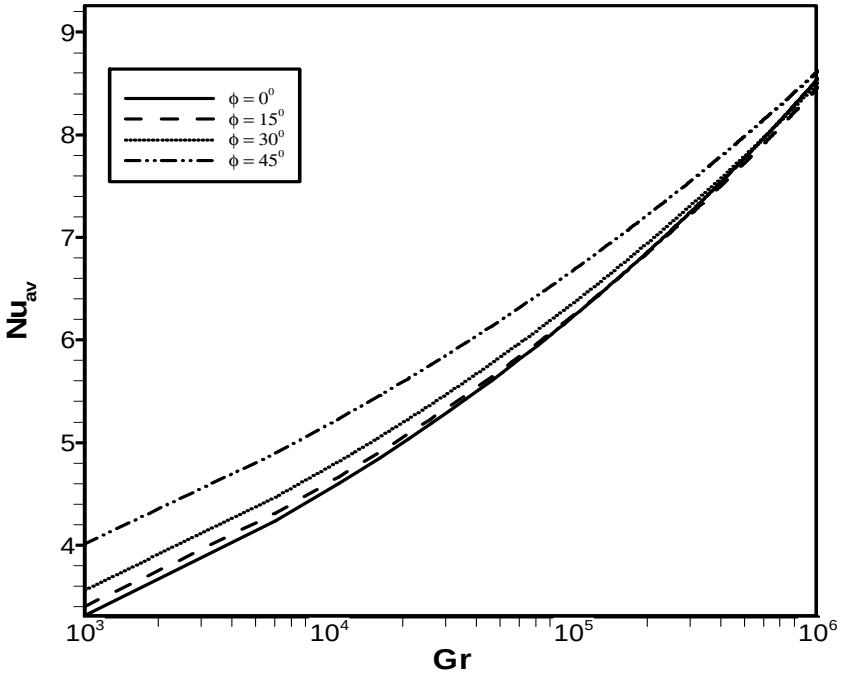

Fig.3.14: Effect of inclination angle on average Nusselt number and Grashof number while *Pr* = 1.0, *dr* = 0.2.

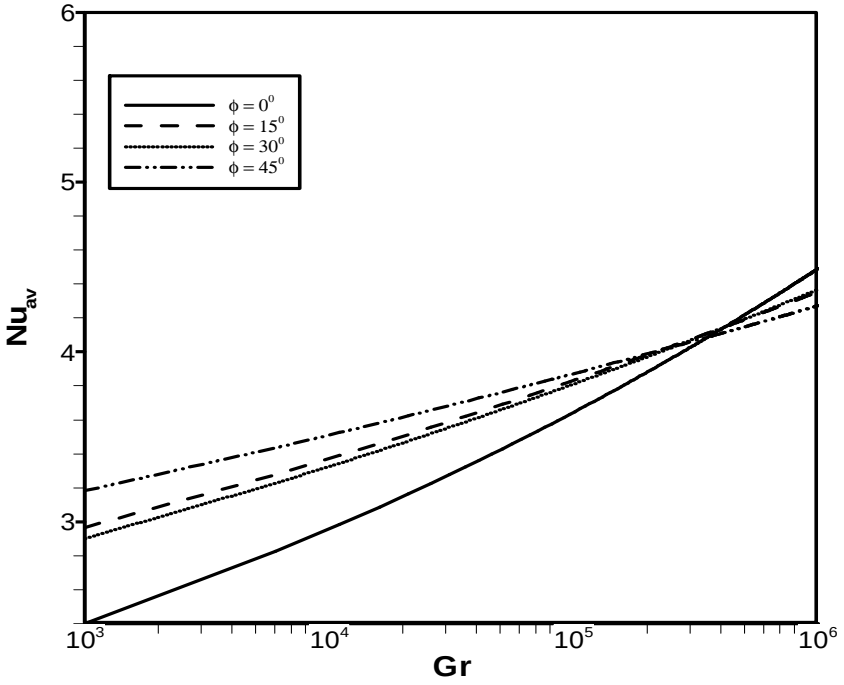

Fig.3.15: Effect of inclination angle on average Nusselt number and Grashof number while *Pr* = 7.0, *dr* = 0.2.

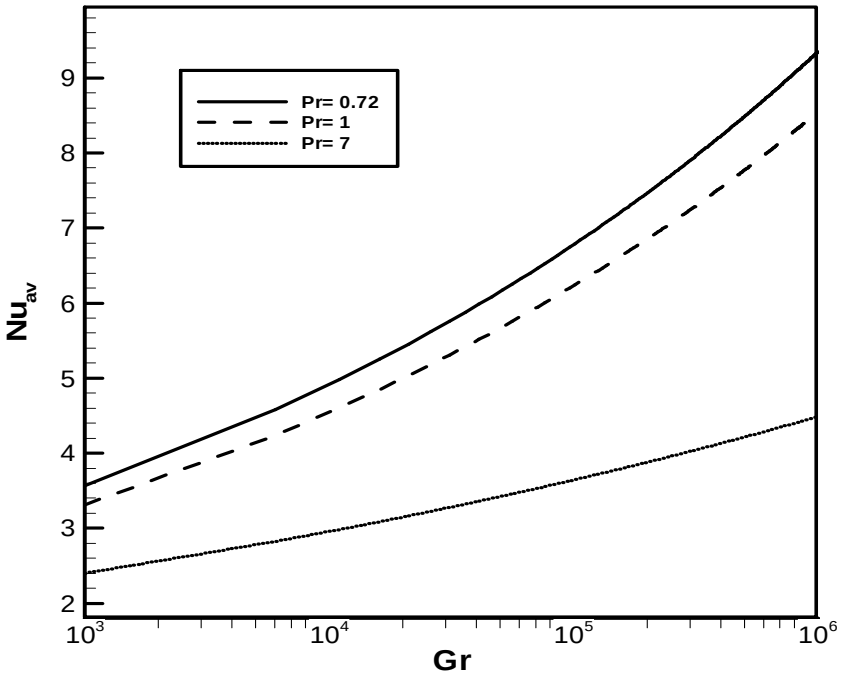

Fig.3.16: Effect of Prandtl number on average Nusselt number and Grashof number while *Pr* = 0.72, 1.0 and 7.0, angle 0^o and *dr* = 0.2.

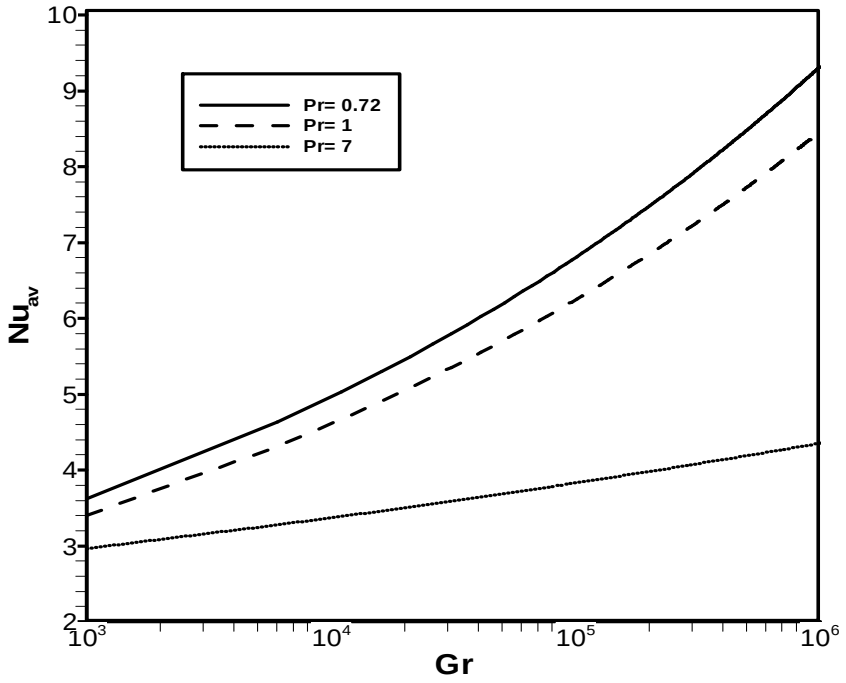

Fig.3.17: Effect of Prandtl number on average Nusselt number and Grashof number while *Pr* = 0.72, 1.0 and 7.0, angle 15^o and *dr* = 0.2.

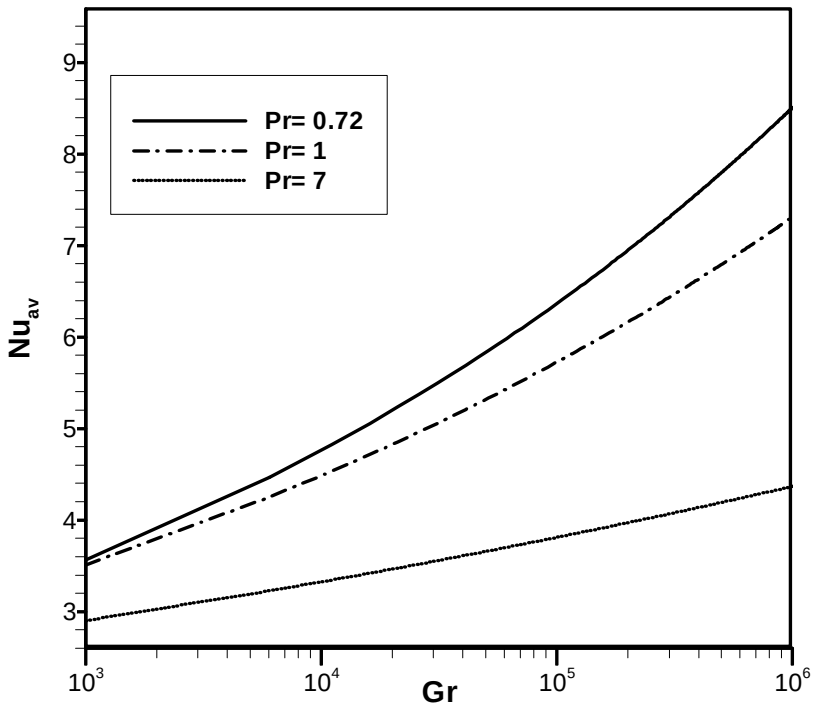

Fig.3.18: Effect of Prandtl number on average Nusselt number and Grashof number while *Pr* = 0.72, 1.0 and 7.0, angle 30^o and *dr* = 0.2.

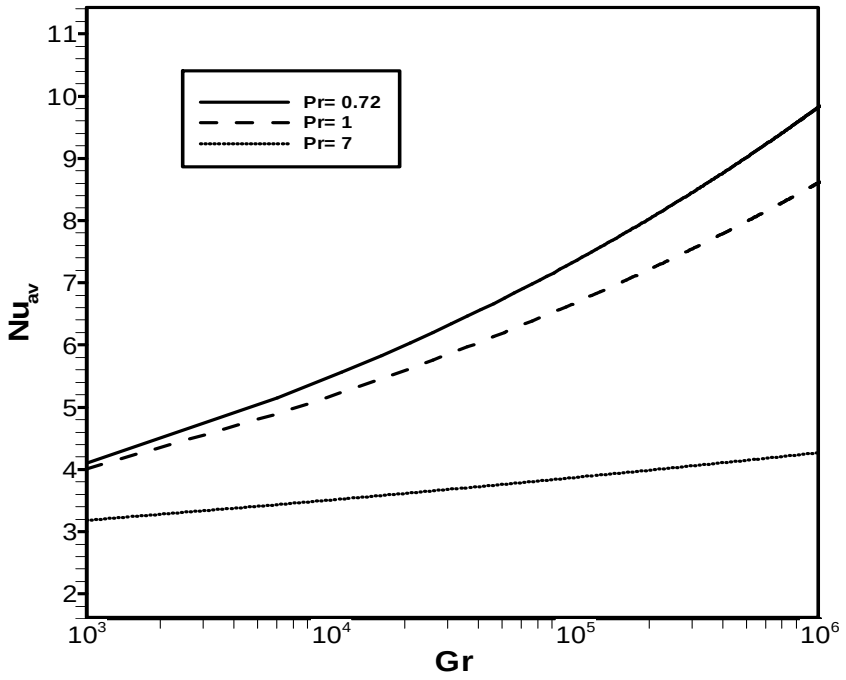

Fig.3.19: Effect of Prandtl number on average Nusselt number and Grashof number while Pr = 0.72, 1.0 and 7.0, angle 45^o and dr = 0.2.

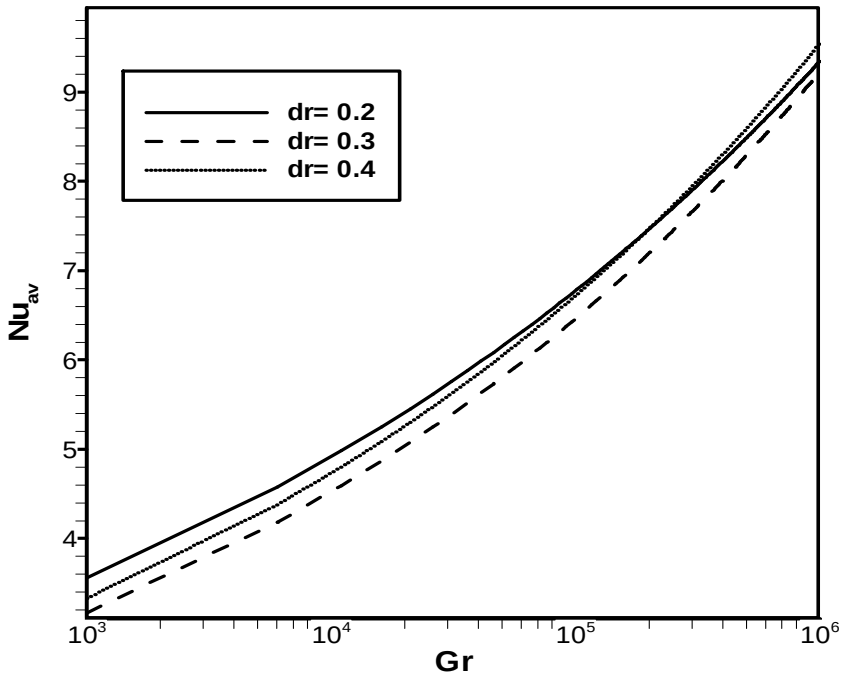

Fig.3.20: Effect of diameter ratio on average Nusselt number and Grashof number while Pr = 0.72, 1.0 and 7.0, angle 0^o.

CHAPTER 4

Numerical Analysis of Two Dimentional Laminar Steady-State Natural Convection Flow in a Tilted Open Square Cavity Having Partially Heated Square Cylinder

4.1 Problem Definition

The heat transfer and the fluid flow in a two-dimensional open square cavity of length L was considered, as shown in the schematic diagram of figure 4.1. The opposite wall to the aperture was first kept to constant heat flux q, while the surrounding fluid interacting with the aperture was maintained to an ambient temperature T_∞. The other two remaining walls were kept cooled Temperature T_c (Top wall) and heated temperature T_h (bottom wall). The square cylinder was assumed to be partially heated. The fluid was assumed with Prandtl number (*Pr* = 0.72, 1.0, 7.0) and Newtonian, and the fluid flow is considered to be laminar. The properties of the fluid were assumed to be constant.

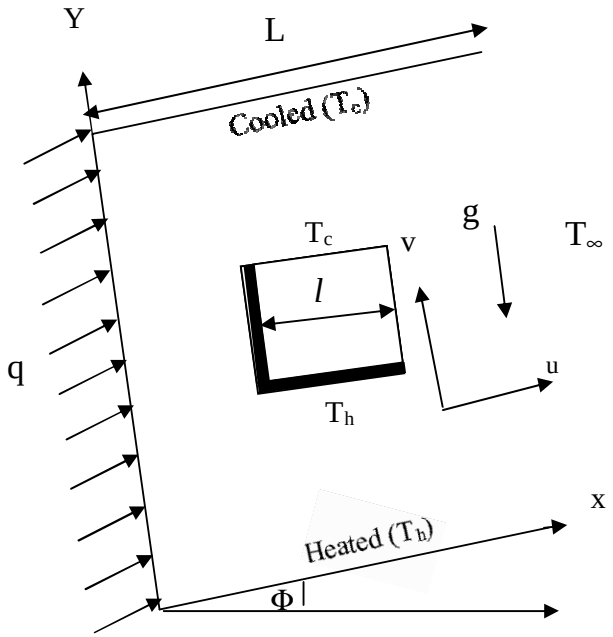

Figure - 4.1 Schematic diagram of the physical system

4.2 Mathematical Modeling

The several steps of the mathematical formulation for the above physical configurations are shown as follows

4.2.1 Governing Equations

The governing equations for steady natural convection flow have been discussed in previous chapter:

4.2.2 Boundary Conditions

The boundary conditions for the present problem are specified as follows:

On the left wall (x = 0): u = v= 0 , $\frac{\partial T(0,y)}{\partial x} = -\frac{q}{k}$

On the right wall (x = 1): u = v = 0, $T_{in} = T_\infty$, $\frac{\partial T}{\partial x}(L,y) = 0$

On the bottom wall (y = 0): u = v = 0, $T = T_h$

On the Upper wall (y = 1): u = v = 0, $T = T_c$

On the cylinder,

At the bottom and left side: u = v = 0, $T = T_h$

At the upper and right side: u = v = 0, $T = T_c$

where x and y are the distances measured along the horizontal and vertical directions, respectively; u and v are the velocity components in the x- and y-direction, respectively; T denotes the temperature; γ and α are the kinematic viscosity and the thermal diffusivity, respectively; p is the pressure and ρ is the density; T_h ,T_c and T_∞ are heated, cooled and ambient temperatures respectively.

4.2.3 Dimensional Analysis

The governing equations in non-dimensional form are written in early chapter.

The following dimensionless scales have used in the non-dimensional Equations (5)-(8):

$$X = \frac{x}{L},\ Y = \frac{y}{L},\ U = \frac{u}{U_o},\ V = \frac{v}{U_o},\quad P = \frac{p - p_\infty}{\rho U_o^2},\ \theta = \frac{T - T_c}{\Delta t}$$

$$= \frac{\nu}{\alpha},\ Gr = \frac{g\,\beta\,\Delta t\,L^3}{\nu^2},\ l_r = \frac{L_s}{L}\ \Delta t = (T_h - T_c)\ \Delta t = \frac{q\,L}{k}$$

Here Gr and Pr are Grashof and Prandtl numbers, respectively. The Grashof number represents the ratio of the buoyancy force to the viscous force acting on the fluid. The reference velocity U_o is related to the buoyancy force term and is defined as

$$U_o = \sqrt{g\,\beta\,L\left(T_h - T_c\right)}.$$

The Nusselt number (Nu) is one of the important dimensionless parameters to be computed for heat transfer analysis in natural convection flow. Also the Nusselt number for free convection is a function of the Grashof number only. The local Nusselt number can be obtained from the temperature field by applying

$$Nu = \frac{1}{\theta(x,0)}dx$$

and the average or overall Nusselt number was calculated by integrating the temperature gradient over the heated wall as

$$Nu_{av} = \int_0^1 \frac{1}{\theta(x,0)}dx$$

with the boundary conditions

On the left wall (X = 0): U = V= 0 , $\frac{\partial\theta(0,Y)}{\partial X} = -1$

On the right wall (X = 1): U = V = 0, θ(1,Y) = 0 if U < 0 and $\frac{\partial\theta}{\partial X}(1,Y) = 0$ if U > 0

On the bottom wall (Y = 0): U = V = 0, θ = 1

On the Upper wall (Y = 1): U = V = 0, θ = 0

On the cylinder,

At the bottom and left side: U = V = 0, θ = 1

At the upper and right side: U = V = 0, θ = 0

4.3 Numerical Analysis

The governing equations along with the boundary conditions are solved numerically, employing Galerkin weighted residual finite element techniques discussed in previous chapter.

4. 3.1 Grid Independence Test

Preliminary results are obtained to inspect the field variables grid independency solutions. Test for the accuracy of grid fineness has been carried out to find out the optimum grid number.

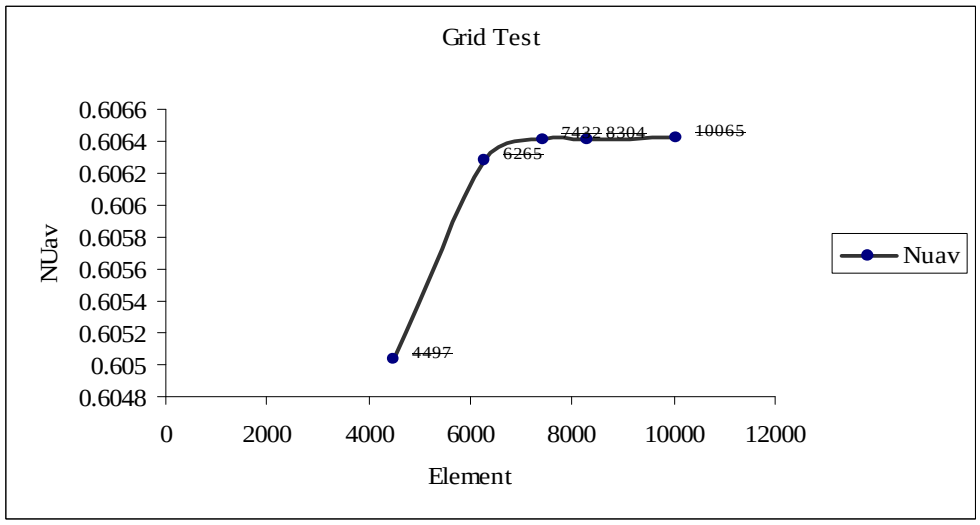

Figure 4.2 Convergence of average Nusselt number with grid refinement for $Gr = 10^6$ and $l_r = 0.2$

In order to obtain grid independent solution, a grid refinement study is performed for a square open cavity with $Gr = 10^6$ and $l_r = 0.2$. Figure 4.2 shows the convergence of the average Nusselt number, Nu_{av} at the heated surface with grid refinement. It is observed that grid independence is achieved with 4803 elements where there is insignificant change in Nu with further increase of mesh elements. Five different non-uniform grids with the following number of nodes and elements were considered for the grid refinement tests: 29808 nodes, 4497 elements; 41300 nodes, 6265 elements; 48840 nodes, 7432 elements; 54557 nodes, 8304 elements; 72408 nodes, 10065 elements. From these values, 54557 nodes, 8304 elements can be chosen throughout the simulation to optimize the relation between the accuracy required and the computing time.

Nodes (elements)	29808 (4497)	41300 (6265)	48840 (7432)	54557 (8304)	72408 (10065)
Nu	0.605032	0.60628	0.60641	0.60641	0.60642
Time (s)	243.406	303.938	476.719	737.656	993.125

Table 4.1: Grid Sensitivity Check at $Pr = 0.72$, $l_r = 0.2$, and $Gr = 10^6$.

4.4 Results and Discussion

The proposed problem in a square open cavity with the left vertical wall is at iso-heat flux has been studied numerically, as shown in Figure 4.1. A partially heated square cylinder is placed at the center of the cavity and the opposite wall to the aperture is heated by iso-flux heat source. The other two remaining walls were kept cooled with Temperature Tc (Top wall) and heated with temperature Th (bottom wall). The Navier-Stokes equations along with the energy equations in two dimensional formed are solved using Galerkin finite element method. Results are obtained for a range of Grashof number from 10^3 to 10^6 at Pr = 0.72, 1.00 and 7.00 with constant physical properties. The parametric studies for a wide range of governing parameters show consistent performance of the present numerical approach to obtain as stream functions and temperature profiles. The computational results indicate that the heat transfer coefficient is strongly affected by Grashof number. Obviously for high values of Grashof number the errors encountered are appreciable and hence it is necessary to perform some grid size testing in order to establish a suitable grid size. Grid independent solution is ensured by comparing the results of different grid meshes for Gr = 10^6, which was the highest Grashof number. The total domain is discretized into 8304 elements that result in 54557 nodes.

In figure 4.3 – 4.12, a comparison between the steady-state patterns of streamlines and isotherms from Grashof numbers of 10^3 to 10^6 alone with different angles of cavity, different Prandtl number (Pr) and different length ratio (dr) are presented. we observe that the heat transfer in the cavity is quasi-conductive at Gr = 10^3 and becomes dominated by convective regime as Gr increases to 10^6. The figures show that as the Grashof number and the inclination angle increases, the buoyancy force increases and the thermal boundary layers become thinner gradually for isotherm .The isotherms pattern show that the cold fluid penetrates right to the hated wall as increases of Gr = 10^3 to 10^6 where the temperature gradient is more steep. The fluid penetrates to heated wall and the isotherm become more packed to cold wall which suggest that the flow moves faster as natural convection is intensified. For the streamlines, the figures show that the fluid enters from the bottom of the aperture, circulates in a clockwise direction following the shape of the cavity, and leaves toward the upper part of the aperture. The streamline patterns is very similar for last one Grashof number and the inclination angle, but the fluid moves faster and created vortices for Gr of 10^3 to10^5. From the figure 4.3 – 4.12,

the velocity gradient increases at lower heated wall and the strength of the circulation increases with the increase of inclination angle of the heated wall. The results in the steady state are obtained for Grashof number 10^3 to 10^6 and the inclination angles of 0^o-45^o of the cavity. The Nusselt number changes substantially with the inclination angle of the cavity for high Grashof numbers. The numerical model predicted Nusselt number oscillations for low angles and high Grashof numbers.

4.4.1 Effects of Inclination Angle

Complex flow pattern characteristics are found for some inclination angles with the increase of the Grashof number. The profiles of isotherm and streamline are presented in Fig. 4.3 to 4.8 with inclination angles of 0^o- 45^o. The steady state can not be secured with the increase of angles of the cavity. In figure 4.3 – 4.8, we observe that the fluid enters and leaves in a very irregular way which indicates an unsteady convection. In the cavity, the cold fluid enters by the lower sections and the hot fluid leaves by the upper sections without regularity. The thermal boundary layer at the top wall becomes much thinner because of the velocity magnitude of the leaving fluid and it is greater than the incoming fluid. The average Nusselt number for different cavity's inclination angles and Grashof numbers, obtained with the present model for Pr = 0.72 and l_r = 0.2 is presented in table 4.2. This presents the average Nusselt numbers for different Gr and different angle of cavity. The average Nusselt number increases with Grashof number at different angle. Therefore, in Table 4.2, the average Nusselt numbers are reported. In Fig.4.13- 4.15, we observe that the heat transfer rate increasing with Grashof number and the increase of inclination angles.

Table 4.2: The Average Nusselt number Nu_{av} for different cavity's inclination angles Φ and Grashof numbers for Pr = 0.72 and l_r = 0.2.

	Nu_{av}			
Φ	Gr=10^3	Gr=10^4	Gr=10^5	Gr=10^6
0^o	0.607032	1.279575	2.466157	4.465709
15^o	0.846723	1.743181	3.411222	6.168179
30^o	0.594534	1.257437	2.472528	4.625688
45^o	0.607886	1.285933	2.54265	4.868601

4.4.2 Effects of Prandtl Number

The flow patterns and heat transfer characteristics affected by different Prandtl number Pr(0.72, 1.00 and 7.00) are shown. It is seen that fluid moves clock wise around the square cylinder and the pattern of isotherms and stream lines are shown in figure 4.9 to 4.10.

In Table 4.3, the average Nusselt numbers obtained for different Prandlt numbers while *Pr* = 0.72, 1.0 and 7.0 and Grashof numbers is presented.

The average Nusselt number variation for different Prandtl numbers *Pr* = 0.72, 1.00, 7.00 with different angle are shown in fig. 4.16 – 4.19. From these figure, we observe that average Nusselt number Nu_{av} increases with increasing of Grashof number *Gr*. In fig. 4.17 and 4.18, we also see that heat transfer rate decrease with increasing Prandtl number *Pr*. Heat transfer characteristics become low for higher Prandtl number *Pr* = 7 and high for lower *Pr* = 0.72. So the results show insignificant for different angles.

Table 4.3: Average Nusselt numbers for different Prandtl number while *Pr* = 0.72, 1.0 and 7.0, angle $\Phi = 0^o$ and l_r = 0.2.

	Nu_{av}			
Pr	$Gr=10^3$	$Gr=10^4$	$Gr=10^5$	$Gr=10^6$
0.72	0.607032	1.279575	2.466157	4.465709
1.0	0.497109	1.104225	2.172888	3.942645
7.0	0.68205	1.432603	2.817915	5.31084

4.4.3 Effects of Length ratio

The average Nusselt numbers for different length while *lr* = 0.2, 0.3 and 0.4 and Grashof numbers, obtained with the present model for angle $\Phi = 0^o$ and Prandlt number Pr = 0.72 is presented in table 4.4. Figure 4.20 shows average Nusselt number increases with increasing of length ratio of the square cylinder for Gr of 10^3 to 10^6 expect l_r = 0.2. This cause, the heated portion is extended of the square cylinder. At 10^6 the average Nusselt number is more for *l*r = 0.2. At 10^6 the Nu_{av} is more for lr = 0.2 and average Nusselt number increases with increasing of Grashof number.

Table 4.4: Average Nusselt numbers for different diameter ratios while l_r = 0.2, 0.3 and 0.4, angle $\Phi = 0^o$ and *Pr* = 0.72.

Nu_{av}				
lr	Gr=10^3	Gr=10^4	Gr=10^5	Gr=10^6
0.2	0.607032	1.279575	2.466157	4.465709
0.3	0.806891	1.450436	2.619125	4.504048
0.4	0.8038	1.462845	2.565466	4.193945

4.5 Chapter Summary

Numerical calculation has been presented for steady state laminar natural convection flow in a square open cavity with the left vertical wall is at iso-heat flux. Here we consider the range of Prandtl numbers (0.72, 1.00 and 7.00) and Grashof numbers (10^3 to 10^6). The calculation of the mean Nusselt number as a function of Pr, length ratio l_r and angle of inclination of the cavity has been presented. The results show:

- Heat transfer depends on Prandtl number and heat transfer rate increases for higher Prandtl number for angle 0^0 and 45^0.Again heat transfer rate decreases for higher Prandtl number and increase for lower Prandtl number at angle 15^0 and 30^0.
- Thermal boundary layer thickness is thinner with increasing of Grashof number.
- The heat transfer rate increases for increasing Grashof number.
- The heat transfer rate Nu_{av} changes with the increase of inclination angles, and average Nusselt number increases with increasing Grashof number.
- The heat transfer rate Nu_{av} increases with the increase of length ratio l_r but decreases when l_r = 0.4 for Grashof number 10^6.
- Various vortices enter the flow field and secondary vortex exist at different places in the cavity.

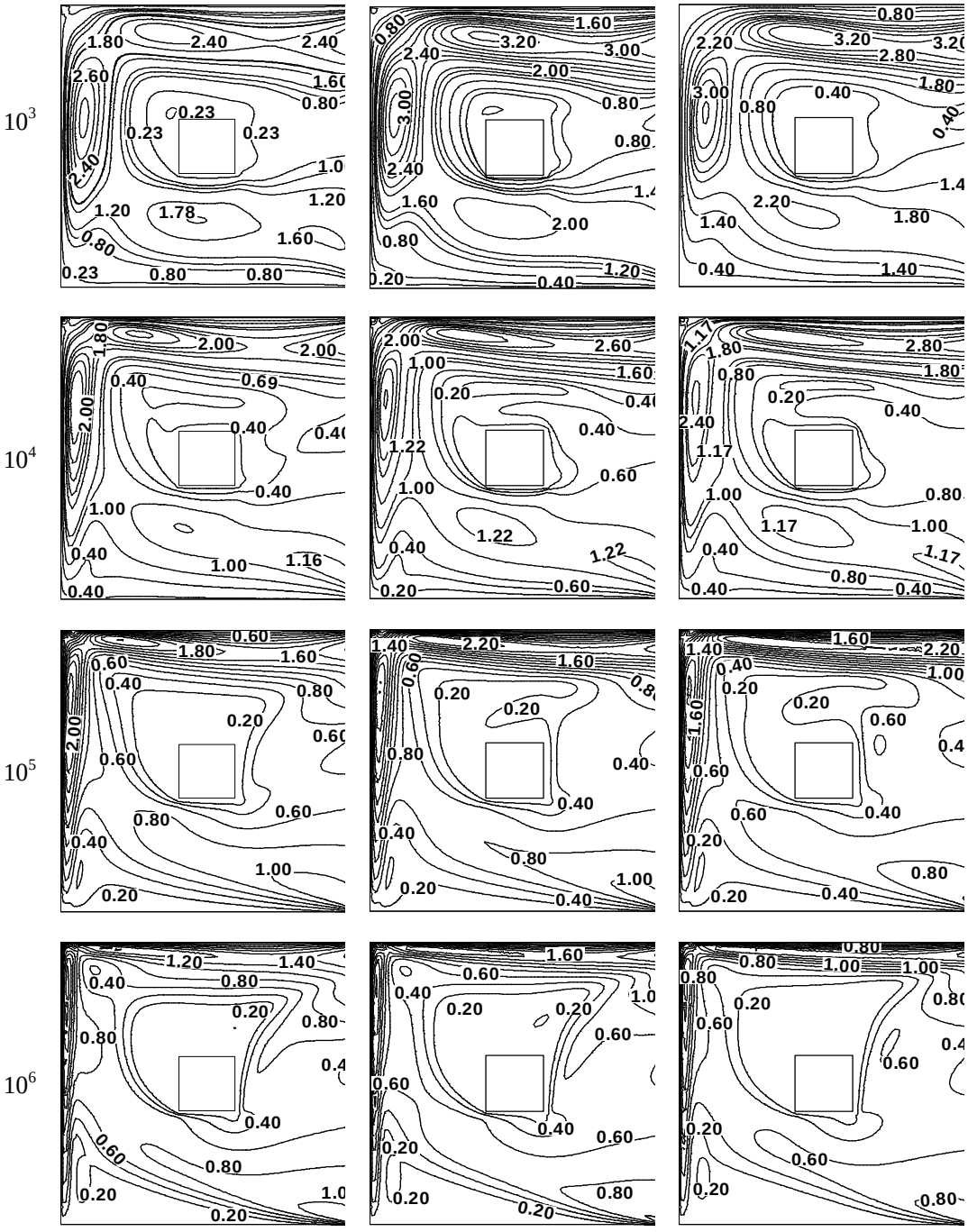

Fig 4.3: Streamline patterns for different angles with *lr* = 0.2 and *Pr* = 0.72

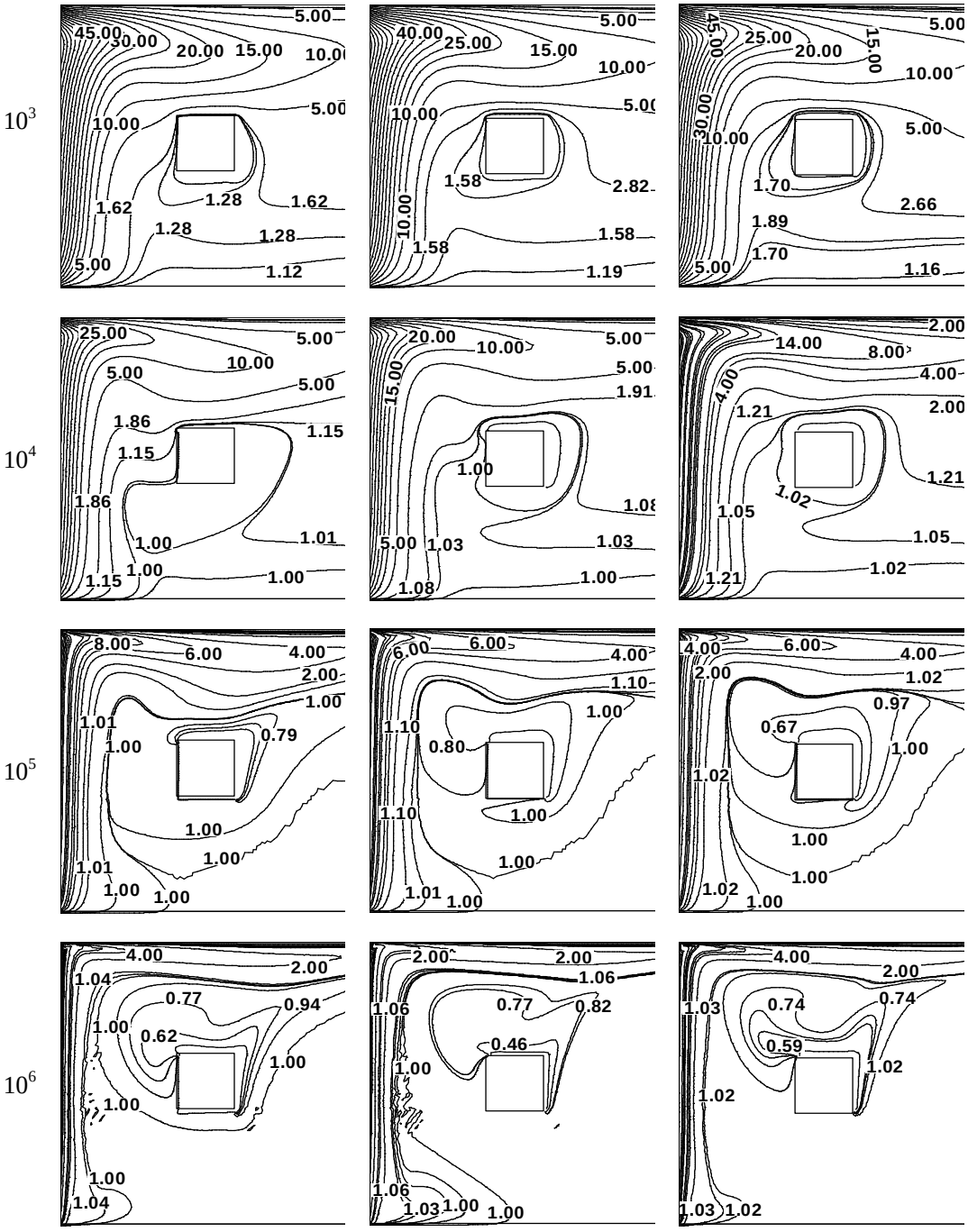

Fig 4.4: Isotherm patterns for different angles with *lr* = 0.2 and *Pr* = 0.72

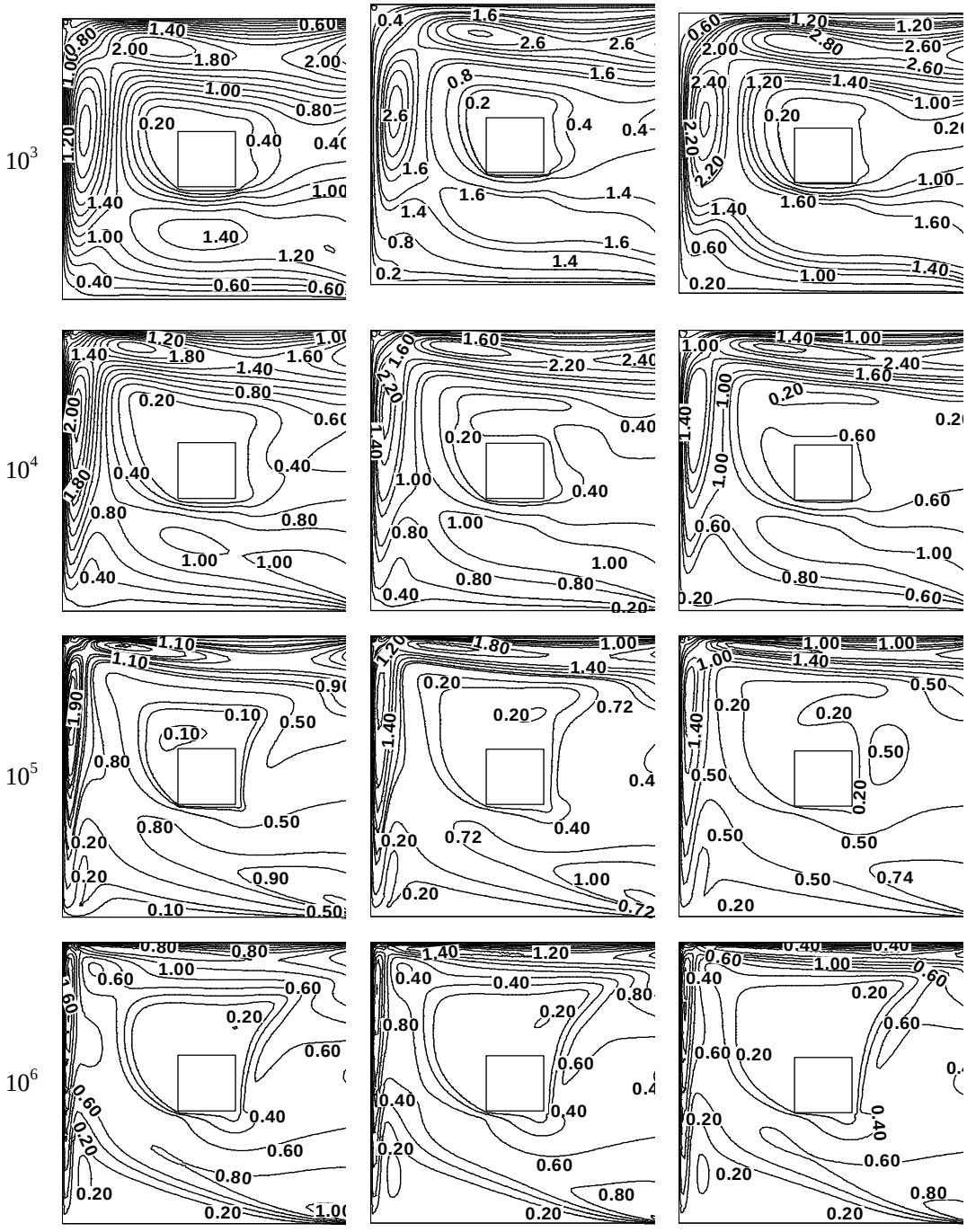

Fig 4.5: Streamline patterns for different angles with *lr* = 0.2 and *Pr* = 1.00

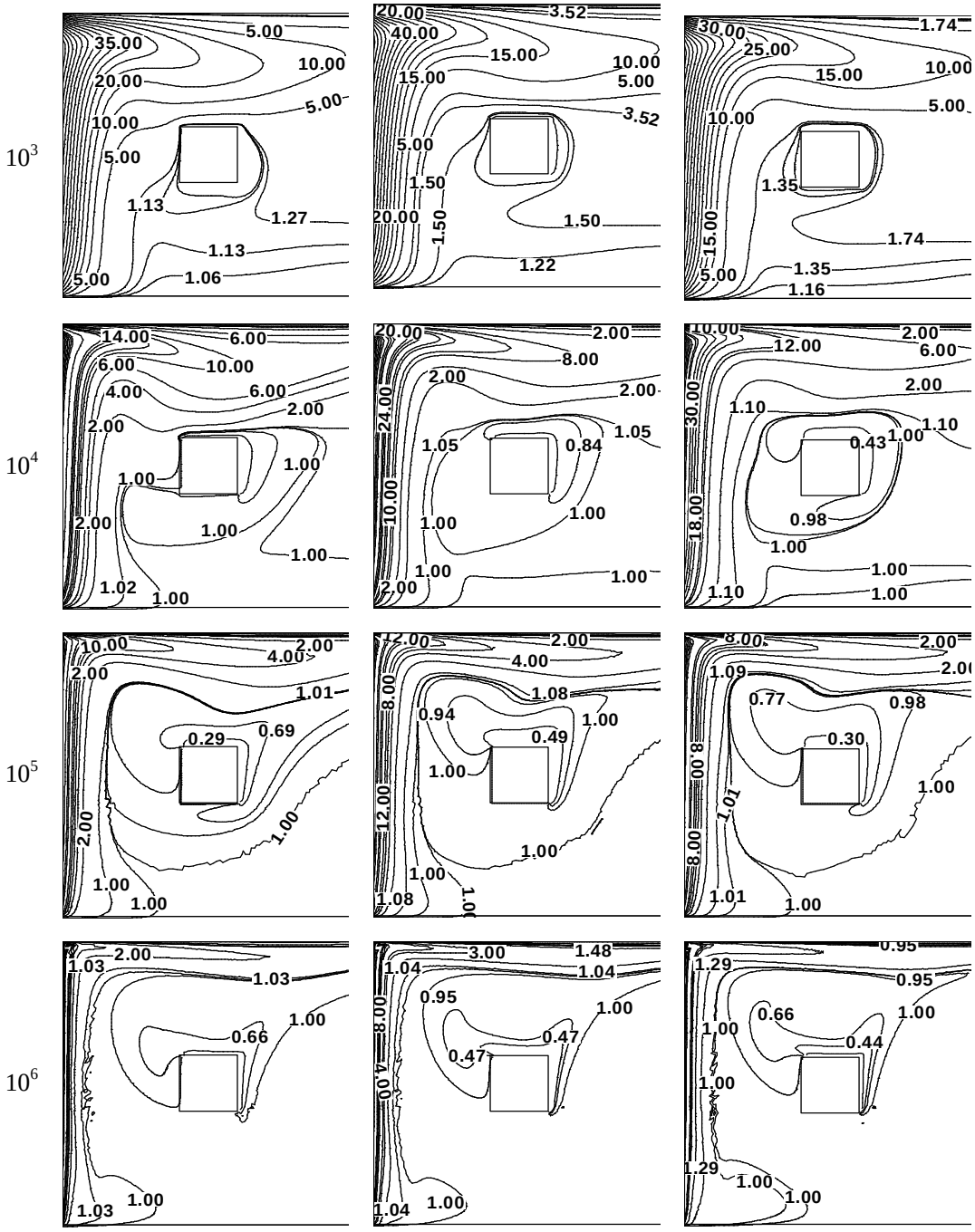

Fig 4.6: Isotherm patterns for different angles with *lr* = 0.2 and *Pr* = 1.00

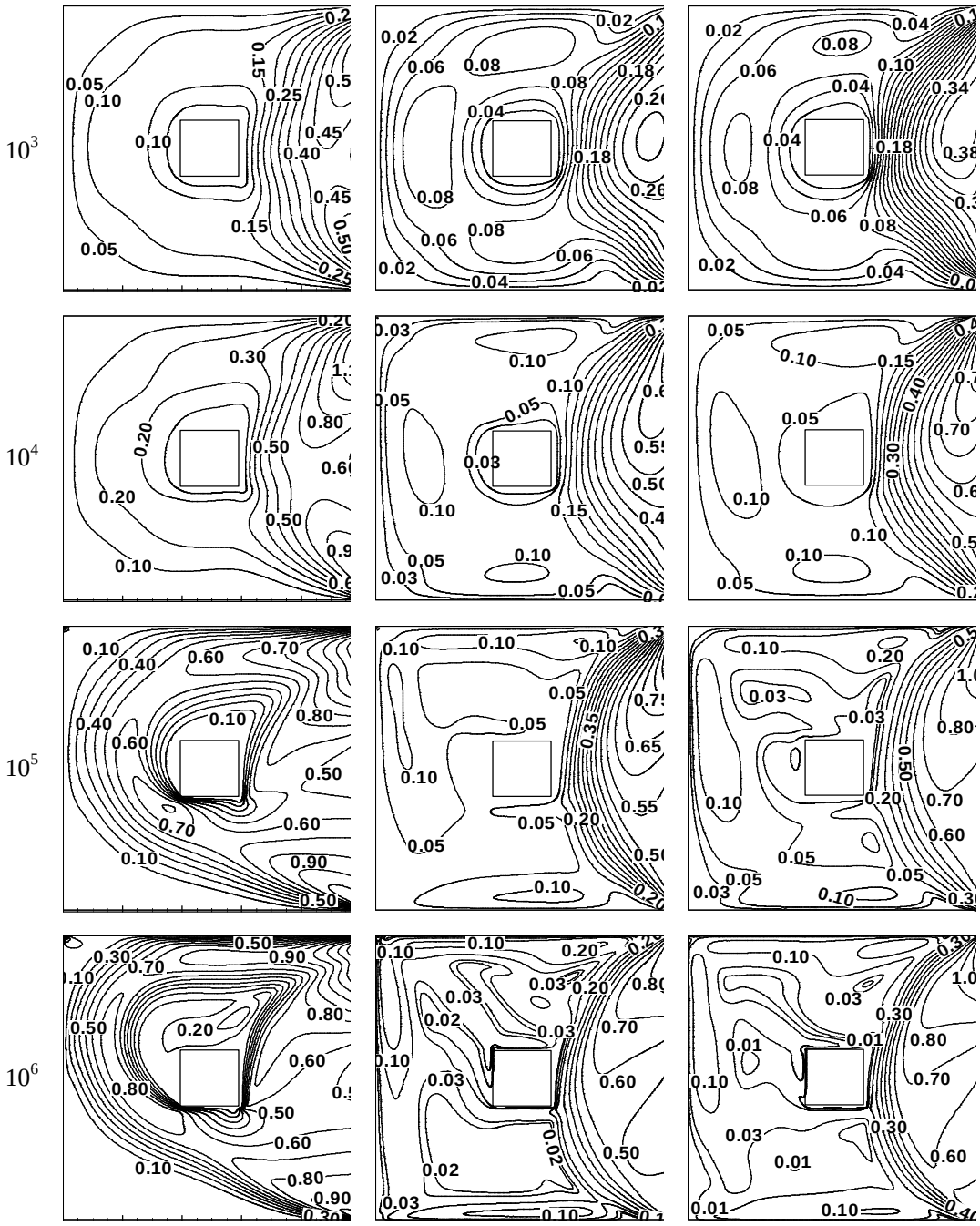

Fig 4.7: Streamline patterns for different angles with *lr* = 0.2 and *Pr* = 7.00

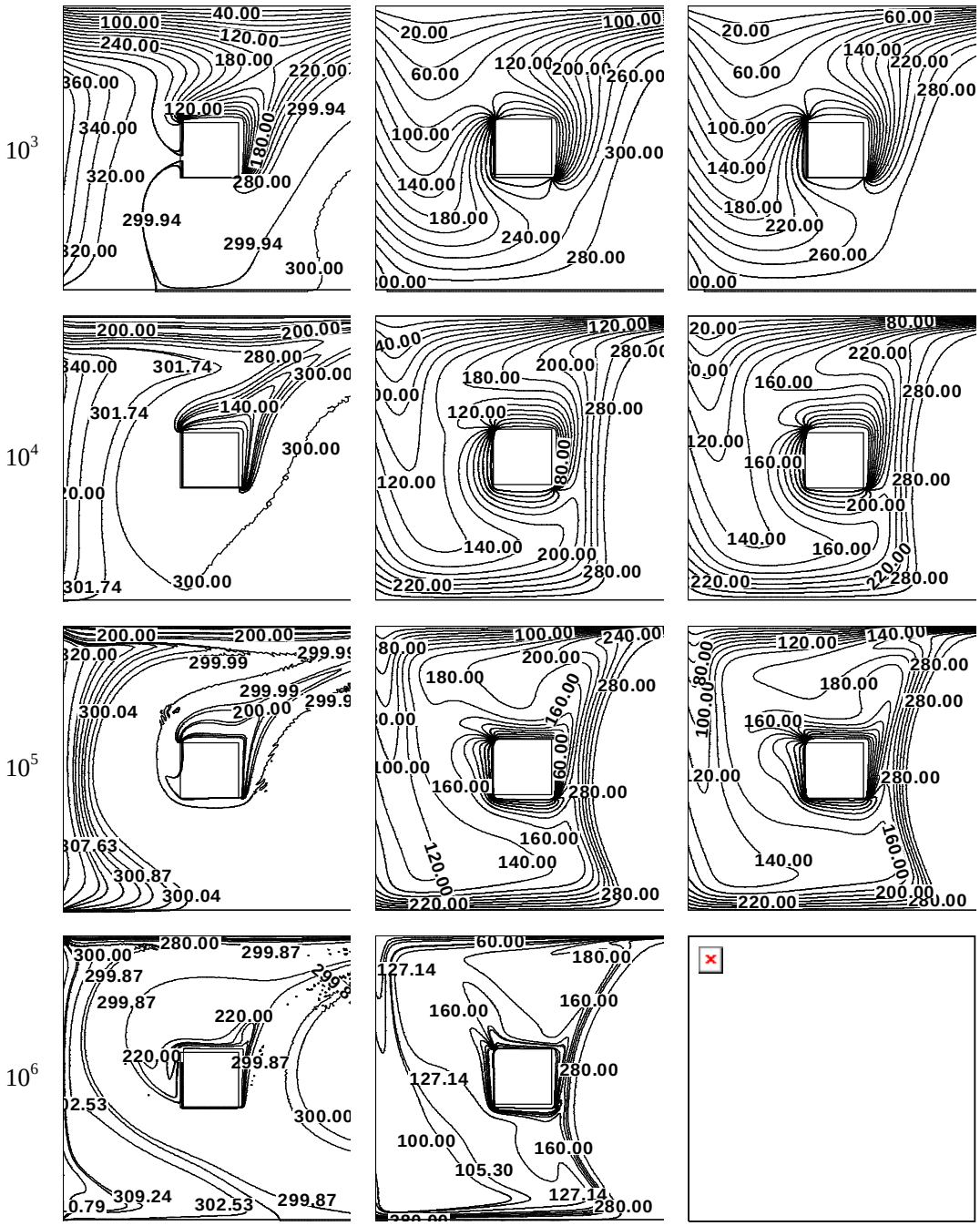

Fig 4.8: Isotherm patterns for different angles with *lr* = 0.2 and *Pr* = 7.00

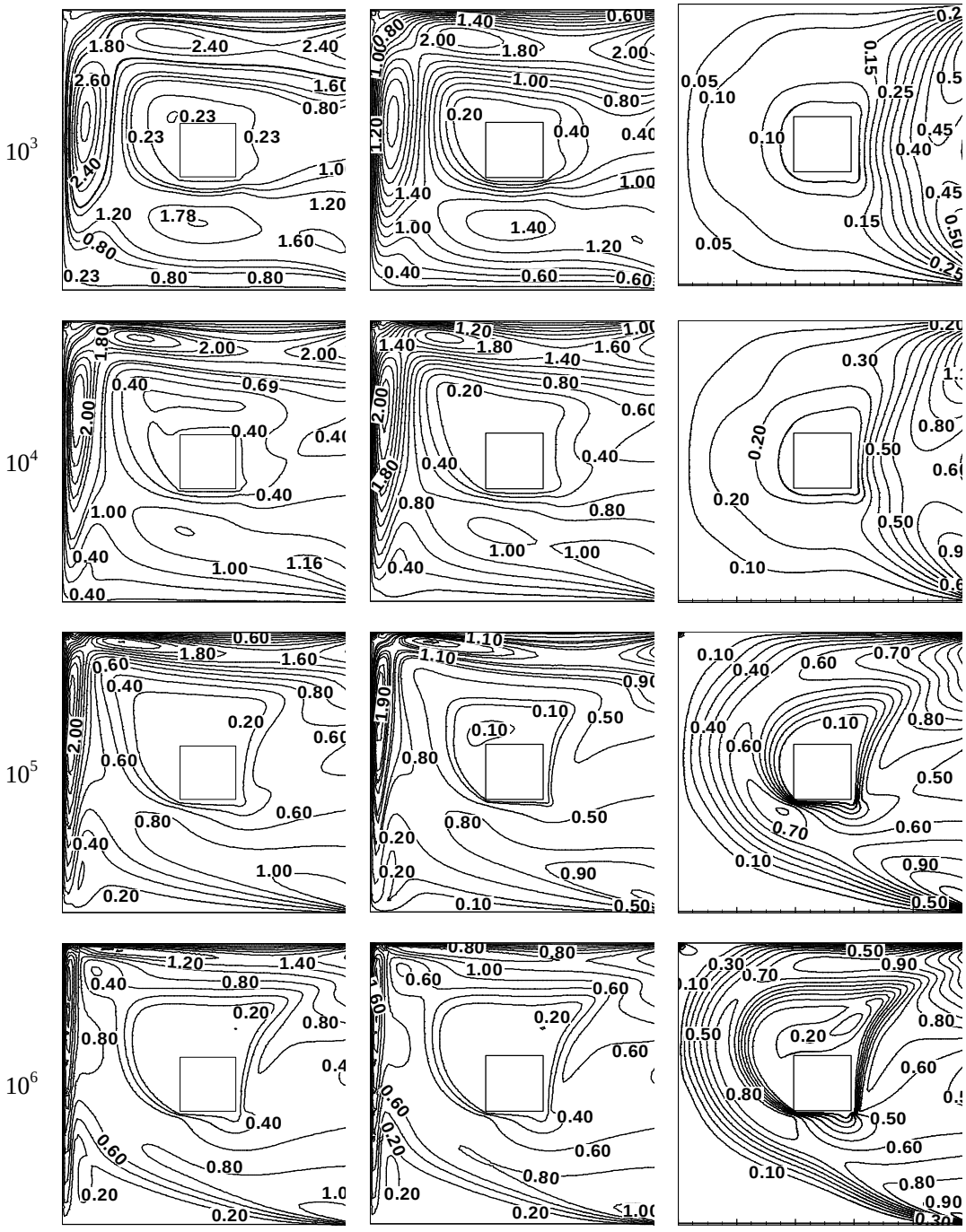

Fig 4.9: Streamline patterns for different Pr with *lr* = 0.2 and Φ= 0°

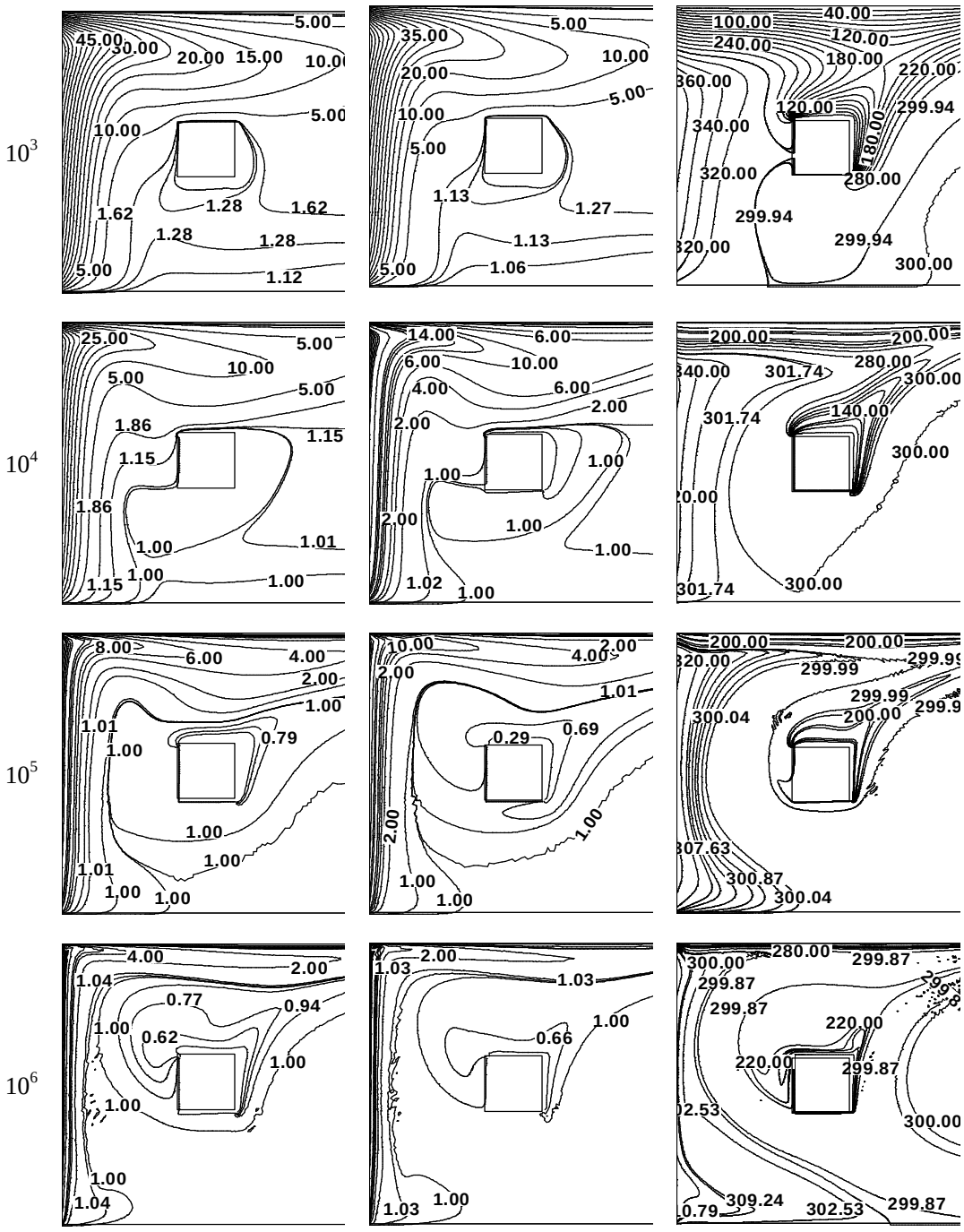

Fig 3.10: Isotherm patterns for different Pr with *lr* = 0.2 and $\Phi = 0^0$

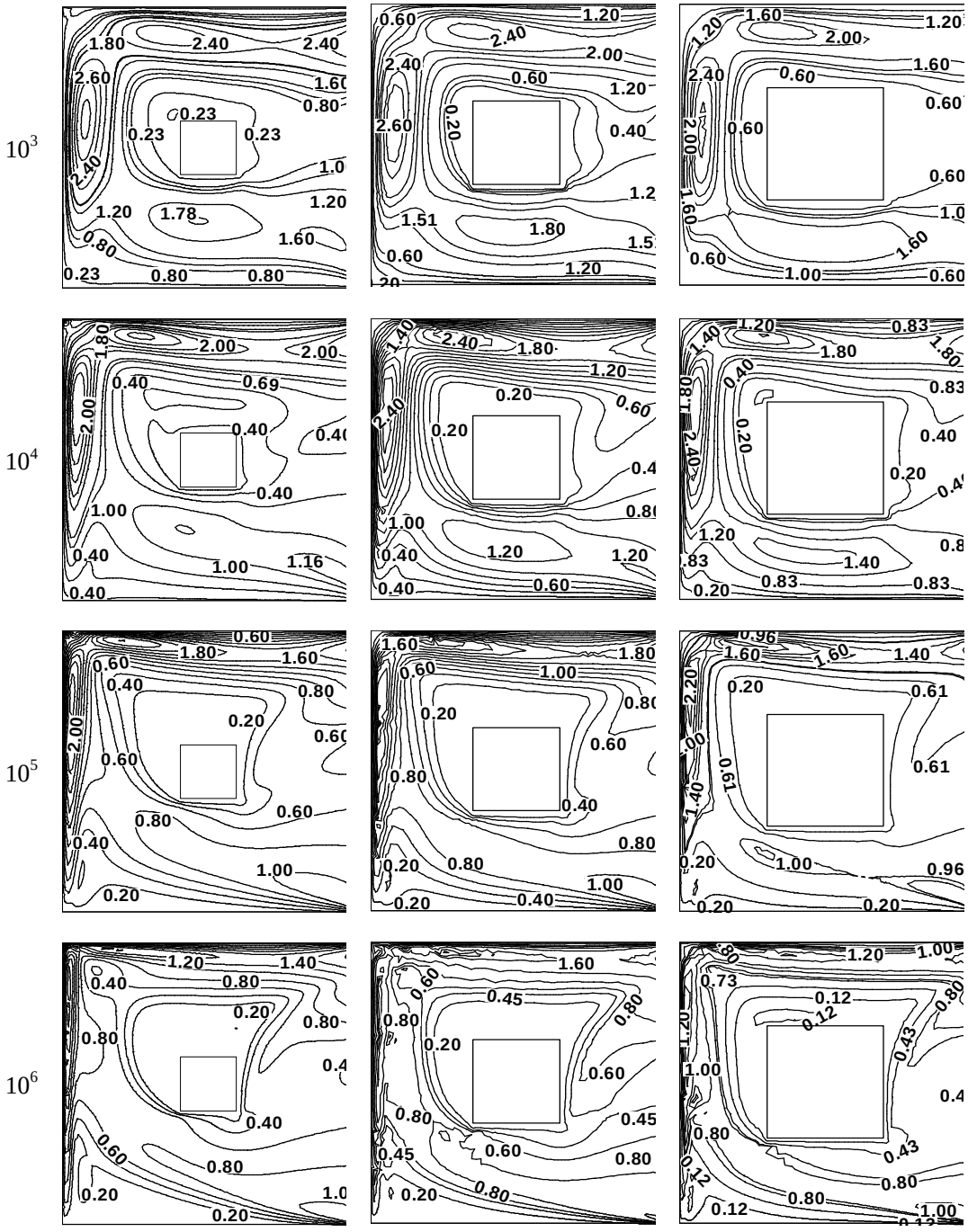

Fig 4.11: Streamline patterns for different *l*r with P*r* = 0.72 and $\Phi = 0^0$

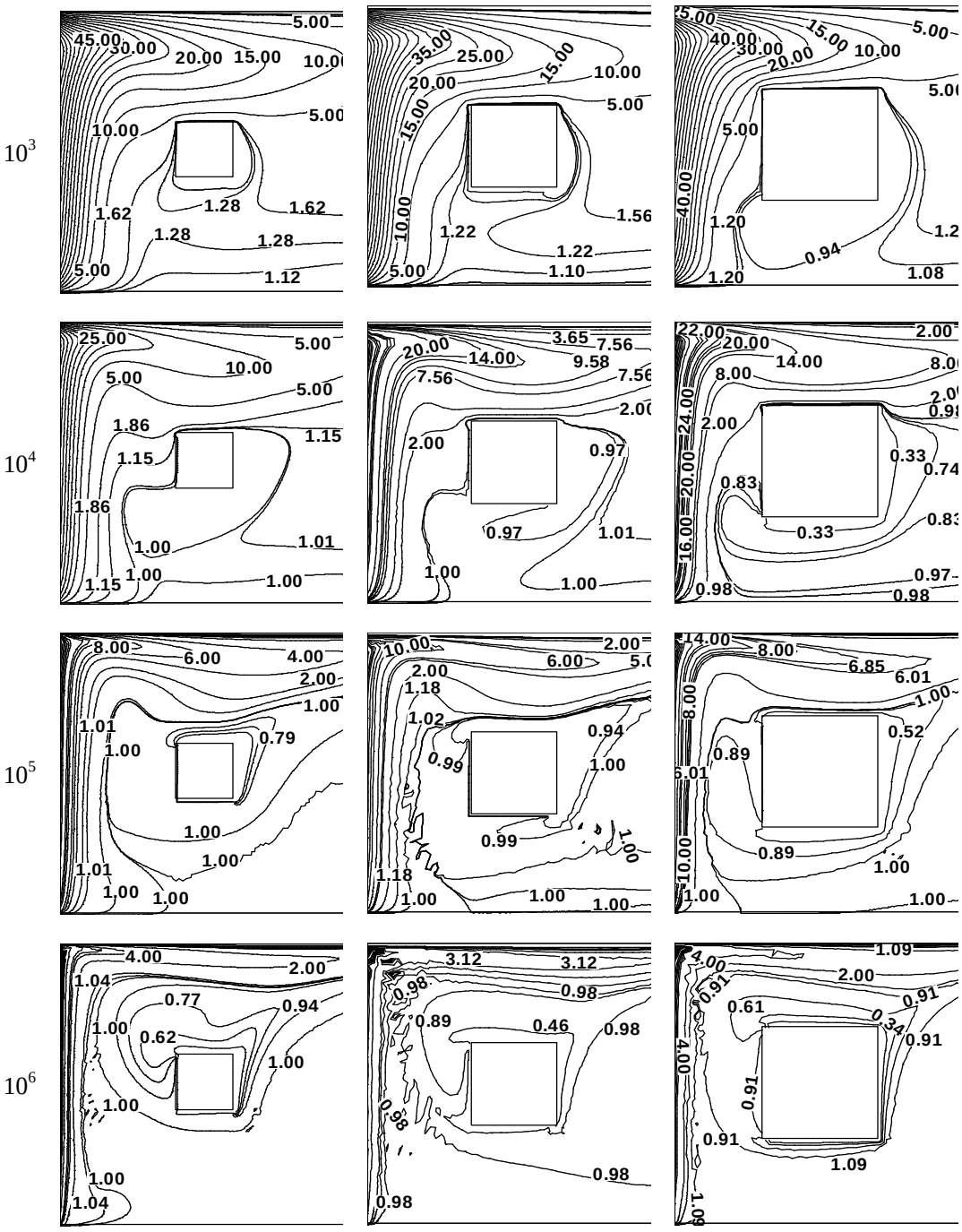

Fig 4.12: Isotherm patterns for different *l*r with *pr* = 0.72 and $\Phi = 0^0$

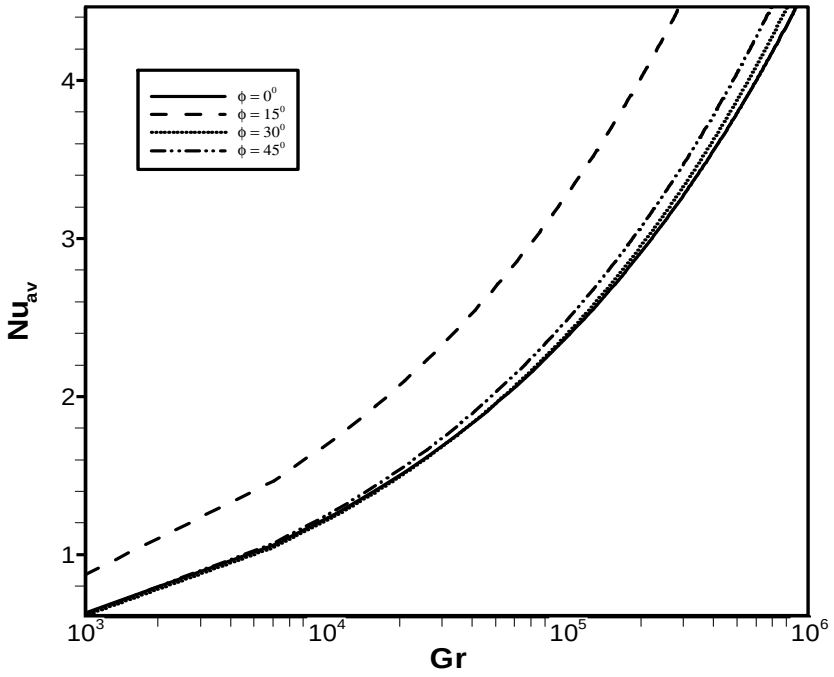

Fig.4.13: Effect of inclination angle on average Nusselt number and Grashof number while Pr = 0.72, l_r = 0.2.

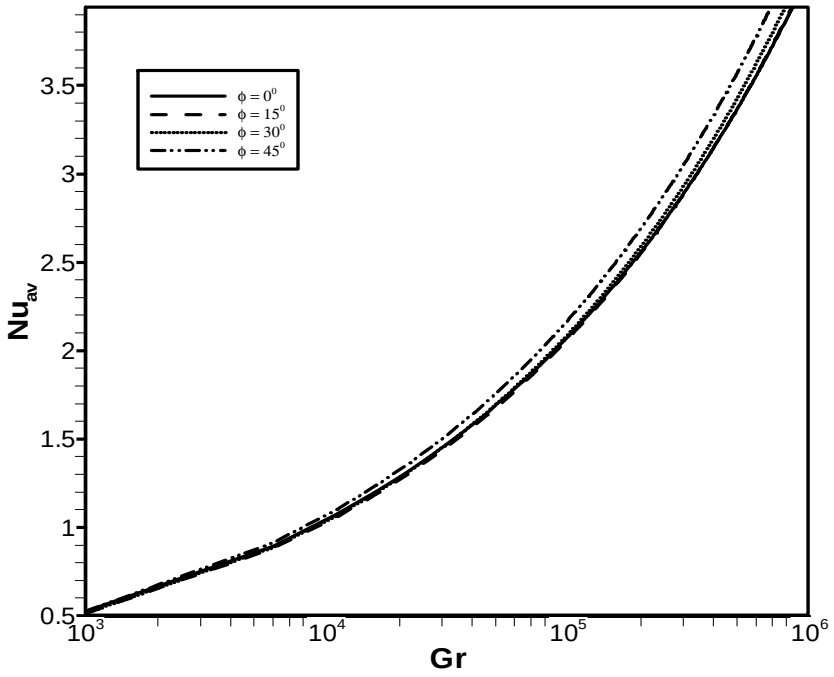

Fig.4.14: Effect of inclination angle on average Nusselt number and Grashof number while Pr = 1.0, l_r = 0.3.

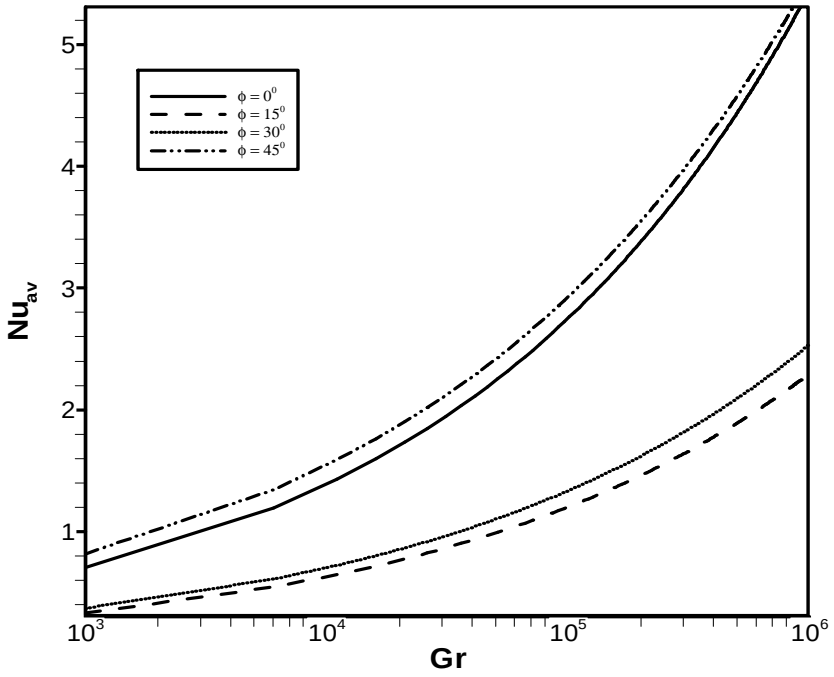

Fig.4.15: Effect of inclination angle on average Nusselt number and Grashof number while Pr = 7.0, l_r = 0.4.

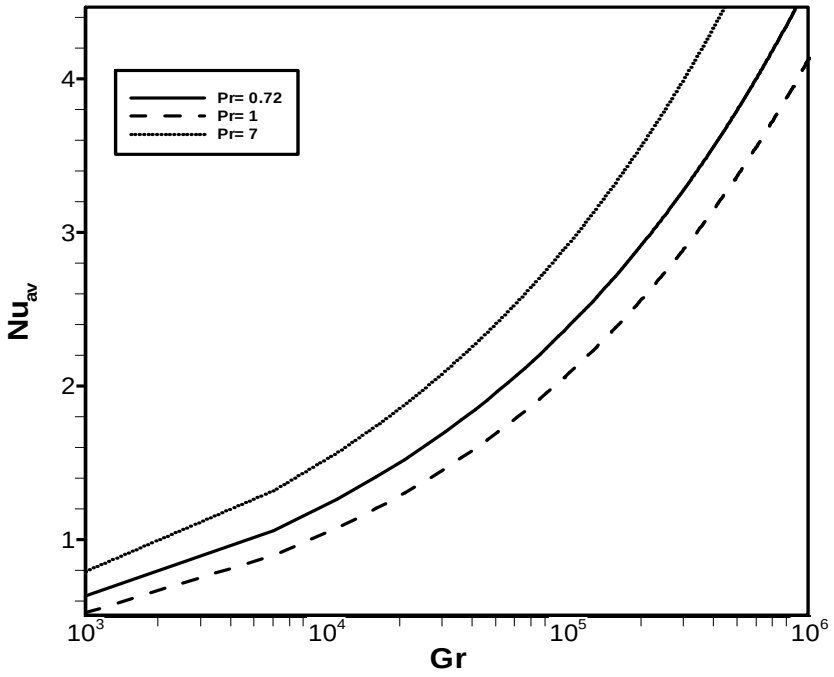

Fig.4.16: Effect of Prandtl number on average Nusselt number and Grashof number while Pr = 0.72, 1.0 and 7.0, angle 0^o and l_r = 0.2.

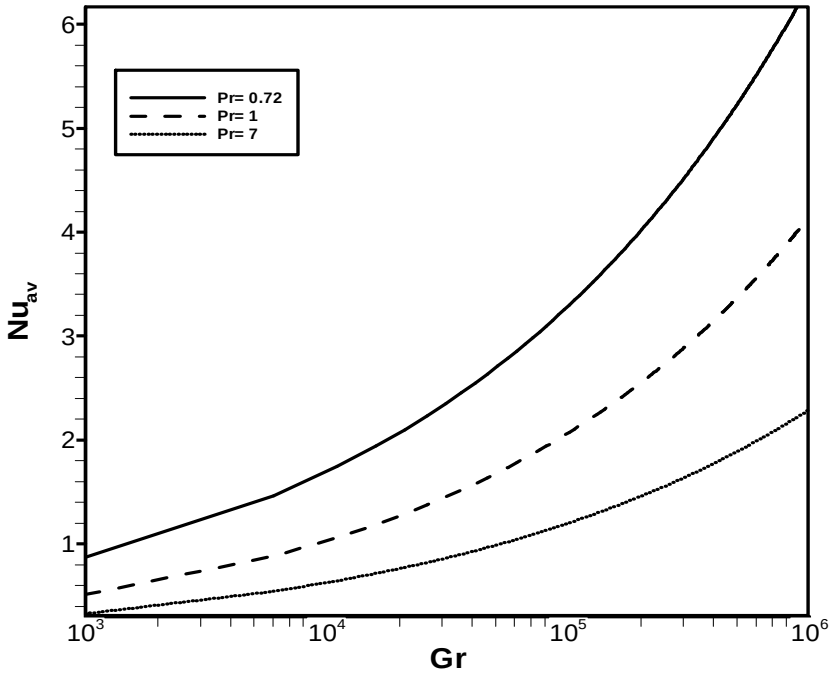

Fig.4.17: Effect of Prandtl number on average Nusselt number and Grashof number while Pr = 0.72, 1.0 and 7.0, angle 15^o and l_r = 0.2.

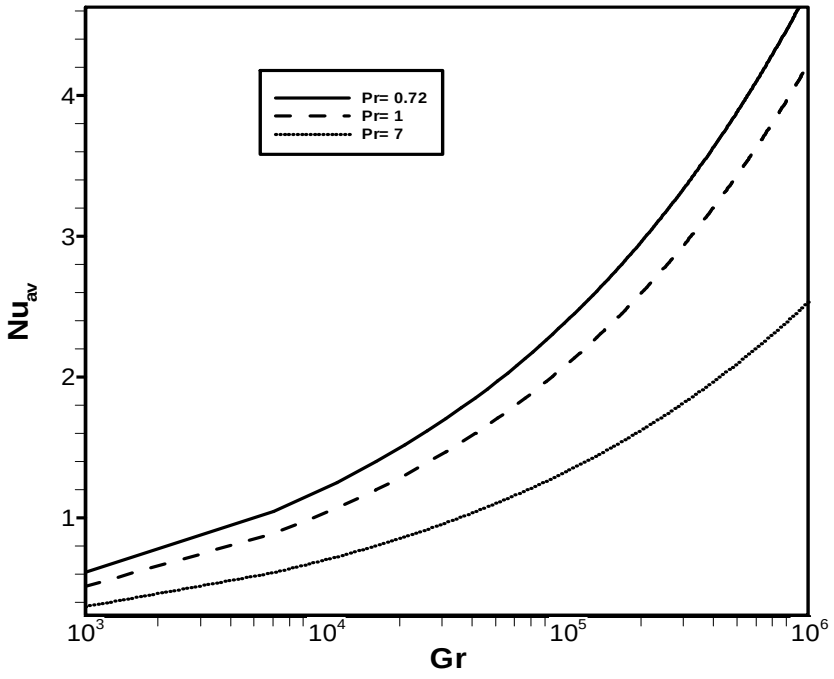

Fig.4.18: Effect of Prandtl number on average Nusselt number and Grashof number while Pr = 0.72, 1.0 and 7.0, angle 30^o and l_r = 0.2.

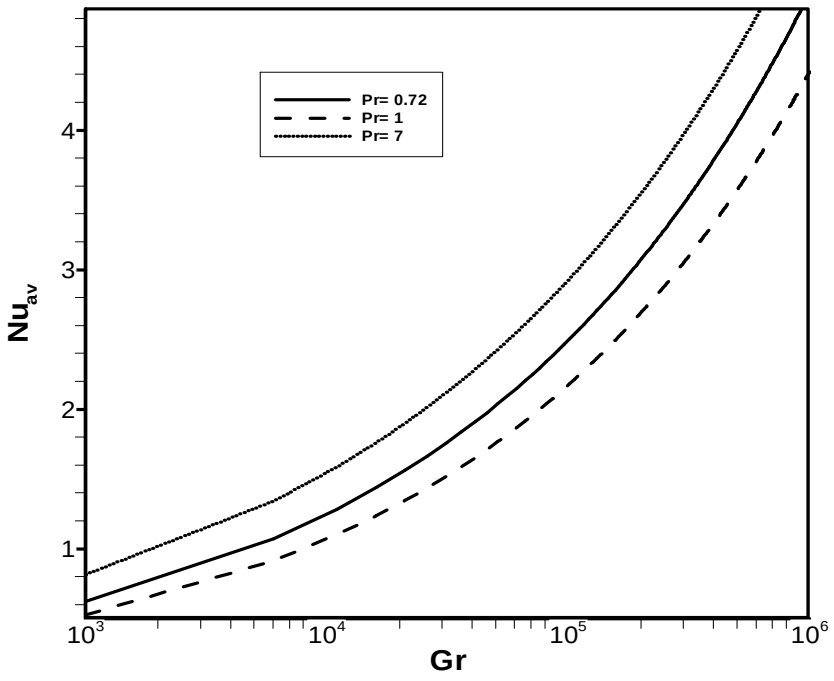

Fig.4.19: Effect of Prandtl number on average Nusselt number and Grashof number while Pr = 0.72, 1.0 and 7.0, angle 45^o and l_r = 0.2.

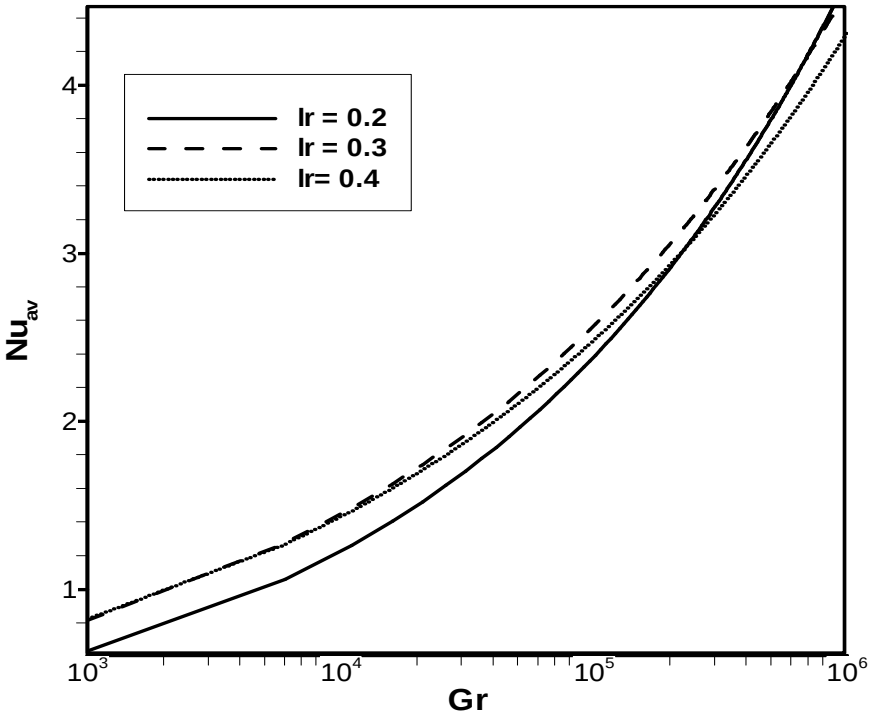

Fig.4.20: Effect of length on average Nusselt number and Grashof number while Pr = 0.72, 1.0 and 7.0, angle 0^o.

CHAPTER 5

5.1 Summary of Major Out Comes

The study has been confined to cases of partially heated circular cylinder and square circular in an open square cavity. In cases of partially heated circular cylinder, the stream line of flow and thermal fields as well as characteristics of heat transfer process particularly its expansion has been evaluated in chapter 3. On the basis of the analysis the following conclusions have been drawn:

(i) The partially heated square cylinder has significant effect on the flow and thermal distributions in an open square cavity. The average Nusselt number (*Nu*) at the hot wall is the highest for the angle 45^0 when Grashof number 10^6, whereas the lowest heat transfer rate for the angle 0^0 when Grashof number 10^3. Moreover, the average Nusselt number, when circular cylinder is considered is higher than those obtained with square cylinder for different angle.

(ii) The heat transfer rate Nu_{av} decreases with the increase of diameter ratio for Gr^3 - Gr^5 and increase of Grashof number Gr^6.

(iii) Heat transfer depends on Prandtl number and heat transfer rate decreases for higher Prandtl number but increase for lower prandtl number.

(iv) Thermal boundary layer thickness is thinner for increasing of Grashof number. The heat transfer rate increases for Grashof number 10^3 to 10^6 gradually.

(v) Various vortices entering into the flow field and a secondary vortex at the center and bottom wall of the cavity is seen in the streamlines.

In cases of partially heated square cylinder, the stream line of flow and thermal fields as well as characteristics of heat transfer process particularly its expansion has been evaluated in chapter 4. On the basis of the analysis the following conclusions have been drawn:

(i) The effect on the flow and thermal distributions in an open square cavity for partially heated square cylinder. The average Nusselt number (Nu) at the hot wall is the highest for the angle 15^0 when Grashof number 10^6, whereas the lowest heat transfer rate for the angle 30^0 when Grashof number 10^3.

(ii) The heat transfer rate Nu_{av} closely ups and down with the increase of inclination angles and average Nusselt number increases with increasing Grashof number.

(iii) Prandtl number influnces isotherms, streamlines and heat transfer rate in the cavity.The heat transfer rate increases with increase of Pr. The average Nusselt number (Nu_{av}) is more for higher Prandtl number at angle 0^0 and 45^0.Again heat transfer rate decreases for higher Prandtl number and increase for lower Prandtl number at angle 15^0 and 30^0.

(iv) The heat transfer rate Nu_{av} increases with the increase of length ratio l_r = 0.2 to 0.3 but decreases when l_r = 0.4 for Grashof number. Thermal boundary layer thickness is thinner for increasing of Grashof number.

(v) Various vortices entering into the flow field and a secondary vortex at different place in the cavity.

5.2 Comparison of Partially heated circular cylinder (PHCC) and square cylinder (PHSC)

The isotherms and streamlines have been influenced by PHCC and PHSC in an open square cavity. The heat transfer rate is higher for PHCC than PHSC at different Gr because of the shape of cylinder. The average Nusselt number increases with the increases of Grashof number Gr = 10^3 -10^6 for both cylinders. In order to validate the numerical code, pure natural convection with Pr = 0.72 in a square open cavity has been solved. The results are compared with PHCC and PHSC. In table 5.1, a comparison between the average Nusselt numbers are presented for both cylinders. The results of both cylinders are almost same. We see that the difference of Nu_{av} are in table 5.1, it shows that the highest difference of Nu_{av} is 1.695381 at Gr = 10^6, the lowest is 0.293443 at Gr = 10^4, with an average difference is 0.705905. The reason for the large difference at high Gr = 10^6 is explained by the fact that the heat transfer is dominated by convection regime.

Table 5.1: Comparison of the results of PHCC and PHSC for the constant surface temperature with Pr = 0.72.

Gr	Nu_{av}		
	PHCC	PHSC	Difference
10^3	3.795779	3.449382	0.346397
10^4	4.608153	4.314710	0.293443
10^5	6.373589	5.885192	0.488397
10^6	9.947833	8.252452	1.695381

5.3 Extension Works

The consequent can be ahead for the additional works on the base of the present research as.

- In the future, the study can be extended by dissimilar physics like radiation effects, heat generation and tube effects.
- Effect of conduction on mixed convection flow in a square open cavity with a heat conducting square cylinder.
- Effect of conduction on mixed convection flow in a square open cavity with a heat conducting circular cylinder.
- The study can be extended for non-uniform surface temperature using different fluids
- The study can be performed by using magnetic cylinder instead of partially heated rectangular cylinder.
- Investigation can be performed by using magnetic fluid within the porous medium and changing the boundary conditions of the cavity's walls.
- Investigation can be performed by using inlet-outlet with various place in the cavity.
- Two-dimensional fluid flow and heat transfer has been analyzed in this thesis. So this consideration may be extended to three-dimensional analyses to explore the effects of parameters on flow fields and heat transfer in cavities. In addition, the problem of fluid flow and heat transfer along with heat generating cylinder may be studied in three-dimensional cases.

References

[1] Arnold, J. N., Catton, I., and Edwards, D. K., "Experimental Investigation of Natural Convection in Inclined Rectangular Regions of Differing Aspect Ratios," Journal of Heat Transfer, Vol. 98, pp.67-71, 1976.

[2] Bilgen, E., and Oztop, H., "Natural convection heat transfer in partially open inclined square cavities", Int. J. of Heat and Mass Transfer, Vol. 48, pp. 1470-1479, 2005.

[3] Chan,Y. L. and Tien, C. L., "A Numerical study of two-dimensional laminar natural convection in a shallow open cavity", Int. J. Heat Mass Transfer, Vol. 28, pp. 603-612,1985.

[4] Chan,Y. L. and Tien, C. L., "A Numerical study of two-dimensional natural convection in square open cavities", Numerical Heat Transfer, Vol. 8, pp. 65-80, 1985.

[5] Chen, C. J. and Talaie, V., "Finite Analytic Numerical Solutions of Laminar Natural Convection in Two-Dimensional Inclined Rectangular Enclosures," ASME paper 85-HT-10, 1985.

[6] Cook, R. D., Malkus, D. S., and Plesha, M. E., "Concepts and applications of finite element analysis", Third Ed., John Wiley & Sons, New York, 1989.

[7] Chung.T.J.,"Computational Fluid Dynamices", Second Ed., Cambridge, 2002.

[8] Dechaumphai, P. Adaptive finite element technique for heat transfer problems, Energy, Heat & Mass transfer, Vol. 17, pp. 87-94, 1995.

[9] Dechaumphai, P., Finite Element Method in Engineering, second Ed., Chulalongkorn University Press, Bangkok,1999.

[10] Elsherbiny, S.M., Raithby, G. D., and Hollands, K. G. T., "Heat Transfer by Natural Convection across Vertical and Incline Air Layers", Transactions of the ASME, Vol. 104, pp. 96-102, 1982.

[11] Frederick, R. L. "Natural convection in an inclined square enclosure with a partition attached to its cold wall", Int. J. Heat and Mass Transfer,Vol. 32, pp. 87–94, 1989.

[12] Ferziger, J. H. and Perić, M., "Computational methods for fluid dynamics", Second Ed., Springer Verlag, Berlin Hedelberg, 1997.

[13] Gallagher, R. H., Simon, B. R., Johnson, P. C. and Gross, J. F., Finite elements in biomechanics, John Wiley & Sons, New York, 1982.

[14] Goutam Saha, Sumon Saha and Md. Arif Hasan Mamun, "A Finite Element Method for Steady-State Natural Convection in a Square Tilt Open Cavity", ARPN Journal of Engineering and Applied Sciences, Vol. 2, No. 2, pp. 41-49, 2007.

[15] Hamady, F. J., Lloyd, J. R., Yang, H. Q., and Yang, K. T., "Study of Local Natural convection Heat Transfer in an Inclined Enclosure," International Journal of Heat and Mass Transfer, Vol. 32, pp.1697-1708, 1989.

[16] Hinojosa, J. F., Estrada, C. A., Cabanillas, R. E., and Alvarez, G., "Nusselt number for the natural convection and surface thermal radiation in a square tilted open cavity", Int. Com. In Heat and Mass Transfer, Vol. 32, pp. 1184-1192, 2005.

[17] Jini, J., The finite element method in electromagnetics, John Wiley & Sons, New York, 1993.

[18] Kangni, A., Ben, R. and Bilgen, E. “Natural convection and conduction in enclosure with multiplevertical partitions”, Int. J. Heat and Mass Transfer,Vol. 34, pp. 2819–2825, 1991.

[19] Kuhn, D. and Oosthuizen, P. H., “Unsteady natural convection in a partially heated rectangular cavity”, ASME Journal of Heat Transfer, Vol. 109, pp. 789–801, 1987.

[20] Kuyper, R.A., Van Der Meer, Th. H., Hoogendoorn, C. J., and Henkes, R. A. W. M., “Numerical Study of Laminar and Turbulent Natural Convection in an Inclined Square Cavity,” International Journal of Heat and Mass Transfer, Vol. 36, No. 11, pp. 2899-2911, 1992.

[21] Lakhal, E. K., Hasnaoui, M.and Vasseur, P., “Numerical study of transient natural convection in a cavity heated periodically with different types of excitations”, International Journal of Heat and Mass Transfer, Vol. 42, No. 21, pp. 3927–3941, 1999.

[22] Le Quere, P., Humphery, J. A., and Sherman, F.S. ”Numerical calculation of thermally driven two-dimensional unsteady laminar flow in cavities of rectangular cross section”, Numerical Heat Transfer, Vol. 4, pp. 249-283,1981.

[23] Lewis, R.W., Morgan, K., Thomas, H. R. and Seetharamu, K. N., The Finite element method in heat transfer analysis, John Wiley & Sons, New York, 1996.

[24] Linthorst, S.J.M., Schinkel, W. M. M., and Hoogendorn, C. J., “Flow Structure with Natural convection in Inclined Air-filled Enclosures,” Journal of Heat Transfer. Vol. 103, pp.535-539, 1981.

[25] Mohamad, A., “Natural convection in open cavities and slots”, Numerical Heat Transfer, Vol. 27, pp. 705-716, 1995.

[26] Ozoe, H., Sayama, H., and Churchill, S. W., “Natural Circulation in an Inclined Rectangular channel at Various Aspect Ratios and Angles—Experimental Measurements,” International Journal of Heat and Mass Transfer, Vol.18, pp.1425-1420, 1975.

[27] Ozoe, H., Sayama, H., and Churchill, S. W., “Natural Convection in an Inclined Square Channel,” International Journal of Heat and Mass Transfer, Vol. 17, pp.401-406,1974.

[28] Patankar, S. V., Numerical Heat Transfer and Fluid Flow, Hemisphere, Washington, DC; McGraw-Hill, New York, 1980.

[29] Penot, F., “Numerical calculation of two-dimensional natural convection in isothermal open cavities”, Numerical Heat Transfer, Vol. 5, pp. 421-437, 1982.

[30] Peraire, J., Vahidati, M., Morgan, K., and Zienkiewicz, O. C. Adaptive remeshing for compressible flow computation, Journal of Computational Physics, Vol.72, pp. 449-466, 1987.

[31] Polat, O. and Bilgen, E. “Laminar natural convection in inclined open shallow cavities”, Int. J. Therm Sci, Vol. 41, pp. 360-368, 2002.

[32] Reddy J.N. and Gartling, “Fundamentals of the Finite Element Method in Heat Transfer”, Second Ed., CRC Press, 2001.

[33] Showole, R.A. and Tarasuk, J.D., “Experimental and numerical studies of natural convection with flow separation in upward-facing inclined open cavities”,Journal of Heat Transfer, Vol. 115, pp. 592-605, 1993.

[34] Soong, C. Y., Tzeng, P. Y., Chiang, D. C., and Sheu, T. S., "Numerical Study on Mode-transition on Natural Convection in Differentially Heated Inclined Enclosures", International Journal of Heat and Mass Transfer, Vol. 39, No. 14, pp. 2869-2882, 1996.

[35] Tasnim, S. T. and Collins, M.R. "Numerical analysis of heat transfer in a square cavity with a baffle on the hot wall", Int. Com. Heat and Mass Transfer, Vol. 31, pp. 639–650, 2004.

[36] Zhong, Z.Y., Yang, K. T., and Lloyd, J. R., "Variable-property Natural convection in tilted Enclosures with Thermal Radiation", Numerical Methods in Heat Transfer, Vol. III, pp. 195-214, 1985.

[37] Zienkiewicz, O. C. and Taylor, R. L. The finite element method, Fourth Ed., McGraw-Hill. 1991.